



universität
wien

DIPLOMARBEIT

Titel der Diplomarbeit

The time-dependent Pauli equation

angestrebter akademischer Grad

Magister der Naturwissenschaften (Mag. rer. nat.)

Verfasser: David Wimmesberger
Matrikelnummer: 0402104
Studienrichtung: A 405 Mathematik
Betreuer: Ao. Univ.-Prof. Dr. Norbert Mauser

Wien, am 26. Juli 2010

Abstract

This diploma thesis deals with the time-dependent Pauli equation as a PDE-model in quantum mechanics that generalizes the time-dependent 'non relativistic' Schrödinger equation to a 'semi-relativistic' model where magnetic field and spin are included. In particular the famous 'spin magnetic field' coupling term that explained some fine structure in spectra is contained in the Pauli equation.

In a hierarchy of models of relativistic quantum mechanics, the Pauli equation is an approximation of the electron part of the 'fully relativistic' Dirac equation at first order in $\frac{1}{c}$, where c is the speed of light.

Since any fast moving charge creates a 'self-consistent' electromagnetic (E-M) field, it is necessary to couple the Pauli equation for fast electrons to PDEs for the E-M field. On a fully relativistic level this is the Maxwell equation, of course.

In order to approximate the Dirac-Maxwell system in a consistent $\frac{1}{c}$ -order approximation we couple the Pauli equation to two Poisson equations, with a vector valued Poisson equation replacing the Maxwell equations by an elliptic equation with the quantum current as source term.

The resulting Pauli-Poiswell system is the main topic of the second part of this thesis, where first we present and analyze appropriate numerical methods : a 'Leap Frog scheme' for the Pauli equation, a 'pseudo Fourier method' for the Poisson equation of the electric potential and a 'relaxation scheme' for the Poisson equation of the magnetic vector potential.

Finally, we present numerical simulations of the time dependent Pauli-Poiswell system and for reduced models like magnetic Schrödinger equations, for different initial conditions.

Zusammenfassung

Diese Diplomarbeit behandelt die zeitabhängige Pauligleichung als quantenmechanisches PDE-Modell, welches die zeitabhängige, 'nichtrelativistische' Schrödingergleichung zu einem 'semirelativistischen' Modell verallgemeinert, das den Spin und das Magnetfeld berücksichtigt. Weiters beinhaltet die Pauligleichung den 'Spin-Magnetfeld Kupplungsterm' - bekannt dafür, einige Feinstrukturen im Spektrum zu begründen.

In der Modellhierarchie der relativistischen Quantenmechanik ist die Pauligleichung eine Approximation erster Ordnung in $\frac{1}{c}$ des Elektronenanteils der 'vollrelativistischen' Diracgleichung (wobei c die Lichtgeschwindigkeit bezeichnet).

Da jeder Ladungsträger in schneller Bewegung ein 'selbstkonsistentes' elektromagnetisches (E-M) Feld erzeugt, muss die Pauligleichung für schnelle Elektronen an PDEs für das E-M Feld gekoppelt werden. Auf vollrelativistischer Ebene ist dies natürlich die Maxwellgleichung.

Um das Dirac-Maxwell-System jedoch konsistent in erster Ordnung in $\frac{1}{c}$ zu approximieren, koppelt man die Pauligleichung an zwei Poissongleichungen (wovon eine vektorwertig ist und die Maxwellgleichungen durch eine elliptische Gleichung mit dem quantenmechanischen Fluss als Quellterm ersetzt).

Das daraus resultierende Pauli-Poiswell-System wird im zweiten Teil dieser Arbeit näher betrachtet: Zuerst werden passende numerische Methoden zur Lösung des Systems eingeführt und analysiert - ein 'Leap Frog'-Schema für die Pauligleichung, eine 'pseudo-Fourier'-Methode für die Poissongleichung des elektrischen Potentials und ein 'Relaxations'-Algorithmus für die Poissongleichung des magnetischen Vektorpotentials.

Weiters werden Ergebnisse numerischer Simulationen präsentiert, welche das zeitabhängige Pauli-Poiswell-System und reduzierte Modelle, wie die magnetische Schrödingergleichung, für verschiedene Startbedingungen behandeln.

Danksagungen

Zuallererst danke ich meinen Betreuern Norbert Mauser und Hans-Peter Stimming, die es mir mit ihren zahlreichen Ratschlägen und Hilfestellungen ermöglichten, mich in das sehr interessante Gebiet der Quantenmechanik einzulesen und diese Arbeit zu verfassen. Danke auch an meine Kollegen am Wolfgang Pauli Institut (WPI), allen voran Dietmar Ölz und Nikolaos Sfakianakis für mathematische Tipps und den wohl besten Kaffee den die Fakultät für Mathematik zu bieten hat.

Weiters danke ich meiner Familie und meiner Freundin Stefanie für ihre Unterstützung während meines Studiums, insbesondere für Motivation und Geduld in arbeitsreichen Zeiten.

Besonderer Dank an Hannes Grimm-Strele fürs Korrekturlesen dieser Diplomarbeit und all meinen Studienkollegen, die die letzten sechs Jahre auch abseits universitärer Einrichtungen zu einer lebenswerten Zeit machten.

Diese Arbeit wurde durch den Wiener Wissenschafts-, Forschungs- und Technologiefonds (WWTF) mit dem Projekt 'TDDFT' (MA-45) und durch die Förderung des WPI durch das österreichische Wissenschaftsministerium unterstützt.

This work was supported by the Vienna Science and Technology Fund (WWTF) via the project 'TDDFT' (MA-45) and by the Austrian ministry of science by its grant for the WPI.

Contents

1	Introduction	7
2	PDE-models in quantum mechanics	10
2.1	Wave aspects of matter	10
2.1.1	The two natures of light	10
2.1.2	De Broglie waves	11
2.2	Statistical interpretation of matter waves	12
2.2.1	The Copenhagen interpretation	12
2.2.2	Expectation values and operators	12
2.2.3	The Heisenberg uncertainty principle	14
2.3	The Schrödinger equation	15
2.3.1	Particle current density	16
3	The Pauli equation	18
3.1	Derivation	18
3.1.1	Coupling to the electromagnetic field: Magnetic Schrödinger equation	18
3.1.2	Spin	19
3.2	Particle current density, conservation of mass	22
3.3	From Dirac-Maxwell to Pauli-Poiswell	24
3.3.1	Scaling of equations	26
3.3.2	'Perturbation theory'	30
3.4	Analytical results	34
3.4.1	Results for the time-dependent Pauli equation	34
3.4.2	Results for the time-dependent Schrödinger-Maxwell system	36
4	Numerical methods	37
4.1	Fourier-pseudospectral derivative	38
4.1.1	Trigonometric interpolation	38
4.1.2	The Fourier-pseudospectral derivative	43
4.2	Relaxation iteration	47
4.2.1	General facts on iterative algorithms	47
4.2.2	Application to a Poisson equation	49

4.3	Finite difference methods	50
4.3.1	Convergence, consistency and stability	51
4.3.2	Von Neumann stability analysis	54
4.3.3	Application to the Pauli equation	57
4.4	Numerical approximation of the Pauli-Poiswell system	61
5	Numerical results	62
5.1	Setup of the numerical experiments	62
5.2	Numerical data	66
A	Curriculum Vitae	92

Chapter 1

Introduction

The time-dependent Pauli equation for the 2-spinor ψ

$$i\hbar \frac{\partial}{\partial t} \psi(\mathbf{x}, t) = \left(\frac{1}{2m} (-i\hbar \nabla - \frac{e}{c} \mathbf{A}(\mathbf{x}, t))^2 + eV(\mathbf{x}, t) + \frac{|e|\hbar}{2mc} \hat{\sigma} \cdot \mathbf{B}(\mathbf{x}, t) \right) \psi(\mathbf{x}, t)$$

is a fundamental equation in quantum mechanics. It is an appropriate model for charged particles which move at intermediate speed compared to the speed of light ('semi-relativistic' particles) taking into account the spin-magnetic field coupling for external fields and/or for self-consistent fields generated by the moving charge itself.

In Chapter 2, an introduction to PDE-models in quantum mechanics is given, including the derivation of the Schrödinger equation.

Chapter 3 deals with the effects caused by spin and the magnetic Schrödinger equation as well as the Pauli equation are introduced. Furthermore, this chapter contains the transition from the Dirac-Maxwell system to the Pauli-Poiswell system:

The Dirac-Maxwell system (i.e.: the Dirac equation for the 4-spinor of a relativistic electron moving in an electromagnetic field coupled to the Maxwell equations for the fields) is a fundamental system in relativistic quantum mechanics. Alas, it is hard to deal with analytically as well as numerically, therefore approximations are needed:

The Pauli equation is an $O(\frac{1}{c})$ -approximation of the 2-spinor of the electron part of the Dirac equation (the positron part is not important in applications). Coupled to two Poisson equations approximating the Maxwell equations (singularly) at order $O(\frac{1}{c})$ this yields the Pauli-Poiswell system.

In Chapter 4, numerical methods to solve the Pauli-Poiswell system are analyzed, results of numerical simulations are presented in chapter 5.

Notation

Throughout this thesis, the following notation is used:

$\Delta_{\mathcal{F}} f \dots$ Fourier-pseudospectral Laplacian of f
 $\sigma^1, \sigma^2, \sigma^3 \dots$ (2x2) Pauli matrices, see page 21
 $\gamma^0, \gamma^1, \gamma^2, \gamma^3 \dots$ (4x4) Dirac matrices, see page 24
 $\odot \dots$ componentwise multiplication
 $\psi(\mathbf{x}, t), \Psi(\mathbf{x}, t) \dots$ wavefunction/spinor of a particle

$\mathbf{A}(\mathbf{x}, t) = (A_1, A_2, A_3)^T \dots$ magnetic vector potential
 $\mathbf{B}(\mathbf{x}, t) \dots$ magnetic field
 $c \dots$ speed of light
 $D_{x^\alpha y^\beta}^{\alpha+\beta} f$ Fourier-pseudospectral derivative of f
 $V(\mathbf{x}, t) \dots$ electric potential
 $\mathbf{E}(\mathbf{x}, t) \dots$ electric field
 $\mathcal{F}, \mathcal{F}(f) \dots$ Fourier transform (of a function f)
 $\mathcal{F}_n, \mathcal{F}_n(f) \dots$ discrete Fourier transform (of a function f)
 $f_{j,k}^n \dots$ approximation of a function f , cf. page 38
 $f^{(m)} \dots$ m -th derivative of a function f
 $h \dots$ scaled Planck constant
 $\hbar \dots$ reduced Planck constant
 $\mathbf{J}(\mathbf{x}, t) = (J_1, J_2, J_3)^T \dots$ current density
 $n(\mathbf{x}, t) \dots$ position density

Vector valued quantities - like \mathbf{A}, \mathbf{x} - are denoted in bold face.

If not otherwise specified, all functions depend on (\mathbf{x}, t) , where $\mathbf{x} \in \mathbb{R}^2$ or \mathbb{R}^3 (usually clear from context) and $t \in \mathbb{R}_0^+$.

Function Spaces:

$\mathcal{C}^\infty(\Omega) \dots$ space of all smooth functions on Ω
 $H^{p,m}(\Omega) \dots$ Sobolev space of degree m on Ω with respect to the Lebesgue- p -norm, $1 \leq$

$p \leq \infty$

$H_0^{p,m}(\Omega) \dots H^{p,m}(\Omega)$ with compact support

$L^p(\Omega) \dots$ space of all Lebesgue-p-integrable functions on Ω , $1 \leq p \leq \infty$

$L_{per}^p(\Omega) \dots L^p(\Omega)$ -space with periodic boundary conditions

$l^p(\mathbb{C}) \dots$ space of all p-summable complex sequences

$S(\Omega) \dots$ Schwartz space of rapidly decreasing functions on Ω

Chapter 2

PDE-models in quantum mechanics

This chapter contains an introduction to the basics of PDE-models used in quantum mechanics. Some of the presented equations originated from intuitive derivations or even postulates, but one has to keep in mind that these models are experimentally verified and generally accepted. Furthermore, there is a relation to classical mechanics: Every classical mechanical quantity has a corresponding quantity in quantum mechanics and the classical one can be regained in the limit $\hbar \rightarrow 0$. This is called *correspondence principle*. Note however that there are quantities, like spin, emerging from the theory of quantum mechanics which do not have a classical counterpart.

For details, see [G].

2.1 Wave aspects of matter

2.1.1 The two natures of light

It is well acknowledged by now, that light has to be described in two different ways, depending on the situation: On the one hand, interference and diffraction effects suggest an interpretation of light as electromagnetic wave. The photoelectric effect on the other hand is an example of a physical phenomenon which can only be explained by the existence of particles associated to light. These 'light particles' are called *photons*.

The photoelectric effect was discovered by *Heinrich Hertz* in 1887 and it describes the ejection of electrons from a metallic surface caused by light.

If monochromatic light shines on a metallic surface, electrons of definite energy get detached. If light was described as wave, one would expect a correlation between the energy of the emitted electrons and the intensity of the light, since the energy of a wave is proportional to its amplitude.

However, increased light intensity only leads to the emission of more electrons, but does

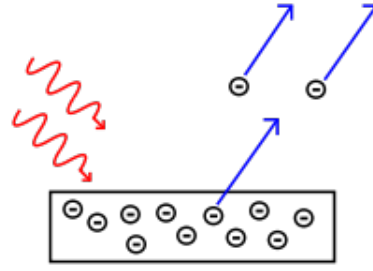


Figure 2.1: Photoelectric Effect

not alter their energy. This can only be achieved by a change in frequency.

Albert Einstein interpreted this effect by postulating a quantization of light into photons with energy $\hbar\omega$ (where $\hbar \sim 1.054571628 \cdot 10^{-34}$ Js is the reduced Planck constant and ω the light's frequency). Increasing the intensity of light also increases the number of photons and therefore more electrons are emitted.

2.1.2 De Broglie waves

Now the question arises, if particles - like electrons - possess wave aspects too. *P. L. V. de Broglie* postulated that similar wave properties can be assigned to matter particles (this was experimentally proved later):

To every free particle with mass m , propagating uniformly at velocity \mathbf{v} , with momentum $\mathbf{p} = m\mathbf{v}$ and energy E corresponds a wave with frequency ν and wave vector \mathbf{k} such that the following hold:

$$E = \tilde{h}\nu = \hbar\omega \quad (\tilde{h} = 2\pi\hbar, \nu = \frac{\omega}{2\pi}) \quad (2.1)$$

$$\mathbf{p} = \hbar\mathbf{k} \quad (2.2)$$

Thus, associated to every particle, there is a plane wave ψ determined up to an amplitude factor a :

$$\psi(\mathbf{x}, t) = a \cdot \exp(i(\mathbf{k} \cdot \mathbf{x} - \omega t)) \stackrel{(2.1), (2.2)}{=} a \cdot \exp\left(\frac{i(\mathbf{p} \cdot \mathbf{x} - Et)}{\hbar}\right) \quad (2.3)$$

According to De Broglie, the wavelength of this wave is $\lambda = \frac{h}{p} = \frac{h}{mv}$. Therefore, for a measurable wavelength, the rest mass m of the particle has to be sufficiently small.

2.2 Statistical interpretation of matter waves

2.2.1 The Copenhagen interpretation

According to the so called *Copenhagen interpretation* the *wave function* ψ is a 'guiding field' for the particle and

$$n(\mathbf{x}, t) := |\psi(\mathbf{x}, t)|^2$$

is introduced as probability density for finding the particle at (\mathbf{x}, t) . This means, the probability of finding the particle in a subset $U \subseteq \mathbb{R}^3$ at time t is

$$\int_U n(\mathbf{x}, t) d\mathbf{x}$$

n has to be normalized to 1, so the amplitude factor a of ψ must be chosen such that

$$\int_{\mathbb{R}^3} n(\mathbf{x}, t) d\mathbf{x} = 1$$

if possible (otherwise, i.e. if $\|\psi\|_2 = \infty$, one can try to normalize the function in a reasonably large box $V \subseteq \mathbb{R}^3$). In the following it is assumed, that the normalization is always possible - this is the case in most applications.

Note that the wave function ψ is not unique. The quantity of interest is $|\psi|^2$ and $e^{i\alpha}\psi$ ($\alpha \in \mathbb{R}$) yields the same probability density. To consider N instead of one particle, one chooses a wave function $\psi(\mathbf{x}, t)$ with $\mathbf{x} \in \mathbb{R}^{3N}$.

ψ is often referred to as the *state* of a quantum mechanical system.

2.2.2 Expectation values and operators

In classical mechanics, a system can be fully described by position and momentum data in phase space. All other 'interesting' quantities - like total energy, angular momentum et cetera - can be derived from these two basic characteristics.

Assume a quantum mechanical system to be in state ψ . If one wants to gather information about position and momentum (for example of an electron described by ψ), the best choice due to the probabilistic approach is to look at expectation values.

$n = \psi\bar{\psi}$ was interpreted as position density, hence the expectation for the position coordinate \mathbf{x} of the electron is:

$$\langle \mathbf{x} \rangle_\psi := \int_{\mathbb{R}^3} \mathbf{x} \psi \bar{\psi} d\mathbf{x} = \int_{\mathbb{R}^3} \psi \mathbf{x} \bar{\psi} d\mathbf{x}$$

For the momentum, consider the following:

If $\mathcal{F}(\psi)(\mathbf{p})$ denotes the Fourier transform of ψ with respect to \mathbf{x} for fixed $t = t_0$, then by Fourier inversion

$$\psi(\mathbf{x}) := \psi(\mathbf{x}, t_0) = \frac{1}{\sqrt[3]{(2\pi)^2}} \int_{\mathbb{R}^3} \mathcal{F}(\psi)(\mathbf{p}) e^{i\mathbf{p}\cdot\mathbf{x}} d\mathbf{x} = \int_{\mathbb{R}^3} \mathcal{F}(\psi)(\mathbf{p}) \psi_{\mathbf{p}}(\mathbf{x}) d\mathbf{x}$$

for $\psi_{\mathbf{p}}(\mathbf{x}) := \frac{1}{\sqrt[3]{(2\pi)^2}} e^{i\mathbf{p}\cdot\mathbf{x}}$. Comparing with (2.3) and choosing the amplitude factor a adequately, one can interpret $\psi_{\mathbf{p}}(\mathbf{x})$ as basic wave function with momentum $\hbar\mathbf{p}$ and $\mathcal{F}(\psi)(\mathbf{p})$ as the 'part of ψ with momentum $\hbar\mathbf{p}$ ' or the probability of the electron - as in the example above - to have a momentum of $\hbar\mathbf{p}$. So $\mathcal{F}(\psi)(\mathbf{p})$ gives a probability density for the momentum in state ψ and leads to the momentum expectation:

$$\begin{aligned} \langle \mathbf{p} \rangle_{\mathcal{F}(\psi)} &= \int_{\mathbb{R}^3} \mathcal{F}(\psi)(\mathbf{p}) \cdot \hbar\mathbf{p} \cdot \overline{\mathcal{F}(\psi)}(\mathbf{p}) d\mathbf{p} = \\ &= \langle \hbar\mathbf{p} \cdot \mathcal{F}(\psi), \mathcal{F}(\psi) \rangle = \langle \mathcal{F}^{-1}(\hbar\mathbf{p} \cdot \mathcal{F}(\psi)), \psi \rangle = \\ &= \langle -i\hbar\nabla\psi, \psi \rangle = \int_{\mathbb{R}^3} (-i\hbar\nabla\psi) \bar{\psi} d\mathbf{x} =: \langle \mathbf{p} \rangle_{\psi} \end{aligned}$$

Introducing the multiplication operator $\hat{\mathbf{x}} := \mathbf{x}$ and the differential operator $\hat{\mathbf{p}} := -i\hbar\nabla$, the above reads:

$$\begin{aligned} \langle \mathbf{x} \rangle_{\psi} &= \int_{\mathbb{R}^3} \hat{\mathbf{x}}\psi \bar{\psi} d\mathbf{x} =: \langle \hat{\mathbf{x}} \rangle_{\psi} \\ \langle \mathbf{p} \rangle_{\psi} &= \int_{\mathbb{R}^3} \hat{\mathbf{p}}\psi \bar{\psi} d\mathbf{x} =: \langle \hat{\mathbf{p}} \rangle_{\psi} \end{aligned}$$

Thus the two basic quantities of a mechanical system can be transferred to a quantum mechanical system via transition to (linear, Hermitian) unbounded operators and their expectation values.

This is true in general (with similar argumentation): If $A(\mathbf{x}, \mathbf{p})$ is a function depending on position and momentum (in classical sense), the quantum mechanical equivalent $\hat{A}(\hat{\mathbf{x}}, \hat{\mathbf{p}})$ is a linear, Hermitian unbounded operator (from now on all mentioned operators in this chapter are assumed to have these properties) found by replacing \mathbf{x} and \mathbf{p} by $\hat{\mathbf{x}}$ and $\hat{\mathbf{p}}$, respectively. Again:

$$\langle A \rangle_{\psi} = \int_{\mathbb{R}^3} \hat{A}(\hat{\mathbf{x}}, \hat{\mathbf{p}}) \psi \bar{\psi} d\mathbf{x} := \langle \hat{A} \rangle_{\psi}$$

Note that due to Hermiticity, the expectation is always real.

Example 1. The total energy of a mechanical system is given by the Hamiltonian function as sum of kinetic and potential energy

$$H(\mathbf{x}, \mathbf{p}) = \frac{\mathbf{p} \cdot \mathbf{p}}{2m} + V(\mathbf{x})$$

where m is the mass (for example of the moving electron). The quantum mechanical analogon is the Hamiltonian operator

$$\hat{H}_0(\hat{\mathbf{x}}, \hat{\mathbf{p}}) = \frac{(-i\hbar\nabla)^2}{2m} + \hat{V}(\hat{\mathbf{x}}) = -\frac{\hbar^2}{2m}\Delta + \hat{V}(\hat{\mathbf{x}})$$

2.2.3 The Heisenberg uncertainty principle

A direct consequence of the probabilistic approach is the *Heisenberg uncertainty principle* which states that the exact position and the exact momentum of an electron cannot be determined simultaneously. As before, $\psi(\mathbf{x})$ denotes a state at a fixed time $t = t_0$.

Variance is a measure for the deviation of the mean value - it is given by

$$\begin{aligned} V_\psi(\mathbf{x}) &:= \langle (\mathbf{x} - \langle \mathbf{x} \rangle_\psi)^2 \rangle_\psi = \langle \mathbf{x}^2 \rangle_\psi - \langle \mathbf{x} \rangle_\psi^2 \\ V_\psi(\mathbf{p}) &:= \langle (\mathbf{p} - \langle \mathbf{p} \rangle_\psi)^2 \rangle_\psi = \langle \mathbf{p}^2 \rangle_\psi - \langle \mathbf{p} \rangle_\psi^2 \end{aligned}$$

And, since one can always choose a coordinate system such that $\langle \mathbf{x} \rangle_\psi = \langle \mathbf{p} \rangle_\psi = 0$:

$$\begin{aligned} V_\psi(\mathbf{x}) &= \langle \mathbf{x}^2 \rangle_\psi \\ V_\psi(\mathbf{p}) &= \langle \mathbf{p}^2 \rangle_\psi \end{aligned}$$

Now for every $\alpha \in \mathbb{R}$:

$$\begin{aligned} 0 &\leq \int_{\mathbb{R}^3} |\alpha \mathbf{x} \psi(\mathbf{x}) + \nabla \psi(\mathbf{x})|^2 d\mathbf{x} = \\ &= \alpha^2 \underbrace{\int_{\mathbb{R}^3} \mathbf{x}^2 |\psi|^2 d\mathbf{x}}_{:=A} + \alpha \underbrace{\int_{\mathbb{R}^3} \mathbf{x} \bar{\psi} \nabla \psi + (\nabla \bar{\psi}) \mathbf{x} \psi d\mathbf{x}}_{:=B} + \underbrace{\int_{\mathbb{R}^3} (\nabla \bar{\psi}) (\nabla \psi) d\mathbf{x}}_{:=C} \\ &= \alpha^2 A + \alpha B + C \end{aligned}$$

This is a polynomial of second order in α and since it is positive semidefinite on \mathbb{R} , it can have at most one real root. Thus necessarily $B^2 - 4AC \leq 0$ and, using

$$A = \int_{\mathbb{R}^3} \mathbf{x}^2 |\psi|^2 d\mathbf{x} = V_\psi(\mathbf{x})$$

$$B = \int_{\mathbb{R}^3} \mathbf{x} \bar{\psi} \nabla \psi + (\nabla \bar{\psi}) \mathbf{x} \psi d\mathbf{x} = \int_{\mathbb{R}^3} \mathbf{x} \nabla (\bar{\psi} \psi) d\mathbf{x} = - \int_{\mathbb{R}^3} \bar{\psi} \psi d\mathbf{x} = -1$$

$$C = \int_{\mathbb{R}^3} (\nabla \bar{\psi}) (\nabla \psi) d\mathbf{x} = - \int_{\mathbb{R}^3} \bar{\psi} \Delta \psi d\mathbf{x} = \frac{1}{\hbar^2} \int_{\mathbb{R}^3} \bar{\psi} (-\hbar^2 \Delta \psi) d\mathbf{x} = \frac{V_\psi(\mathbf{p})}{\hbar^2}$$

($\psi \xrightarrow{|\mathbf{x}| \rightarrow \infty} 0$) one can see that

$$\frac{\hbar^2}{4} \leq V_\psi(\mathbf{x}) V_\psi(\mathbf{p})$$

This is the uncertainty principle - if $V_\psi(\mathbf{x}) \rightarrow 0$, $V_\psi(\mathbf{p})$ has to tend to infinity and vice versa.

Remark 2. For operators \hat{L}, \hat{M} one can show:

- $V_\psi(\hat{L}) = 0 \Leftrightarrow \psi$ is an eigenfunction (or in this context: eigenstate) of \hat{L} .
- Although commonly known for position and momentum, there are uncertainty relations for other quantities too: If the eigenstates of \hat{L} form a complete orthonormal set in $L^2(\mathbb{R}^3)$ and $[\hat{L}, \hat{M}]_- := \hat{L}\hat{M} - \hat{M}\hat{L} = \hat{C} \neq 0$, then

$$-\frac{\langle \hat{C} \rangle_\psi^2}{4} \leq V_\psi(\hat{L}) V_\psi(\hat{M})$$

Otherwise, for $[\hat{L}, \hat{M}]_- = 0$, two cases can occur: If \hat{L} is not degraded (i.e. for every eigenvalue of \hat{L} there is exactly one eigenstate), then \hat{L} and \hat{M} are simultaneously exactly measurable in all states ψ . If \hat{L} is degraded, one can at least find eigenstates in which this is possible.

Another example of a pair of 'canonically conjugated' operators is the energy operator $\hat{E} = i\hbar \frac{\partial}{\partial t}$ together with the time operator t .

2.3 The Schrödinger equation

Until now it is not clear how to find the states describing a system. This will be the task of this chapter. At first, consider the energy operator $\hat{E} := i\hbar \frac{\partial}{\partial t}$. Applying it on the wave function of a free particle, one can see that the energy E of the particle is an eigenvalue of \hat{E} :

$$\psi(\mathbf{x}, t) = a \exp\left(\frac{i(\mathbf{p} \cdot \mathbf{x} - Et)}{\hbar}\right)$$

$$\hat{E}\psi = i\hbar \frac{\partial}{\partial t} a \exp\left(\frac{i(\mathbf{p} \cdot \mathbf{x} - Et)}{\hbar}\right) = E a \exp\left(\frac{i(\mathbf{p} \cdot \mathbf{x} - Et)}{\hbar}\right) = E\psi$$

On the other hand we already deduced the Hamiltonian \hat{H} for calculating the expectation E of energy:

$$\langle \hat{H} \rangle_\psi = \int_{\mathbb{R}^3} \hat{H}\psi\bar{\psi}d\mathbf{x} = E = E \int_{\mathbb{R}^3} \psi\bar{\psi}d\mathbf{x} = \int_{\mathbb{R}^3} E\psi\bar{\psi}d\mathbf{x} = \int_{\mathbb{R}^3} \hat{E}\psi\bar{\psi}d\mathbf{x} = \langle \hat{E} \rangle_\psi$$

Therefore, both operators can be set equal:

$$\hat{H}\psi(\mathbf{x}, t) = \hat{E}\psi(\mathbf{x}, t) = E\psi(\mathbf{x}, t) \quad (2.4)$$

This gives the general form of the time-dependent *Schrödinger equation*:

$$i\frac{\partial}{\partial t}\psi(\mathbf{x}, t) = \hat{H}\psi(\mathbf{x}, t) \quad (2.5)$$

If \hat{H} acts only on the space variables, the separation ansatz $\psi(\mathbf{x}, t) = \tilde{\psi}(\mathbf{x})f(t)$ leads to the *stationary Schrödinger equation*:

$$i\hbar\tilde{\psi}(\mathbf{x})\frac{\partial}{\partial t}f(t) \stackrel{(4)}{=} \left(\hat{H}\tilde{\psi}(\mathbf{x})\right)f(t)$$

$$i\hbar\frac{\dot{f}(t)}{f(t)} = \frac{\hat{H}\tilde{\psi}(\mathbf{x})}{\tilde{\psi}(\mathbf{x})} = E$$

hence

$$f(t) = c \exp\left(-i\frac{E}{\hbar}t\right)$$

and

$$\hat{H}\tilde{\psi}(\mathbf{x}) = E\tilde{\psi}(\mathbf{x}) \quad (2.6)$$

which is an eigenvalue equation.

2.3.1 Particle current density

Conservation of mass is usually expressed in the conservation law

$$\frac{\partial}{\partial t}n(\mathbf{x}, t) + \operatorname{div}\mathbf{J}(\mathbf{x}, t) = 0 \Rightarrow \frac{\partial}{\partial t} \int_U n(\mathbf{x}, t)d\mathbf{x} + \int_{\partial U} \mathbf{J}(\mathbf{x}, t) \cdot \mathbf{nd}S = 0$$

It states that if the electric charge density n in $U \subseteq \mathbb{R}^3$ changes, then a current \mathbf{J} flows through its surface. A similar equation for the flow density appears in fluid mechanics and other theories of mathematical physics. The goal of this section is to derive a continuity

equation for the particle probability density $n = \bar{\psi}\psi$.

In a volume element $U \subseteq \mathbb{R}^3$ no particles can be created or annihilated. Thus if n changes, there has to be a flux \mathbf{J} through the surface ∂U :

$$\frac{\partial}{\partial t}n(\mathbf{x}, t) + \operatorname{div}\mathbf{J}(\mathbf{x}, t) = 0 \quad (2.7)$$

To deduce an expression for \mathbf{J} one starts with the time dependent Schrödinger equation (assume, that the wave function ψ is normalized on U) and gets by conjugation:

$$\frac{\partial}{\partial t}\psi = \frac{\hat{H}\psi}{i\hbar} \quad \text{and} \quad \frac{\partial}{\partial t}\bar{\psi} = -\frac{\hat{H}^*\bar{\psi}}{i\hbar}$$

Multiplying the left equation by $\bar{\psi}$, the complex conjugate by ψ and adding both:

$$\frac{\partial}{\partial t}\underbrace{(\bar{\psi}\psi)}_n + \frac{i}{\hbar}(\bar{\psi}\hat{H}\psi - \psi\hat{H}^*\bar{\psi}) = 0$$

Now for $\hat{H} = \frac{1}{2m}\hat{\mathbf{p}}^2 + \underbrace{\hat{V}(\hat{\mathbf{x}})}_{=V(\mathbf{x})}$:

$$\begin{aligned} 0 &= \frac{\partial}{\partial t}n + \frac{i\hbar}{2m}(\psi\Delta\bar{\psi} - \bar{\psi}\Delta\psi) = \frac{\partial}{\partial t}n + \frac{i\hbar}{2m}\nabla \cdot (\psi\nabla\bar{\psi} - \bar{\psi}\nabla\psi) = \\ &= \frac{\partial}{\partial t}n + \frac{i\hbar}{2m}\operatorname{div}(\psi\nabla\bar{\psi} - \bar{\psi}\nabla\psi) \end{aligned}$$

Comparing with equation (2.7), one arrives at

$$\mathbf{J} = \frac{i\hbar}{2m}(\psi\nabla\bar{\psi} - \bar{\psi}\nabla\psi)$$

In the special case of a wave function of a free particle $\psi(\mathbf{x}, t) = a \cdot \exp\left(\frac{i(\mathbf{p}\cdot\mathbf{x} - Et)}{\hbar}\right)$, this yields the current density:

$$\mathbf{J} = \frac{a^2}{m} \mathbf{p}$$

Chapter 3

The Pauli equation

In the previous chapter, the Schrödinger equation was introduced in a very general form. Choosing a Hamiltonian as before

$$\hat{H}(\hat{\mathbf{x}}, \hat{\mathbf{p}}) = \hat{H}_0(\hat{\mathbf{x}}, \hat{\mathbf{p}}) := -\frac{\hbar^2}{2m}\Delta + V(\mathbf{x})$$

it yields a description of a particle moving in a given, time-independent electric field $\mathbf{E} = -\nabla V$. Influences of magnetic fields however are not included in this model.

If such an influence has to be considered, the situation changes and further effects - like spin - become important for the model. This gives rise to new Schrödinger equations (the 'magnetic' ones) and finally to the Pauli equation (which is also a Schrödinger equation).

3.1 Derivation

3.1.1 Coupling to the electromagnetic field: Magnetic Schrödinger equation

If a charged particle of charge e moves in an electromagnetic field, the *Lorentz force*

$$\mathbf{F} = e(\mathbf{E} + \frac{\mathbf{v}}{c} \times \mathbf{B})$$

acts on it. Here \mathbf{E} and \mathbf{B} denote electric and magnetic field, c is the speed of light in vacuum. Therefore, quantities proportional to $\frac{1}{c}$ or $\frac{1}{c^2}$, which will appear frequently in the following, can be considered to be 'small' or 'very small'.

It is common to express the electric and magnetic field strengths by the corresponding

potentials $\mathbf{A}(\mathbf{x}, t)$ and $V(\mathbf{x}, t)$ via

$$\begin{aligned}\mathbf{E} &= -\nabla V - \frac{\partial \mathbf{A}}{\partial t} \frac{1}{c} \\ \mathbf{B} &= \nabla \times \mathbf{A}\end{aligned}$$

In classical mechanics this motion is described by the Hamiltonian function

$$H(\mathbf{x}, \mathbf{p}, t) = \frac{1}{2m} \left(\mathbf{p} - \frac{e}{c} \mathbf{A}(\mathbf{x}, t) \right)^2 + eV(\mathbf{x}, t)$$

Following the recipe from above, the corresponding Hamiltonian reads as follows (here it is assumed, that \mathbf{A} and V act as multiplication operators, therefore $\hat{\mathbf{A}} = \mathbf{A}$, $\hat{V} = V$):

$$\begin{aligned}\hat{H}(\mathbf{x}, \mathbf{p}, t) &= \frac{1}{2m} \left(-i\hbar\nabla - \frac{e}{c} \hat{\mathbf{A}}(\hat{\mathbf{x}}, t) \right)^2 + e\hat{V}(\hat{\mathbf{x}}, t) = \\ &= -\frac{\hbar^2}{2m} \Delta + \frac{ie\hbar}{2mc} \mathbf{A}(\mathbf{x}, t) \cdot \nabla + \underbrace{\frac{ie\hbar}{2mc} \nabla \cdot \mathbf{A}(\mathbf{x}, t)}_{=0 \text{ in most common examples}} + \frac{e^2}{2mc^2} \mathbf{A}^2(\mathbf{x}, t) + eV(\mathbf{x}, t) \\ \Rightarrow \hat{H}(\mathbf{x}, \mathbf{p}, t) &= \underbrace{\hat{H}_0(\mathbf{x}, \mathbf{p}, t)}_{\substack{:= \frac{\hat{\mathbf{p}}^2}{2m} + eV \\ \text{motion in free case}}} - \underbrace{\frac{e}{2mc} \mathbf{A}(\mathbf{x}, t) \cdot \hat{\mathbf{p}}}_{\text{coupling term}} + \underbrace{\frac{e^2}{2mc^2} \mathbf{A}^2(\mathbf{x}, t)}_{O(\frac{1}{c^2})}\end{aligned}$$

Hence motion under the influence of an electromagnetic field is described by the magnetic Schrödinger equation

$$i\hbar \frac{\partial}{\partial t} \psi = \left(\frac{1}{2m} \left(\hat{\mathbf{p}} - \frac{e}{c} \mathbf{A}(\mathbf{x}, t) \right)^2 + eV(\mathbf{x}, t) \right) \psi \quad (3.1)$$

Note that up to now, ψ is still a scalar quantity, this will change now in order to incorporate effects caused by spin in the model.

3.1.2 Spin

Around 1920, experiments (like *Stern-Gerlach*, *Doublet Splitting* and *Einstein-de Haas*) suggested that elementary particles have an intrinsic angular momentum, the *spin*.

The Stern-Gerlach experiment:

A beam of silver atoms is directed through an inhomogeneous magnetic field and the distribution is measured after passing the field. The atoms are in ground state, therefore they should not be influenced by the field. However, the distribution of the atoms when

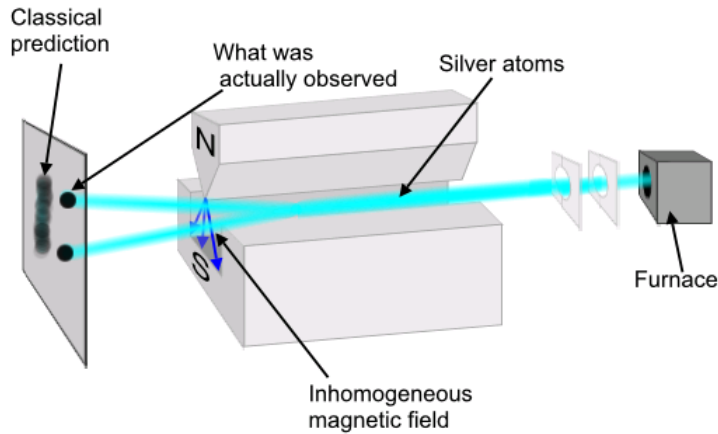


Figure 3.1: Stern-Gerlach experiment

the magnetic field is turned on differs from the distribution without the field.

Therefore, the atoms must have an intrinsic magnetic moment. And since one can exclude the nuclei as its origin physically, it has to be caused by the surrounding electrons.

The beam is split into two components of equal intensity, so one can assume that the electrons' magnetic moment can have only two orientations of same absolute value - parallel or antiparallel to the magnetic field.

Further experiments proved this assumption and led to the following result: Every electron has a magnetic moment caused by an intrinsic angular momentum (*spin*) of $\frac{\hbar}{2}$ or $-\frac{\hbar}{2}$. Moreover, spin is a property of all elementary particles.

Mathematically, spin leads to the introduction of a new degree of freedom in the wave function ψ - which can take only the two values $s_{\uparrow} = \frac{\hbar}{2}$ ('spin up') and $s_{\downarrow} = -\frac{\hbar}{2}$ ('spin down'). Here one axis relatively to which the spin can take the two possible orientations has to be fixed, usually this is the z-axis.

Until now the function

$$n(\mathbf{x}, t) = |\psi(\mathbf{x}, t)|^2$$

was interpreted as a probability density for finding the electron at time t . Now there is a probability $|\psi_{\uparrow}(\mathbf{x}, t)|^2 := |\psi(\mathbf{x}, s_{\uparrow}, t)|^2$ of finding the electron in a 'spin-up-state' at (\mathbf{x}, t) and $|\psi_{\downarrow}(\mathbf{x}, t)|^2 := |\psi(\mathbf{x}, s_{\downarrow}, t)|^2$ of finding the electron in a 'spin-down-state'. Therefore one introduces the following notation:

$$\psi(\mathbf{x}, t) := \begin{pmatrix} \psi_{\uparrow}(\mathbf{x}, t) \\ \psi_{\downarrow}(\mathbf{x}, t) \end{pmatrix}$$

ψ is called *spinor* or in this special case *2-spinor* and the normalization reads:

$$\begin{aligned} \int_{\mathbb{R}^3} \bar{\psi}(\mathbf{x}, t) \psi(\mathbf{x}, t) d\mathbf{x} &= \int_{\mathbb{R}^3} \begin{pmatrix} \bar{\psi}_\uparrow(\mathbf{x}, t) & \bar{\psi}_\downarrow(\mathbf{x}, t) \end{pmatrix} \begin{pmatrix} \psi_\uparrow(\mathbf{x}, t) \\ \psi_\downarrow(\mathbf{x}, t) \end{pmatrix} d\mathbf{x} \\ &= \int_{\mathbb{R}^3} |\psi_\uparrow(\mathbf{x}, t)|^2 + |\psi_\downarrow(\mathbf{x}, t)|^2 d\mathbf{x} = 1 \end{aligned}$$

In order to calculate the spin of a state, a suitable operator is needed.

Consider the following: For fixed time t , the expectation of the z-coordinate of the spin is given by

$$\int_{\mathbb{R}^3} \frac{\hbar}{2} |\psi_\uparrow(\mathbf{x}, t)|^2 + (-\frac{\hbar}{2}) |\psi_\downarrow(\mathbf{x}, t)|^2 d\mathbf{x} = \int_{\mathbb{R}^3} \underbrace{\frac{\hbar}{2} \begin{pmatrix} 1 & 0 \\ 0 & -1 \end{pmatrix}}_{\hat{\sigma}_z} \begin{pmatrix} \psi_\uparrow(\mathbf{x}, t) \\ \psi_\downarrow(\mathbf{x}, t) \end{pmatrix} \overline{\begin{pmatrix} \psi_\uparrow(\mathbf{x}, t) \\ \psi_\downarrow(\mathbf{x}, t) \end{pmatrix}} d\mathbf{x}$$

So for $\hat{S}_z := \frac{\hbar}{2} \hat{\sigma}_z$:

$$\int_{\mathbb{R}^3} \frac{\hbar}{2} |\psi_\uparrow(\mathbf{x}, t)|^2 + (-\frac{\hbar}{2}) |\psi_\downarrow(\mathbf{x}, t)|^2 d\mathbf{x} = \int_{\mathbb{R}^3} \hat{S}_z \psi(\mathbf{x}, t) \bar{\psi}(\mathbf{x}, t) d\mathbf{x}$$

This is an operator for measuring the spin of a state with respect to the z-axis. Spin is an angular momentum, therefore one can use commutation relations for the components of general angular momentum operators to conclude for the remaining spin components:

$$\hat{S}_x = \frac{\hbar}{2} \hat{\sigma}_x = \frac{\hbar}{2} \begin{pmatrix} 0 & 1 \\ 1 & 0 \end{pmatrix}$$

$$\hat{S}_y = \frac{\hbar}{2} \hat{\sigma}_y = \frac{\hbar}{2} \begin{pmatrix} 0 & -i \\ i & 0 \end{pmatrix}$$

The matrices $\sigma_x, \sigma_y, \sigma_z$ are called *Pauli matrices*. For details on the last calculation, cf. [G], chapter 12.4 .

The total spin is given by

$$\hat{S}^2 := \hat{S}_x^2 + \hat{S}_y^2 + \hat{S}_z^2$$

To derive an equation describing a system including the effects caused by the interaction of spin with the magnetic field, one starts with equation (3.1) and adds terms which couple spin and magnetic field. This yields the *Pauli equation*, which is a coupled system of two

scalar PDEs

$$i\hbar \frac{\partial}{\partial t} \psi(\mathbf{x}, t) = \left(\frac{1}{2m} (-i\hbar \nabla - \frac{e}{c} \mathbf{A}(\mathbf{x}, t))^2 + eV(\mathbf{x}, t) + \frac{|e|\hbar}{2mc} \hat{\sigma} \cdot \mathbf{B}(\mathbf{x}, t) \right) \psi(\mathbf{x}, t) \quad (3.2)$$

where $\hat{\sigma}$ is a three-'vector' containing the Pauli matrices and $\hat{\sigma} \cdot \mathbf{B}$ has to be interpreted as

$$(\text{curl} \mathbf{A})_1 \sigma_x + (\text{curl} \mathbf{A})_2 \sigma_y + (\text{curl} \mathbf{A})_3 \sigma_z$$

The Pauli equation is an appropriate model for 'semi-relativistic' charged particles, i.e. which move at intermediate speed compared to the speed of light and where the spin-magnetic field coupling (via $\hat{\sigma} \cdot \mathbf{B}$) is significant for external fields and/or for self-consistent fields generated by the moving charge itself.

3.2 Particle current density, conservation of mass

Similar to the Schrödinger equation one wants to deduce conservation laws as well as an expression for the particle current density \mathbf{J} of the Pauli equation.

For the following calculation, the gradient of the 2-spinor ψ is needed - it is defined by:

$$\nabla \psi = \nabla \begin{pmatrix} \psi_1 \\ \psi_2 \end{pmatrix} := \begin{pmatrix} \frac{\partial \psi_1}{\partial x_1} & \frac{\partial \psi_1}{\partial x_2} & \frac{\partial \psi_1}{\partial x_3} \\ \frac{\partial \psi_2}{\partial x_1} & \frac{\partial \psi_2}{\partial x_2} & \frac{\partial \psi_2}{\partial x_3} \end{pmatrix}$$

and

$$\mathbf{A} \cdot \nabla \psi := \begin{pmatrix} \frac{\partial \psi_1}{\partial x_1} & \frac{\partial \psi_1}{\partial x_2} & \frac{\partial \psi_1}{\partial x_3} \\ \frac{\partial \psi_2}{\partial x_1} & \frac{\partial \psi_2}{\partial x_2} & \frac{\partial \psi_2}{\partial x_3} \end{pmatrix} \begin{pmatrix} A_1 \\ A_2 \\ A_3 \end{pmatrix}$$

Another formal definition:

$$\text{div}(\mathbf{A}\psi) := (\text{div} \mathbf{A})\psi + \mathbf{A} \cdot \nabla \psi \quad (3.3)$$

Similar operations are defined for $\bar{\psi} = \begin{pmatrix} \bar{\psi}_1 & \bar{\psi}_2 \end{pmatrix}$ with adjusted dimensions of matrices and dot-products.

Let's start with the Pauli equation and the corresponding adjoint equation

$$\begin{aligned} i\hbar \partial_t \psi &= \frac{1}{2m} \left(-i\hbar \nabla - \frac{e}{c} \mathbf{A} \right)^2 \psi + eV\psi + \frac{|e|\hbar}{2mc} \hat{\sigma} \cdot \mathbf{B}\psi \\ -i\hbar \partial_t \bar{\psi} &= \frac{1}{2m} \left(-i\hbar \nabla + \frac{e}{c} \mathbf{A} \right)^2 \bar{\psi} + eV\bar{\psi} + \frac{|e|\hbar}{2mc} \hat{\sigma} \cdot \mathbf{B}\bar{\psi} \end{aligned}$$

Note that $\mathbf{A}, \mathbf{B}, V$ are real and that the Pauli matrices are hermitian. Multiplying the first equation with $\bar{\psi}$ from the left, the second one with ψ from the left yields:

$$\begin{aligned} i\hbar\bar{\psi}\partial_t\psi &= \frac{1}{2m}\bar{\psi}\left((-i\hbar\nabla - \frac{e}{c}\mathbf{A})^2\psi\right) + eV\bar{\psi}\psi + \frac{|e|\hbar}{2mc}\hat{\sigma}\cdot\mathbf{B}\bar{\psi}\psi \\ -i\hbar(\partial_t\bar{\psi})\psi &= \frac{1}{2m}\left((-i\hbar\nabla + \frac{e}{c}\mathbf{A})^2\bar{\psi}\right)\psi + eV\bar{\psi}\psi + \frac{|e|\hbar}{2mc}\hat{\sigma}\cdot\mathbf{B}\bar{\psi}\psi \end{aligned}$$

The parts containing the magnetic Schrödinger operator are expanded as follows:

$$\begin{aligned} \bar{\psi}\left((-i\hbar\nabla - \frac{e}{c}\mathbf{A})^2\psi\right) &= -\hbar^2\bar{\psi}\Delta\psi + \frac{i\hbar e}{c}\bar{\psi}\operatorname{div}(\mathbf{A}\psi) + \frac{i\hbar e}{c}\bar{\psi}(\mathbf{A}\cdot\nabla\psi) + \frac{e^2}{c^2}\mathbf{A}^2\bar{\psi}\psi \\ \left((-i\hbar\nabla + \frac{e}{c}\mathbf{A})^2\bar{\psi}\right)\psi &= -\hbar^2(\Delta\bar{\psi})\psi - \frac{i\hbar e}{c}\operatorname{div}(\mathbf{A}\bar{\psi})\psi - \frac{i\hbar e}{c}(\mathbf{A}\cdot\nabla\bar{\psi})\psi + \frac{e^2}{c^2}\mathbf{A}^2\bar{\psi}\psi \end{aligned}$$

Subtraction of the two equations yields:

$$\begin{aligned} i\hbar\partial_t(\bar{\psi}\psi) &= -\frac{\hbar^2}{2m}(\bar{\psi}\Delta\psi - (\Delta\bar{\psi})\psi) + \frac{i\hbar e}{2mc}(\bar{\psi}\operatorname{div}(\mathbf{A}\psi) + \operatorname{div}(\mathbf{A}\bar{\psi})\psi + \bar{\psi}(\mathbf{A}\cdot\nabla\psi) + (\mathbf{A}\cdot\nabla\bar{\psi})\psi) \\ &= -\frac{\hbar^2}{2m}\operatorname{div}((\bar{\psi}\nabla\psi)^t - (\nabla\bar{\psi})\psi) + \frac{i\hbar e}{2mc}(\bar{\psi}((\operatorname{div}\mathbf{A})\psi + \mathbf{A}\cdot\nabla\psi) + ((\operatorname{div}\mathbf{A})\bar{\psi} + \mathbf{A}\cdot\nabla\bar{\psi})\psi \\ &\quad + \bar{\psi}(\mathbf{A}\cdot\nabla\psi) + (\mathbf{A}\cdot\nabla\bar{\psi})\psi) \\ &= -\frac{\hbar^2}{2m}\operatorname{div}((\bar{\psi}\nabla\psi)^t - (\nabla\bar{\psi})\psi) + \frac{i\hbar e}{2mc}((\operatorname{div}\mathbf{A})\bar{\psi}\psi + \bar{\psi}(\mathbf{A}\cdot\nabla\psi) + (\operatorname{div}\mathbf{A})\bar{\psi}\psi \\ &\quad + (\mathbf{A}\cdot\nabla\bar{\psi})\psi + \bar{\psi}(\mathbf{A}\cdot\nabla\psi) + (\mathbf{A}\cdot\nabla\bar{\psi})\psi) \\ &= -\frac{\hbar^2}{2m}\operatorname{div}((\bar{\psi}\nabla\psi)^t - (\nabla\bar{\psi})\psi) + \frac{i\hbar e}{2mc}(2(\operatorname{div}\mathbf{A})\bar{\psi}\psi + 2\mathbf{A}\cdot\nabla(\bar{\psi}\psi)) \\ &\stackrel{(3.3)}{=} -\frac{\hbar^2}{2m}\operatorname{div}((\bar{\psi}\nabla\psi)^t - (\nabla\bar{\psi})\psi) + \frac{i\hbar e}{mc}\operatorname{div}(\mathbf{A}\bar{\psi}\psi) \end{aligned}$$

Comparing with the continuity equation (2.7) yields the current density

$$\tilde{\mathbf{J}} = -\frac{i\hbar}{2m}((\bar{\psi}\nabla\psi)^t - (\nabla\bar{\psi})\psi) - \frac{e}{mc}(\mathbf{A}\bar{\psi}\psi)$$

To include the additional magnetic moment caused by spin, a divergence-free term has to be added to complete the expression for the current density:

$$\mathbf{J} = -\frac{i\hbar}{2m}((\bar{\psi}\nabla\psi)^t - (\nabla\bar{\psi})\psi) - \frac{e}{mc}(\mathbf{A}\bar{\psi}\psi) - \frac{|e|\hbar}{2m}\operatorname{curl}(\bar{\psi}\hat{\sigma}\psi) \quad (3.4)$$

This is consistent with the *conservation of mass*, since integration with respect to \mathbf{x}

yields:

$$\begin{aligned} \partial_t \int_{\mathbb{R}^3} \bar{\psi} \psi d\mathbf{x} &= - \int_{\mathbb{R}^3} \operatorname{div} \mathbf{J} d\mathbf{x} = \frac{i\hbar}{2m} \int_{\mathbb{R}^3} \operatorname{div} (\bar{\psi} \nabla \psi - (\nabla \bar{\psi}) \psi) d\mathbf{x} + \frac{e}{mc} \int_{\mathbb{R}^3} \operatorname{div} (\mathbf{A} \bar{\psi} \psi) d\mathbf{x} + \\ &+ \frac{|e|\hbar}{2m} \int_{\mathbb{R}^3} \underbrace{\operatorname{div} (\operatorname{curl} \bar{\psi} \hat{\sigma} \psi)}_{=0} d\mathbf{x} = 0 \end{aligned}$$

3.3 From Dirac-Maxwell to Pauli-Poiswell

In this section, an application of the Pauli equation is presented. The equation arises as semi-relativistic approximation to the Dirac equation, which provides an even more exact model of charged particles in electromagnetic fields than the Pauli equation. However, the Dirac equation contains terms describing positrons which are not necessary in applications. Furthermore, a coupling to the fully relativistic Maxwell-equations for the self-consistent fields yields a very complex system - therefore approximations have to be considered.

In the following, ψ denotes the 2-spinor of the Pauli equation and Ψ is the 4-spinor used in the *Dirac equation* (including two additional components for antimatter).

Coupling the Dirac equation to the Maxwell equations for electromagnetic fields yields the *Dirac-Maxwell system*.

The Dirac equation reads:

$$i\hbar \partial_t \Psi = -i\hbar c \sum_{k=1}^3 \gamma^0 \gamma^k \partial_k \Psi + mc^2 \gamma^0 \Psi - e \sum_{k=1}^3 A_k \gamma^0 \gamma^k \Psi + eV \Psi \quad (3.5)$$

$$\Psi(\mathbf{x}, 0) = \Psi_I(\mathbf{x}) \quad (3.6)$$

As before, V denotes the electric potential of the electromagnetic field and \mathbf{A} its magnetic vector potential,

$$\gamma^0 = \begin{pmatrix} 1 & 0 & 0 & 0 \\ 0 & 1 & 0 & 0 \\ 0 & 0 & 1 & 0 \\ 0 & 0 & 0 & 1 \end{pmatrix}, \gamma^1 = \begin{pmatrix} 0 & 0 & 0 & 1 \\ 0 & 0 & 1 & 0 \\ 0 & -1 & 0 & 0 \\ -1 & 0 & 0 & 0 \end{pmatrix}, \gamma^2 = \begin{pmatrix} 0 & 0 & 0 & -i \\ 0 & 0 & i & 0 \\ 0 & i & 0 & 0 \\ -i & 0 & 0 & 0 \end{pmatrix}, \gamma^3 = \begin{pmatrix} 0 & 0 & 1 & 0 \\ 0 & 0 & 0 & -1 \\ -1 & 0 & 0 & 0 \\ 0 & 1 & 0 & 0 \end{pmatrix}$$

are the *Dirac matrices* (which are closely related to the *Pauli matrices*, see below) and

$$\partial_t = \frac{\partial}{\partial t}, \quad \partial_k = \frac{\partial}{\partial x_k} \quad (k = 1, 2, 3).$$

Note that as in (3.2), the last two terms in equation (3.5) represent the coupling of the spin to the electromagnetic field.

The densities for position and current for the Dirac equation are defined as follows:

$$n(\mathbf{x}, t) := \Psi(\mathbf{x}, t) \cdot \bar{\Psi}(\mathbf{x}, t) \quad (3.7)$$

$$J_k(\mathbf{x}, t) := \gamma^0 \gamma^k \Psi(\mathbf{x}, t) \cdot \bar{\Psi}(\mathbf{x}, t), \quad k = 1, 2, 3 \quad (3.8)$$

Note that in contrast to the Schrödinger equation and Pauli equation, the expression of the Dirac current does not contain derivatives.

The electromagnetic field is described by the Maxwell equations, cf. [G1]:

$$\nabla \cdot \mathbf{B} = 0 \quad (3.9)$$

$$\nabla \times \mathbf{E} + \frac{1}{c} \partial_t \mathbf{B} = 0 \quad (3.10)$$

$$\nabla \cdot \mathbf{E} = 4\pi n \quad (3.11)$$

$$\frac{1}{c} \partial_t \mathbf{E} - \nabla \times \mathbf{B} = -\frac{4\pi}{c} \mathbf{J} \quad (3.12)$$

Where \mathbf{E} denotes the electric field, \mathbf{B} the magnetic field. To couple the Dirac equation to the Maxwell equations it is common to introduce \mathbf{E} and \mathbf{B} with help of the potentials in the following way:

$$V = V_{int} + V_{ext} \quad (3.13)$$

$$\mathbf{A} = \mathbf{A}_{int} + \mathbf{A}_{ext} \quad (3.14)$$

$$\mathbf{B} = \nabla \times \mathbf{A}_{int} \quad (3.15)$$

$$\mathbf{E} = -\nabla V_{int} - \frac{1}{c} \partial_t \mathbf{A}_{int} \quad (3.16)$$

$$\nabla \cdot \mathbf{A}_{int} + \frac{1}{c} \partial_t V_{int} = 0 \quad (3.17)$$

The last equation represents the Lorentz gauge, V_{int} and \mathbf{A}_{int} are the self-consistent parts of the potentials (see below) and $V_{ext}, \mathbf{A}_{ext}$ the parts acting externally on the particle.

Putting (3.15)-(3.17) into (3.9)-(3.12) yields the Maxwell equations for the self-consistent parts $V_{int}, \mathbf{A}_{int}$ of the potentials:

Using this definition of the fields, equations (3.9) and (3.10) are always satisfied.

$$(3.17) \Rightarrow \begin{cases} -\frac{1}{c}\partial_t(\nabla V_{int}) = \nabla(\nabla \cdot \mathbf{A}_{int}) & * \\ -\frac{1}{c^2}\partial_{tt}^2 V_{int} = \frac{1}{c}\partial_t(\nabla \cdot \mathbf{A}_{int}) & ** \end{cases}$$

Now

$$(3.11) \Rightarrow \nabla \cdot \left(-\nabla V_{int} - \frac{1}{c}\partial_t \mathbf{A}_{int} \right) = 4\pi n \\ \Rightarrow -\Delta V_{int} - \frac{1}{c}\partial_t(\nabla \cdot \mathbf{A}_{int}) = 4\pi n$$

$$\stackrel{**}{\Rightarrow} -\frac{1}{c^2}\partial_{tt}^2 V_{int} + \Delta V_{int} = -4\pi n \quad (3.18)$$

$$(3.12) \Rightarrow \frac{1}{c}\partial_t \left(-\nabla V_{int} - \frac{1}{c}\partial_t \mathbf{A}_{int} \right) - \nabla \times (\nabla \times \mathbf{A}_{int}) = -\frac{4\pi}{c}\mathbf{J} \\ \Rightarrow -\frac{1}{c}\partial_t(\nabla V_{int}) - \frac{1}{c^2}\partial_{tt}^2 \mathbf{A}_{int} - \nabla(\nabla \cdot \mathbf{A}_{int}) + \Delta \mathbf{A}_{int} = -\frac{4\pi}{c}\mathbf{J}$$

$$\stackrel{*}{\Rightarrow} -\frac{1}{c^2}\partial_{tt}^2 \mathbf{A}_{int} + \Delta \mathbf{A}_{int} = -\frac{4\pi}{c}\mathbf{J} \quad (3.19)$$

Equations (3.5),(3.18) and (3.19) form the Dirac-Maxwell system. It is a *self-consistent* model, i.e. it takes the effects caused by the additional electromagnetic field induced by the movement of the electron on the particle itself into account. This fact is modelled by the coupling of position and current density to the potentials in (3.18) and (3.19).

The Dirac-Maxwell system is hard to handle analytically as well as numerically (up to date there is no proof of global well-posedness) - confer [M] or [MM]. Therefore, one searches an approximation to a self-consistent system which is easier to solve but preserves the main properties of interest - i.e. self-consistency, the relativistic effects and, in particular, spin-magnetic field coupling. This is the goal of this section.

3.3.1 Scaling of equations

Before continuing the quest for a suitable approximation, a brief interlude about scaling of equations is needed:

Considering a differential equation used as a model for a physical process, it is clear that

the (fine-) structure of the equation and its solutions depend on the unit system for which the model was developed.

E.g. for a system depending on space and time, there is a big difference if time is measured in nanoseconds or hours. Here 'measuring' means comparison with units.

To get rid of this dependency on units, it is desirable to write the model equation in a more general - dimensionless - form. In this context, 'dimension' means a qualitative description of a measurable physical quantity. To every dimension there is a corresponding unit in a unit system. In the example above, nanoseconds and hours are units of dimension time.

There are seven fundamental dimensions, from which all other dimensions are derived: M (mass), L (length), T (time), Θ (temperature), E (electric current), I (intensity of light) and A (amount of a substance).

Nondimensionalization is the process of rescaling equations to render them dimensionless. It can be interpreted as a switch to proportions instead of measurements against units. This is done by dividing dimensionful parameters and variables by appropriate reference values - this usually leads to equations of easier structure.

Note that this process is not unique! Different choices of reference values yield different dimensionless problems.

In the Dirac-Maxwell system one can choose to nondimensionalize the two main physical constants $\frac{1}{c}$ (which is of dimension $\frac{T}{L}$) and \hbar (with dimension $\frac{ML^2}{T}$).

The corresponding dimensionless parameters are

$$\varepsilon := \frac{x^*}{t^*c} = \frac{v^*}{c} \tag{3.20}$$

$$h := \frac{\hbar}{m(v^*)^2t^*} \tag{3.21}$$

for a reference length x^* , time t^* and velocity $v^* := \frac{x^*}{t^*}$ that remain to be specified.

To rescale the system (3.5),(3.18),(3.19), define the following scaled quantities (the '*'-sign denotes a reference value for the corresponding parameter or variable):

$$\begin{aligned}
 \mathbf{y} &= (y_1, y_2, y_3)^t := x^*(x_1, x_2, x_3)^t = x^* \mathbf{x} \\
 \tau &:= t^* t \\
 \Phi(\mathbf{y}, \tau) &:= \psi^* \Psi \left(\frac{\mathbf{y}}{x^*}, \frac{\tau}{t} \right) = \psi^* \Psi(\mathbf{x}, t) \\
 \tilde{A}(\mathbf{y}, \tau) &:= A^* \mathbf{A}(\mathbf{x}, t) = A^* \mathbf{A}_{int}(\mathbf{x}, t) + A^* \mathbf{A}_{ext}(\mathbf{x}, t) \\
 \tilde{V}(\mathbf{y}, \tau) &:= A^* V(\mathbf{x}, t) = A^* V_{int}(\mathbf{x}, t) + A^* V_{ext}(\mathbf{x}, t) \\
 \tilde{n}(\mathbf{y}, \tau) &:= \Phi(\mathbf{y}, \tau) \cdot \bar{\Phi}(\mathbf{y}, \tau) \\
 \tilde{J}_k(\mathbf{y}, \tau) &:= \gamma^0 \gamma^k \Phi(\mathbf{y}, \tau) \cdot \bar{\Phi}(\mathbf{y}, \tau), \quad k = 1, 2, 3
 \end{aligned}$$

Thus, using the chain rule:

$$\begin{aligned}
 \frac{\partial \Phi}{\partial \tau} &= \psi^* \frac{\partial \Psi}{\partial t} \frac{\partial t}{\partial \tau} = \frac{\psi^*}{t^*} \frac{\partial \Psi}{\partial t} \\
 \partial_k \Phi &= \frac{\psi^*}{x^*} \partial_k \Psi, \quad k = 1, 2, 3 \\
 \nabla \Phi &= \frac{\psi^*}{x^*} \nabla \Psi \\
 \nabla \cdot \Phi &= \frac{\psi^*}{x^*} \nabla \cdot \Psi \\
 \Delta \Phi &= \frac{\psi^*}{(x^*)^2} \Delta \Psi \\
 \tilde{\mathbf{J}} &= |\psi^*|^2 \mathbf{J} \\
 \tilde{n} &= |\psi^*|^2 n
 \end{aligned}$$

Now, putting this into the Dirac equation:

$$\begin{aligned}
 i\hbar \frac{t^*}{\psi^*} \frac{\partial \Phi}{\partial \tau} &= i\hbar \frac{\partial \Psi}{\partial t} = -i\hbar c \sum_{k=1}^3 \gamma^0 \gamma^k \partial_k \Psi + mc^2 \gamma^0 \Psi - e \sum_{k=1}^3 A_k \gamma^0 \gamma^k \Psi + eV \Psi \\
 &= -i\hbar c \frac{x^*}{\psi^*} \sum_{k=1}^3 \gamma^0 \gamma^k \partial_k \Phi + \frac{mc^2}{\psi^*} \gamma^0 \Phi - \frac{e}{A^* \psi^*} \sum_{k=1}^3 \tilde{A}_k \gamma^0 \gamma^k \Phi + \frac{e}{A^* \psi^*} \tilde{V} \Phi
 \end{aligned}$$

Equivalently:

$$i\hbar t^* \frac{\partial \Phi}{\partial \tau} = -i\hbar c x^* \sum_{k=1}^3 \gamma^0 \gamma^k \partial_k \Phi + mc^2 \gamma^0 \Phi - \frac{e}{A^*} \sum_{k=1}^3 \tilde{A}_k \gamma^0 \gamma^k \Phi + \frac{e}{A^*} \tilde{V} \Phi$$

Now, using definition (3.20) and (3.21):

$$\begin{aligned}\hbar t^* &= m(x^*)^2 h \\ \hbar c x^* &= \frac{(x^*)^2}{\varepsilon t^*} \hbar = \frac{(x^*)^4 m h}{\varepsilon (t^*)^2} = m(x^*)^2 \frac{(x^*)^2 \hbar}{\varepsilon (t^*)^2} \\ m c^2 &= m(x^*)^2 \frac{1}{\varepsilon^2 (t^*)^2}\end{aligned}$$

and

$$i m(x^*)^2 h \frac{\partial \Phi}{\partial \tau} = -i m(x^*)^2 \frac{(x^*)^2 \hbar}{\varepsilon (t^*)^2} \sum_{k=1}^3 \gamma^0 \gamma^k \partial_k \Phi + m(x^*)^2 \frac{\gamma^0}{\varepsilon^2 (t^*)^2} \Phi - \frac{e}{A^*} \sum_{k=1}^3 \tilde{A}_k \gamma^0 \gamma^k \Phi + \frac{e}{A^*} \tilde{V} \Phi$$

After dividing by $m(x^*)^2$ and choosing $x^* = t^* = 1$, $A^* = \frac{e}{m}$ ($\Rightarrow \varepsilon = \frac{1}{c}$, $h = \frac{\hbar}{m}$):

$$i h \frac{\partial \Phi}{\partial \tau} = -\frac{i \hbar}{\varepsilon} \sum_{k=1}^3 \gamma^0 \gamma^k \partial_k \Phi + \frac{1}{\varepsilon^2} \gamma^0 \Phi - \sum_{k=1}^3 \tilde{A}_k \gamma^0 \gamma^k \Phi - \tilde{V} \Phi \quad (3.22)$$

$$\Phi(\mathbf{y}, 0) = \Phi_I(\mathbf{y}) \quad (3.23)$$

With properly rescaled initial value $\Phi_I(\mathbf{y})$.

Next, adjust equation (3.18):

$$\begin{aligned}-\frac{1}{c^2} \partial_{tt}^2 V_{int} + \Delta V_{int} &= -4\pi n \\ -\frac{(t^*)^2}{c^2 A^*} \frac{\partial^2}{\partial \tau^2} \tilde{V}_{int} + \frac{(x^*)^2}{A^*} \Delta \tilde{V}_{int} &= -\frac{4\pi}{|\psi^*|^2} \tilde{n} \\ -\frac{m}{c^2 e} \frac{\partial^2}{\partial \tau^2} \tilde{V}_{int} + \frac{m}{e} \Delta \tilde{V}_{int} &= -\frac{4\pi}{|\psi^*|^2} \tilde{n}\end{aligned}$$

Choosing $\psi^* = \sqrt{\frac{4\pi e}{m}}$ this is equivalent to

$$\Delta \tilde{V}_{int} - \varepsilon^2 \frac{\partial^2}{\partial \tau^2} \tilde{V}_{int} = -\tilde{n} \quad (3.24)$$

Analogously, in the this new scaling equation (3.19) reads:

$$\Delta \tilde{A}_{int} - \varepsilon^2 \frac{\partial^2}{\partial \tau^2} \tilde{A}_{int} = -\varepsilon \tilde{\mathbf{J}} \quad (3.25)$$

3.3.2 'Perturbation theory'

Back to the search for approximations to the Dirac-Maxwell system: An approximation to an equation is another equation - preferably of simpler structure - whose solutions approximate the solutions of the original one (in a sense to be specified).

Considering the Dirac-Maxwell system in the new scaling - equations (3.22), (3.24) and (3.25) - possible approximations are the equations resulting from the formal 'limit' $\varepsilon \rightarrow 0$ or $\varepsilon^2 \rightarrow 0$. But it is not clear if these are actual approximations and how this limit is defined. For a rigorous treatment, basic facts from perturbation theory are necessary - therefore a short introduction to this field is given - further information and references can be found in [H].

As a general rule, formal limits of equations yield approximations if the limiting process does not change the order of the equation.

Definition 3. Let $(B, \|\cdot\|)$ be a Banach space and $u \in B$. The formal series

$$\sum_{k=0}^{\infty} u_k \varepsilon^k$$

is called *asymptotic expansion* of u with respect to ε if

$$\left\| u - \sum_{k=0}^n u_k \varepsilon^k \right\| = o(\varepsilon^n), \quad \text{for all } n \geq 0$$

If this is satisfied only for $n \leq N$, the expansion is called *asymptotic expansion of order N* .

Remark 4. It is customary to write

$$u = v + o(f(\varepsilon))$$

instead of

$$\|u - v\| = o(f(\varepsilon))$$

And similar for all other 'O-notations'.

To deal with differential equations in this context, let $(B_1, \|\cdot\|_1), (B_2, \|\cdot\|_2)$ be Banach spaces and consider the family of operators $\{T_\varepsilon \mid \varepsilon \in [0, a)\}$, satisfying

$$T_\varepsilon : B_1 \rightarrow B_2$$

Thus (following the ideas above), if one searches approximations to the differential equation

$$T_\varepsilon u_\varepsilon = 0$$

the question is whether solutions u_0 of the so called *reduced problem*

$$T_0 u_0 = 0$$

approximate solutions of the original problem, i.e. if:

$$\lim_{\varepsilon \rightarrow 0} u_\varepsilon = u_0 \text{ in } \|\cdot\|_1$$

There are several criteria guaranteeing this convergence, but they are not trivial - cf. [H].

To improve the approximation u_0 , one can try to expand $T_\varepsilon u$ asymptotically for fixed $u \in B_1$ which yields an expansion of the form

$$T_\varepsilon u = \sum_{k=0}^N T_k u \varepsilon^k + O(\varepsilon^N)$$

and

$$\sum_{k=0}^N T_k u \varepsilon^k = 0$$

is an approximation to the original equation. $\sum_{k=0}^N T_k u \varepsilon^k$ is called *correction of order N*.

In the scaling used above, the linear Pauli equation reads

$$ih\partial_t \psi = \frac{1}{2} (ih\nabla + \varepsilon \mathbf{A})^2 \psi - V\psi - \frac{\varepsilon h}{2} \sum_{k=1}^3 \sigma^k \text{curl}_k(\mathbf{A})\psi$$

One can show ([M],[MM]) that it is an $O(\varepsilon)$ approximation for the electron component of the Dirac equation. It is sufficient to consider this component, as the positron component is not important in most applications. The transition from Dirac equation to Pauli equation is quite involved and not part of this thesis. For further information, confer the list of references at the end of this section.

For the self-consistent coupling one could use the Maxwell equations again, but to preserve order one switches to first order corrections. These can be found by a formal asymptotic expansion of the electromagnetic fields and the corresponding potentials. Combining, this

leads to the so called *Pauli-Poiswell system*

$$ih\partial_t\psi = \frac{1}{2}(ih\nabla + \varepsilon\mathbf{A})^2\psi - V\psi - \frac{\varepsilon h}{2}\sum_{k=1}^3\sigma^k\text{curl}_k(\mathbf{A})\psi \quad (3.26)$$

$$\psi(\mathbf{x}, 0) = \psi_I(\mathbf{x}) \quad (3.27)$$

$$n(\mathbf{x}, t) = |\psi_1(\mathbf{x}, t)|^2 + |\psi_2(\mathbf{x}, t)|^2 \quad (3.28)$$

$$J_k(\mathbf{x}, t) = \text{Im}(\bar{\psi}(h\partial_k + i\varepsilon A_k)\psi) + \text{curl}_k(\bar{\psi} \cdot \vec{\sigma}\psi), \quad k = 1, 2, 3 \quad (3.29)$$

$$V = V_{int} + V_{ext} \quad (3.30)$$

$$\mathbf{A} = \mathbf{A}_{int} + \mathbf{A}_{ext} \quad (3.31)$$

$$\Delta V_{int} = -n \quad (3.32)$$

$$\Delta \mathbf{A}_{int} = -\varepsilon \mathbf{J} \quad (3.33)$$

for the electron component. In equation (3.29), the Dirac current was replaced by the Pauli current; here $\{\sigma_x, \sigma_y, \sigma_z\} = \{\sigma_1, \sigma_2, \sigma_3\}$.

The structure of this system is considerably less complex. The transition from Dirac-Maxwell to Pauli-Poiswell simplifies the spinor and the (hyperbolic) wave equations for the fields are replaced by (elliptic) Poisson equations.

Remark 5. • The described transition from Dirac-Maxwell system to Pauli-Poiswell system is only a formal motivation since e.g. the Maxwell equations depend singularly on ε . The coupling of the Pauli equation to the two Poisson equations (3.32) and (3.33) is rather heuristic. Anyway, this model catches the main properties of the solutions as shown in simulations (see chapter 5).

- This model can be used analogously in two space dimensions. Assume the electron moves only in the x_2x_3 -plane, then the magnetic vector potential reads as follows:

$$\mathbf{A}(x_1, x_2, x_3, t) = \begin{pmatrix} 0 \\ A_2(x_2, x_3, t) \\ A_3(x_2, x_3, t) \end{pmatrix}$$

Thus, the curl in equation (3.26) becomes

$$\nabla \times \mathbf{A}(x_1, x_2, x_3, t) = \begin{pmatrix} \partial_2 A_3(x_2, x_3, t) - \partial_3 A_2(x_2, x_3, t) \\ 0 \\ 0 \end{pmatrix}$$

- In (3.29), the last term involving the curl can be dropped in calculations. As mentioned in section 3.2 it represents the (minor) influence of spin on the particle current density.

Relativistic Corrections of Second Order

For the sake of completeness a short remark on approximations of the Dirac equation up to order two in ε . This equation reads

$$i\partial_t\psi = (i\hbar\nabla + \varepsilon\mathbf{A})^2\psi - V\psi - \frac{\varepsilon}{2}\sum_{k=1}^3\sigma^k\text{curl}_k(\mathbf{A})\psi + \\ + \frac{\varepsilon^2}{8}\partial_x^4\psi + \frac{\varepsilon^2}{4}\Delta(V\psi) - \frac{i\varepsilon^2}{2}\sum_{k=1}^3\sigma^k E_k\psi - \frac{\varepsilon^2}{4}\mathbf{E}\cdot\nabla\psi$$

The most interesting $O(\varepsilon^2)$ -term is $\frac{\varepsilon^2}{4}\Delta(V\psi)$. It corresponds to the so called *Darwin term* which is related to the *zitterbewegung*. The *zitterbewegung* (German for 'trembling motion') is an effect following from the Dirac equation for relativistic electrons which describes high frequency oscillations of the particles near their position expectation. Cf. [M] for further details.

Further References

The aim of this section is to enrich the list of references, which were already mentioned earlier in this chapter.

- [BM] and [M1] are the only works concerning the derivation of the linear Pauli equation in the time-dependent case.
- [BM1] and [BM2] are the only rigorous results on the derivation of nonlinear time-dependent Pauli and Schrödinger equations starting from the Dirac equation or the Klein-Gordon equation (which is more or less the 'squared Dirac equation').
- In [MS], the nonrelativistic limit is combined with the classical limit. The result and the methods apply to the limit from the Pauli-Poiswell system to the Vlasov-Poisson system as well.
- In [SC], an alternative approach to derive the Pauli equation as approximation to the Dirac equation is presented.

3.4 Analytical results

In this section, some partial results concerning the existence of solutions of the time-dependent Pauli equation and the Schrödinger-Maxwell system (which has the same analytical properties as Pauli-Maxwell) are presented. For nonlinear PDEs in general, only special results can be achieved. Especially for rigorous analysis of time-dependent problems results are rare, but as they are of growing importance, this should change in near future.

We did not tackle the open problem of proving global existence (in time) of unique solutions for the Pauli-Poiswell system in this thesis

3.4.1 Results for the time-dependent Pauli equation

The following result is for a time-dependent magnetic Schrödinger equation in three spacial dimensions, but it should hold for the Pauli equation too, as the coupling term $\hat{\sigma} \cdot \mathbf{B}$ does not change the analytic properties too much. It is taken from the book of Cycon, Froese, Kirsch and Simon ([CF]), who extend a result of Tip ([T1]) to this special case. At first, a definition is needed:

Definition 6. Let $(B_1, \|\cdot\|_1), (B_2, \|\cdot\|_2)$ be Banach spaces and T_1, T_2 be operators with

$$T_i : D(T_i) \subseteq B_1 \rightarrow B_2$$

Then T_1 is called T_2 – bounded or *relatively bounded with respect to T_2* , if

$$D(T_2) \subseteq D(T_1)$$

and if there are constants $a, b \geq 0$ such that

$$\|T_1 u\|_2 \leq a \|T_2 u\|_2 + b \|u\|_2$$

for all $u \in D(T_2)$. The infimum of all a for which a b exists such that this equation holds is called the T_2 – bound of T_1 .

Now, if $H(t)$ is defined as the closure of $(\hat{\mathbf{p}} - \mathbf{A}(t))^2 + V$ on $S(\mathbb{R}^3)$, $\mathbf{A}(t) := (A \cos(\omega t), A \sin(\omega t), 0)^t$ with positive frequency $\omega > 0$, $A > 0$ and the electric potential V is assumed to be rotationally invariant, time independent and relatively bounded with respect to the Laplace operator $-\Delta$ on $L^2(\mathbb{R}^3)$ with relative bound smaller than 1. Furthermore, V has to be essentially bounded outside a ball.

Then the two-parameter unitary propagator

$$U(t, s) := e^{-i\omega L_z t} e^{-i(t-s)H} e^{i\omega L_z s}$$

solves the operator equation

$$\begin{aligned} i\frac{\partial}{\partial t}U(t, s) &= H(t)U(t, s) \\ U(0, 0) &= 1 \end{aligned}$$

where $H = (\hat{\mathbf{p}} - a)^2 + V - \omega L_z$, $a = (A, 0, 0)^t$ and $L_z = -i\hbar(x\partial_y - y\partial_x)$ is the angular momentum operator with respect to the z-axis.

Consequently, following [T1],

$$U(t) := U(t, 0) = e^{-i\omega L_z t} e^{-i(t-s)H}$$

is a solution operator for the magnetic Schrödinger equation

$$i\frac{\partial}{\partial t}\psi = H(t)\psi$$

on $D(H(t)) = H^{2,2}(\mathbb{R}^3)$. This means that for every initial value $u_0 \in D(H(t))$ $U(t)u_0$ is a solution of this equation.

In [BB], Bouguerra, Bounames, Maamache and Saadi calculate an exact expression for the wavefunction ψ of the Pauli equation in two spacial dimensions with harmonic oscillator potential $V(r, t) = \frac{1}{2}m(t)\omega^2(t)r^2$ in presence of the *Aharonov-Bohm effect*, i.e. a kind of nonlocal interaction of a nonrelativistic spin- $\frac{1}{2}$ -particle with the magnetic vector potential. The resulting spinor is given in polar coordinates via:

$$\begin{pmatrix} \psi_1(r, \varphi, t) \\ \psi_2(r, \varphi, t) \end{pmatrix} = \sum_{m,n} \frac{a_{m,n}}{\rho} e^{i\frac{M\hat{p}}{2\hbar\rho}r^2 + i\alpha_{m,n}} \begin{pmatrix} \chi_{m,n}^1(r, \varphi, t, \nu) \\ \chi_{m,n}^2(r, \varphi, t, \nu) \end{pmatrix}$$

where $a_{m,n}$ are constants, ν is a flux parameter and the functions $\rho, \alpha_{m,n}, \chi^1, \chi^2$ are determined via auxiliary differential equations.

In [YA] Yamasaki mentions so called WKB-solutions for the nonrelativistic Pauli equation. These solutions are calculated via approximation by an asymptotic expansion in \hbar .

A stochastic approach is taken in [AJ] to determine the spinor of a nonrelativistic spin- $\frac{1}{2}$ -particle. Here, solving the Pauli equation amounts to solving an equivalent system of four stochastic differential equations.

Works on the stationary Pauli equation include the extensive treatment of Erdős and Solovej, e.g. [ES], [ES1] or [E].

3.4.2 Results for the time-dependent Schrödinger-Maxwell system

Now some results for coupled Schrödinger-Maxwell systems are presented. In many cases, the standing wave ansatz

$$\psi(\mathbf{x}, t) = u(\mathbf{x})e^{i\omega t}$$

is chosen. It yields a stationary Schrödinger equation for the amplitude $u(\mathbf{x})$. To render the Maxwell equations stationary, the *electrostatic case* $\mathbf{A} = 0$ and $\partial_t V = 0$ is considered. This leads to a (time-independent) system of the form

$$\begin{aligned} -c_1\Delta u + c_2Vu + c_3\Phi u - c_4|u|^{p-s}u - c_5g &= 0 \\ -c_6\Delta\Phi - c_7u^2 &= 0 \end{aligned}$$

with constants c_i (possibly partly equal to 0) and varying $s \in \mathbb{N}$ - depending on the paper.

There are many results on systems of this form, e.g. Candela and Salvatore show in [CS] that such a system, restricted to a ball B with zero boundary values, has infinitely many radially symmetric solutions $(u_n, \Phi_n) \in H_0^{2,1}(B) \times H_0^{2,1}(B)$ for $p = 5$, $g(\mathbf{x}) = g(|\mathbf{x}|) \in L^2(B)$ satisfying

$$\int_B |u_n| d\mathbf{x} \rightarrow \infty \text{ for } n \rightarrow \infty$$

Other works using this approach are for example [AP], where the whole-space case is treated and the recent results of Azzollini, d'Avenia and Pomponio [AA], where more general nonlinearities are considered.

Chapter 4

Numerical methods

In this chapter an overview of the numerical methods used to solve the Pauli-Poiswell system in two dimensions is given. As mentioned before (in remark 5), the magnetic field $\mathbf{B} = \text{curl}\mathbf{A}$ acts perpendicularly on the xy -plane (if interpreted as projection of the x_2x_3 -plane in \mathbb{R}^3) in this case.

The numerical methods of interest are: Finite difference schemes, relaxation iteration and pseudospectral derivatives. The nonlinear coupling occurring in the Pauli-Poiswell system makes a rigorous convergence analysis of the numerical schemes very difficult. Therefore only results for the linear case are presented at this point. For rigorous analysis of a numerical method for a nonlinear Schrödinger-Poisson coupling, confer for example [L], where an operator splitting method is used.

For this, the domain is restricted to a square $Q := [a, b] \times [a, b] \subseteq \mathbb{R}^2$ in space and periodic boundary conditions are assumed.

Moreover, Q is discretized in the following way:

In x -direction, the N points

$$x_0 = a < x_1 < \dots < x_{N-1}$$

are defined as

$$x_j := a + j \frac{b-a}{N}, \quad j = 0, \dots, N-1$$

such that $[a, b]$ is divided into N subintervals of length $\Delta x := \frac{b-a}{N}$. In y -direction, y_0, \dots, y_{N-1} are given analogously.

This results into a grid of points (x_j, y_k) , $j, k \in \{0, \dots, N-1\}$ covering Q . Additionally, time is discretized into $t_0 = 0, t_1, t_2, \dots$ after choosing a *timestep* Δt .

For any function

$$f : Q \times \mathbb{R}_0^+ \rightarrow \mathbb{C}$$

an approximation to f (calculated by a numerical algorithm) in (x_j, y_k) at time t_n is denoted by $f_{j,k}^n$.

4.1 Fourier-pseudospectral derivative

The basic idea of this method of numerical differentiation is to consider the derivative of an interpolating polynomial of a function f an approximation to f' .

4.1.1 Trigonometric interpolation

Since periodic functions are to be interpolated (periodic boundary conditions are used), the appropriate interpolation method is trigonometric interpolation, which will be introduced in this section. First the one-dimensional case is considered, which can be generalized to multidimensional problems.

1D Trigonometric interpolation

For simplicity, assume $f : I \subseteq \mathbb{R} \rightarrow \mathbb{C}$ is periodic with period 2π (other periods can be reduced to this case via variable transformations - see below). Due to periodicity one can restrict considerations to the interval $[0, 2\pi]$. As before, let

$$x_j := \frac{2\pi j}{N}, j = 0, \dots, N-1$$

be a discretization of $[0, 2\pi]$ and $(f_j)_{j=0}^{N-1}$ the corresponding function values of f in the nodes.

Since $\cos(jx), \sin(jx)$ both have period 2π , it is straight forward to try to interpolate f by a linear combination of these trigonometric functions. Thus, one searches a polynomial

$$q_N(f)(x) = \frac{a_0}{2} + \sum_{l=0}^M (a_l \cos(lx) + b_l \sin(lx)) + \frac{a_{(M+1)}}{2} \cos((M+1)x) \delta_{(N \bmod 2), 0}$$

with $q_N(f)(x_j) = f_j$ (where $N = 2M + 1$ and $\delta_{m,n}$ is the Kronecker-delta - the last term vanishes if N is even).

Setting $a_m = c_m$ and $b_m = ic_m$, this can be transformed to

$$p_N(f)(x) := \sum_{l=0}^{N-1} c_l e^{ilx}$$

$$p_N(f)(x_j) = f_j, \quad j = 0, \dots, N-1$$

and with $z := e^{ix}$, $\omega_j = e^{ix_j} = e^{i\frac{2\pi j}{N}}$ one arrives at

$$\tilde{p}_N(f)(z) = \sum_{l=0}^{N-1} c_l z^l$$

$$\tilde{p}_N(f)(\omega_j) = f_j, \quad j = 0, \dots, N-1 \quad (4.1)$$

The polynomial $\tilde{p}_N(f)$ (and therefore $p_N(f)$ and $q_N(f)$) exists and is unique (because of the uniqueness of interpolating polynomials in general (cf. [S])).

To calculate the coefficients $(c_m)_m$, consider

$$\begin{aligned} \omega_l^j \omega_l^k &= e^{i\frac{2\pi l(j+k)}{N}} = \omega_l^{j+k} \\ \omega_l^{-k} &= e^{-i\frac{2\pi lk}{N}} = \overline{\omega_l^k} \end{aligned}$$

to conclude:

Lemma 7. $v^{(m)} := (\omega_0^m, \omega_1^m, \dots, \omega_{N-1}^m)$, $m = 0, \dots, N-1$ is an orthonormal basis of \mathbb{C}^N with respect to the weighted standard inner product

$$\langle x, y \rangle_{\mathbb{C}^N} := \frac{1}{N} \sum_{l=0}^{N-1} x_l \overline{y_l}$$

Proof: Choose $m, n \in \{0, 1, \dots, N-1\}$, then

$$\langle v^{(m)}, v^{(n)} \rangle = \sum_{l=0}^{N-1} \omega_l^m \overline{\omega_l^n} = \sum_{l=0}^{N-1} \omega_l^{m-n} = N\delta_{m,n}$$

The case $m = n$ is clear, for $m - n = k \neq 0$:

$$\sum_{l=0}^{N-1} \omega_l^k = \sum_{l=0}^{N-1} \left(e^{\frac{2\pi ik}{N}} \right)^l = \frac{1 - e^{2\pi ik}}{1 - e^{\frac{2\pi ik}{N}}} = 0$$

□

Setting $f_v = (f_0, \dots, f_{N-1}) \in \mathbb{C}^N$, one can see that the coefficients $(c_m)_m$ have to satisfy

(compare equation (4.1)):

$$f_v = \sum_{l=0}^{N-1} c_l v^{(l)}$$

$$\Rightarrow c_m = \langle f_v, v^{(m)} \rangle_{\mathbb{C}^N} = \frac{1}{N} \sum_{l=0}^{N-1} f_l \omega_l^{-m}, l = 0, \dots, N-1 \quad (4.2)$$

Definition 8. • The linear and invertible map

$$\mathcal{F}_N : \mathbb{C}^N \rightarrow \mathbb{C}^N$$

$$(f_j)_j \rightarrow (c_m)_m$$

which maps the sampling points of a function f to the coefficients of the interpolating trigonometric polynomial corresponding to the described calculation is called *discrete Fourier transform* (DFT). Usually, c_m is denoted by \hat{f}_m .

The DFT's computational cost is $O(N^2)$ operations, but using the special structure of the sums (4.2), one can reduce this to $O(N \log_2 N)$ for $N = 2^m$ - these algorithms are called *fast Fourier transforms* (FFTs).

- The inverse map \mathcal{F}_N^{-1} is called *Fouriersynthesis*. $\mathcal{F}_N^{-1}((c_m)_m)$ corresponds to the evaluation of the trigonometric polynomial with coefficients $(c_m)_m$ in the nodes $(x_j)_j$. \mathcal{F}_N^{-1} is given by

$$f_j = \sum_{l=0}^{N-1} c_l \omega_l^j, j = 0, \dots, N-1$$

Remark 9. • The derivative of $p_N(f)(x)$ is given by

$$p'_N(f)(x) = \sum_{l=0}^{N-1} il c_l e^{ilx}$$

Therefore, differentiation in x is equal to a multiplication of the coefficients by constants:

$$(c_m)_m \mapsto (im \cdot c_m)_m$$

- In general

$$p'_N(f) \neq p_N(f')$$

This is only true for $f \in \text{span} \{e^{ilx} \mid l = 0, \dots, N-1\}$.

- Let $v \in \mathbb{C}^N$, then $\mathcal{F}_N(v)$ and $\mathcal{F}_N^{-1}(v)$ can be expressed with help of the $N \times N$ Vandermonde matrices

$$F_N := \frac{1}{N} \left(\omega_{k-1}^{1-j} \right)_{j,k=1}^N$$

$$F_N^{-1} := \left(\omega_{k-1}^{j-1} \right)_{j,k=1}^N$$

via

$$\mathcal{F}_N(v) = F_N \cdot v, \quad \mathcal{F}_N^{-1}(v) = F_N^{-1} \cdot v$$

Now assume $f : [a, b] \rightarrow \mathbb{C}$ is a function defined on an arbitrary real interval. In this case one can use the variable transformation

$$x \mapsto \frac{(x-a)2\pi}{b-a}$$

to reduce the problem to the interval $[0, 2\pi]$. The interpolating polynomial for N nodes becomes

$$p(x) = \sum_{l=0}^{N-1} \hat{f}_l e^{il \frac{(x-a)2\pi}{b-a}}$$

and differentiation in Fourier space changes to

$$(\hat{f}_m)_m \mapsto \left(im \frac{(x_m - a)2\pi}{b-a} \hat{f}_m \right)_m$$

2D Trigonometric interpolation

The two dimensional case can be treated in an analogous way by introducing the following inner product:

Definition 10. Let $X, Y \in \mathbb{C}^{N \times N}$, $X = (x_{i,j})_{i,j}$, $Y = (y_{i,j})_{i,j}$. Define:

$$\langle X, Y \rangle_{\times} := \frac{1}{N^2} \sum_{l_1=0}^{N-1} \sum_{l_2=0}^{N-1} x_{l_1, l_2} \bar{y}_{l_1, l_2}$$

This is clearly an inner product on $\mathbb{C}^{N \times N}$ since it corresponds to the weighted standard inner product on \mathbb{C}^{N^2} .

Lemma 11. Let $(v^{(m)})_{m=0}^{N-1}$, $(w^{(n)})_{n=0}^{N-1}$ be orthonormal bases of \mathbb{C}^N with respect to the weighted standard inner product and

$$V^{(m,n)} := (v_i^{(m)} \cdot w_j^{(n)})_{i,j=0}^{N-1} \in \mathbb{C}^{N \times N}$$

Then $(V^{(m,n)})_{m,n=0}^{N-1}$ is an orthonormal basis of $\mathbb{C}^{N \times N}$ with respect to $\langle \cdot, \cdot \rangle_{\times}$.

Proof: Choose $m, n, m', n' \in \{0, 1, \dots, N-1\}$, then

$$\begin{aligned}
 \langle V^{(m,n)}, V^{(m',n')} \rangle_{\times} &= \frac{1}{N^2} \sum_{l_1=0}^{N-1} \sum_{l_2=0}^{N-1} V_{l_1, l_2}^{(m,n)} \overline{V_{l_1, l_2}^{(m',n')}} \\
 &= \frac{1}{N^2} \sum_{l_1=0}^{N-1} \sum_{l_2=0}^{N-1} v_{l_1}^{(m)} w_{l_2}^{(n)} \overline{v_{l_1}^{(m')}} \overline{w_{l_2}^{(n')}} \\
 &= \frac{1}{N} \sum_{l_1=0}^{N-1} v_{l_1}^{(m)} \overline{v_{l_1}^{(m')}} \cdot \frac{1}{N} \sum_{l_2=0}^{N-1} w_{l_2}^{(n)} \overline{w_{l_2}^{(n')}} \\
 &= \langle v^{(m)}, v^{(m')} \rangle_{\mathbb{C}^N} \cdot \langle w^{(n)}, w^{(n')} \rangle_{\mathbb{C}^N} \\
 &= \delta_{m,m'} \cdot \delta_{n,n'} = \delta_{(m,n), (m',n')}
 \end{aligned}$$

Here $\delta_{(m,n), (m',n')}$ is equal to 1 if both $m = m'$ and $n = n'$ hold, else it is equal to 0. □

Now let $f : \Omega := [0, 2\pi] \times [0, 2\pi] \rightarrow \mathbb{C}$ and $(x_j, y_k) := \left(\frac{2\pi j}{N}, \frac{2\pi k}{N}\right)$, $j, k = 0, \dots, N-1$ be a discretization of Ω as before. The function values of f in these nodes are denoted by $f_{j,k}$.

Following analogous arguments as in the 1D-case, one searches an interpolating polynomial

$$p_N(f)(x, y) = \sum_{l_1, l_2=0}^{N-1} c_{l_1, l_2} e^{il_1 x} e^{il_2 y} = \sum_{l_1, l_2=0}^{N-1} c_{l_1, l_2} \underbrace{e^{i(l_1 x + l_2 y)}}_{=: c^{l_1, l_2}(x, y)}$$

with

$$p_N(f)(x_j, y_k) = f_{j,k}, \quad j, k = 0, \dots, N-1$$

Setting $z = e^{ix}$, $s = e^{iy}$, $\omega_j = e^{ix_j}$, $\eta_k = e^{iy_k}$ this transforms to

$$\tilde{p}_N(f)(z, s) = \sum_{l_1, l_2=0}^{N-1} c_{l_1, l_2} z^{l_1} s^{l_2}$$

$$\tilde{p}_N(f)(\omega_j, \eta_k) = f_{j,k}, \quad j, k = 0, \dots, N-1$$

As in the 1D-case, existence and uniqueness of these polynomials is guaranteed.

Now for $f_V := (f_{i,j})_{i,j} \in \mathbb{C}^{N \times N}$ and the orthonormal basis $V^{(m,n)} := (\omega_j^m \cdot \eta_k^n)_{j,k}$ (according

to Lemma 11), the coefficients $(c_{j,k})_{j,k}$ must satisfy

$$f_V = \sum_{l_1, l_2=0}^{N-1} c_{l_1, l_2} V^{(l_1, l_2)}$$

hence

$$c_{m,n} = \langle f_V, V^{m,n} \rangle_{\times} = \frac{1}{N^2} \sum_{l_1, l_2=0}^{N-1} f_{l_1, l_2} \overline{V_{l_1, l_2}^{m,n}} = \frac{1}{N^2} \sum_{l_1, l_2=0}^{N-1} f_{l_1, l_2} \omega_{l_1}^{-m} \eta_{l_2}^{-n}$$

Definition 12. The linear and invertible map

$$\mathcal{F}_N : \mathbb{C}^{N \times N} \rightarrow \mathbb{C}^{N \times N}$$

$$(f_{j,k})_{j,k} \rightarrow (c_{m,n})_{m,n}$$

is called (*2D-*)*discrete Fourier transform* (DFT), $c_{n,m}$ is often written as $\hat{f}_{n,m}$. The *Fourier synthesis* is given by:

$$f_{j,k} = \sum_{l_1, l_2=0}^{N-1} c_{l_1, l_2} \omega_{l_1}^j \eta_{l_2}^k$$

The 2D-DFT can be calculated via 1D-DFTs - one for each coordinate direction. This corresponds to $O(N \log_2 N)$ operations (when using FFTs).

Written in matrix form, the calculation reads

$$\mathcal{F}_N(f) = F_{N,y} \cdot F_{N,x} \cdot f_V = F_{N,x} \cdot F_{N,y} \cdot f_V$$

where $F_{N,x}, F_{N,y}$ denote the DFT-matrices with respect to the corresponding coordinate direction.

Remark 13. As before, there is a connection between differentiation in x, y and multiplication of the coefficients $(c_{m,n})_{m,n}$ by constants:

$$\frac{\partial}{\partial x} p_N(f)(x, y) = \sum_{l_1, l_2=0}^{N-1} i l_1 c_{l_1, l_2} e^{i(l_1 x + l_2 y)}$$

$$\frac{\partial}{\partial y} p_N(f)(x, y) = \sum_{l_1, l_2=0}^{N-1} i l_2 c_{l_1, l_2} e^{i(l_1 x + l_2 y)}$$

4.1.2 The Fourier-pseudospectral derivative

As mentioned above, the goal of this section is to find an approximation to the derivative of a function f by using the derivative of interpolating polynomials. The following definition

considers only the 2D-case (since it will be used later), but all other dimensions can be treated in an analogous way.

Definition 14. Let $f : \Omega := [0, 2\pi] \times [0, 2\pi] \rightarrow \mathbb{C}$ and $p_N(f) : \Omega \rightarrow \mathbb{C}$ the interpolating trigonometric polynomial to f corresponding to the nodes $(x_j, y_k)_{j,k=0}^{N-1}$, then the *Fourier-pseudospectral derivative* of f (of order N) is defined by

$$D_{x^\alpha y^\beta}^{\alpha+\beta} f(x, y) := \frac{\partial^{\alpha+\beta}}{\partial x^\alpha \partial y^\beta} p_N(f)(x, y) = \sum_{l_1, l_2=0}^{N-1} \left(i^{\alpha+\beta} l_1^\alpha l_2^\beta \right) \hat{f}_{l_1, l_2} \zeta^{l_1, l_2}(x, y), \quad (x, y) \in \Omega$$

For example:

$$\frac{\partial^2}{\partial x^2} f(x, y) \approx D_{x^2}^2 f(x, y) = \sum_{l_1, l_2=0}^{N-1} -l_1^2 \hat{f}_{l_1, l_2} \zeta^{l_1, l_2}(x, y)$$

$$\frac{\partial^2}{\partial y^2} f(x, y) \approx D_{y^2}^2 f(x, y) = \sum_{l_1, l_2=0}^{N-1} -l_2^2 \hat{f}_{l_1, l_2} \zeta^{l_1, l_2}(x, y)$$

In the following, the *Fourier-pseudospectral Laplacian* will be denoted by

$$\Delta_{\mathcal{F}} f := \left(D_{x^2}^2 + D_{y^2}^2 \right) f$$

and in the 1D-case, notation is simplified by

$$f' \approx Df, \quad f'' \approx D^2 f \dots$$

Remark 15. According to Definition 8, one has to apply the inverse Fourier transform on $D_{x^\alpha y^\beta}^{\alpha+\beta} f$ to evaluate the pseudospectral derivative in the nodes. Thus, for example, the approximate partial derivative with respect to x of a sample f_V of f is given by:

$$\left(\frac{\partial}{\partial x} f \right)_V \approx \mathcal{F}_N^{-1} (\mathfrak{M} \odot \mathcal{F}_N f_V)$$

Where \mathfrak{M} is the matrix containing the Fourier multipliers and \odot denotes componentwise multiplication. Using FFTs, this calculation needs $O(N \log_2 N)$ operations.

Application to linear PDEs

The discussed methods can be used to approximately solve PDEs. This is outlined by considering the example of the 2D Poisson equation with periodic boundary conditions:

$$\Delta u(x, y) = g(x, y), \quad x, y \in [0, 2\pi] \times [0, 2\pi]$$

Choosing a discretization $(x_j, y_k)_{j,k=0}^{N-1}$, one can construct a numerical solution by switching to pseudospectral derivatives and interpolating polynomials:

$$\begin{aligned}\Delta_{\mathcal{F}}u &= p_N(g) \\ \Rightarrow \Delta p_N(u) &= p_N(g)\end{aligned}$$

This leads to the following equations for the discrete Fourier coefficients:

$$\begin{aligned}-(j^2 + k^2)\hat{u}_{j,k} &= \hat{g}_{j,k}, \quad j, k = 0, \dots, N-1 \\ \Rightarrow \hat{u}_{j,k} &= -\frac{\hat{g}_{j,k}}{j^2 + k^2}\end{aligned}$$

Therefore

$$p_N(u)(x, y) \approx \sum_{l_1, l_2=0}^{N-1} -\frac{\hat{g}_{l_1, l_2}}{l_1^2 + l_2^2} \zeta^{l_1, l_2}(x, y) \quad (4.3)$$

Numerically the approximation to the solution u is calculated via

$$u_V \approx F_N^{-1} (\mathfrak{M}^{-2} \odot F_N g_V) \quad (4.4)$$

where \mathfrak{M}^{-2} is a matrix containing the Fourier multipliers. Values at the boundary have to be adjusted to satisfy the boundary conditions.

Error analysis

In the following, estimates on the error of pseudospectral derivatives and their application to PDEs are presented. Details and proofs can be found in [CH] and [BD].

Proposition 16. Let $f : [0, 2\pi] \rightarrow \mathbb{C}$, $p_N(f)$ the interpolating trigonometric polynomial for x_j , $j = 0, \dots, N-1$ defined as before. Then

(i) $\exists C_1 > 0$

$$\|f - p_N(f)\|_{H^{p,l}} \leq C_1 N^{l-m} \|f^{(m)}\|_{L^2}, \quad \text{if } f \in H^{p,m}(0, 2\pi), \quad 0 \leq l \leq m, \quad m \geq 1$$

(ii) $\exists C_2 > 0$:

$$\|f - p_N(f)\|_{L^\infty} \leq C_2 N^{-m} \log N \|f^{(m)}\|_{L^\infty}, \quad \text{if } f \in H^{\infty,m}, \quad m \geq 1$$

Thus, interestingly, the accuracy of the interpolation depends on the regularity of f . As

consequence of Proposition 16 one gets:

Theorem 17 (Accuracy of the Fourier-pseudospectral derivative). Let $f : [0, 2\pi] \rightarrow \mathbb{C}$, then, if Df, D^2f are Fourier-pseudospectral derivatives of order 1 and 2 with respect to N nodes:

(i) $\exists C_1 > 0$:

$$\|f' - Df\|_{L^2} \leq C_1 N^{1-m} \|f^{(m)}\|_{L^2}, \text{ if } f \in H^{p,m}, m \geq 1$$

(ii)

$$\|f' - Df\|_{L^2} \leq C_\eta N e^{-N\frac{\eta}{2}}, \text{ for all } 0 < \eta < \eta_0$$

If f is analytic in $\Omega := \{z \in \mathbb{C} \mid |\operatorname{Im}z| < \eta_0\} \cap (0, 2\pi)$ ($C_\eta > 0$ depends on η).

(iii) $\exists C_2 > 0$:

$$\|f'' - D^2f\|_{L^2} \leq C_2 N^{2-m} \|f^{(m)}\|_{L^2}, \text{ if } f \in H^{p,m}, m \geq 2$$

Hence, if f is analytic, the error committed by approximating by pseudospectral derivatives decays faster than every power of N^{-1} for $N \rightarrow \infty$. This is called *exponential accuracy* or *spectral accuracy*.

According to [BD], 16 (i.) and therefore 17 (i.) and (iii.) can be generalized to two dimensions yielding the same bounds.

Corollary 18 (Accuracy of the pseudospectral solution of Poisson's equation). The approximate solution to Poisson's equation

$$\Delta u(x, y) = g(x, y), (x, y) \in (0, 2\pi) \times (0, 2\pi)$$

calculated as above is of spectral accuracy.

Proof: According to 16 and 17

$$\begin{aligned} p_N(u) &= u + O(e^{-N}) \\ \Delta p_N(u) &= \Delta u + O(e^{-N}) \\ p_N(\Delta u) &= \Delta u + O(e^{-N}) \end{aligned}$$

and therefore

$$\Delta p_N(u) = \underbrace{p_N(\Delta u)}_{p_N(g)} + O(e^{-N})$$

Every approximation taken is of spectral accuracy, hence the algorithm maintains this level of accuracy.

4.2 Relaxation iteration

In the first part of this section, basic results on iterative algorithms are given. The second part contains a discussion of an algorithm to solve equation (3.33). The application of a pseudospectral method is not successful in this case, since the multiplication by the wave function ψ makes a comparison of Fourier multipliers as in (4.3) impossible.

For details and proofs confer [K].

4.2.1 General facts on iterative algorithms

The algorithms of interest are of the form

$$\mathbf{x}_{k+1} = \mathbf{b} + M\mathbf{x}_k, \quad k \geq 0 \quad (4.5)$$

where $\mathbf{b}, \mathbf{x}_k \in \mathbb{C}^N$, $M \in \mathbb{C}^{N \times N}$ nonsingular, with given initial value $\mathbf{x}_0 \in \mathbb{C}^N$.

Definition 19. Let $\|\cdot\|$ be a norm on \mathbb{C}^N , then the corresponding *induced matrix norm* on $\mathbb{C}^{N \times N}$ is defined as

$$\|M\| := \sup_{\mathbf{x} \in \mathbb{C}^N, \|\mathbf{x}\|=1} \|M\mathbf{x}\|, \quad \text{for every } M \in \mathbb{C}^{N \times N}$$

Proposition 20. If $\|M\| < 1$, then $I - M$ is invertible and (4.5) converges to

$$\mathbf{x}^* = (I - M)^{-1}\mathbf{b}$$

for every starting point $\mathbf{x}_0 \in \mathbb{C}^N$ with respect to the given norm $\|\cdot\|$. Furthermore, \mathbf{x}^* is a fixed point of the iteration:

$$(I - M)\mathbf{x}^* = \mathbf{b}$$

$$\Rightarrow \mathbf{x}^* = \mathbf{b} + M\mathbf{x}^*$$

Induced matrix norms are not the best tool to analyse the convergence behaviour iterative algorithms, since it is not always clear how to determine a norm in which $\|M\| < 1$ - or if this is true for any norm. A better way is to look at the *spectral radius*, which is an intrinsic property of every matrix:

Definition 21. Let $M \in \mathbb{C}^{N \times N}$, then the *spectral radius* of M is defined as

$$\rho(M) := \max \{ \lambda \in \mathbb{C} \mid \lambda \text{ is an eigenvalue of } M \}$$

Lemma 22 (Properties of the spectral radius). Let $M \in \mathbb{C}^{N \times N}$, then for any induced matrix norm $\|\cdot\|$:

- i. $\rho(M) \leq \|M\|$
- ii. $\rho(M) = \lim_{n \rightarrow \infty} \|M^n\|^{\frac{1}{n}}$

The proof of the first statement is straightforward, the second statement is shown in [Y] in a very general form.

This leads to the main result of this section:

Theorem 23. Let $M \in \mathbb{C}^{N \times N}$, then $I - M$ is invertible and there is a norm $\|\cdot\|$ on \mathbb{C}^n such that (4.5) converges for every $\mathbf{x}_0 \in \mathbb{C}^N$ to

$$\mathbf{x}^* = (I - M)^{-1} \mathbf{b} \quad (4.6)$$

if and only if

$$\rho(M) < 1$$

As consequence of 22 (ii.), one can see that for arbitrary $\alpha \in \mathbb{C}$

$$\rho(\alpha M) = |\alpha| \rho(M)$$

This fact will be used later to accelerate convergence of iterative algorithms - the smaller the spectral radius of the iteration matrix M , the faster the convergence:

If $\rho(M) < 1$, define the error in the k -th step as

$$\mathbf{e}_k := \mathbf{x}_k - \mathbf{x}^*, \quad k \geq 0$$

Let $\lambda \in \mathbb{C}$ be an eigenvalue of M and choose x_0 such that $\mathbf{e}_0 = \mathbf{x}_0 - \mathbf{x}^*$ is an eigenvector corresponding to λ . Then:

$$\begin{aligned} \mathbf{x}_1 &= M\mathbf{x}_0 + \mathbf{b} \stackrel{(4.6)}{=} M\mathbf{x}_0 + (I - M)\mathbf{x}^* = M\mathbf{x}_0 - M\mathbf{x}^* + \mathbf{x}^* \\ \Rightarrow \mathbf{e}_1 &= \mathbf{x}_1 - \mathbf{x}^* = M\mathbf{x}_0 - M\mathbf{x}^* = M\mathbf{e}_0 = \lambda\mathbf{e}_0 \end{aligned}$$

Hence

$$\mathbf{e}_k = \lambda^k \mathbf{e}_0 \text{ for every } k \geq 0$$

and

$$\|\mathbf{e}_k\| = |\lambda|^k \|\mathbf{e}_0\| \leq \rho(M)^k \|\mathbf{e}_0\|$$

Thus a small spectral radius is necessary for fast convergence.

A useful termination criterion for an iterative algorithm is to look at the difference

$$\epsilon_k := \|\mathbf{x}_k - \mathbf{x}_{k-1}\|$$

Since convergence is assured, this must tend to zero and one can terminate the iteration as soon as an error bound ϵ_{max} is reached.

4.2.2 Application to a Poisson equation

When approximating the Pauli-Poiswell system numerically in the proposed way (see below, at the end of this chapter), one encounters equations of the following form (compare (3.33)):

$$\Delta A_k(\mathbf{x}, t^n) = -\varepsilon h \text{Im}(\bar{\psi}(\mathbf{x}, t^n) \partial_k \psi(\mathbf{x}, t^n)) - \varepsilon^2 |\psi(\mathbf{x}, t^n)|^2 A_k(t^n, \mathbf{x}) \quad (4.7)$$

For a timestep t^n , $\mathbf{x} \in \mathbb{R}^2$ and $k \in \{1, 2\}$.

Discretization in space with N gridpoints in each coordinate direction leads to $N \times N$ matrices A_j^n approximating $A_j(\cdot, t^n)$ and ψ^n approximating $\psi(\cdot, t^n)$. $|\psi^n|^2$ is approximated by $n^n = (\psi^n)^* \psi^n$. Before deriving an iterative method to solve this equation, note that the stated convergence results of the previous section are valid for matrices instead of vectors too (when interpreting a $\mathbb{C}^{N \times N}$ matrix as \mathbb{C}^{N^2} vector).

Now the exact derivatives are replaced by Fourier-pseudospectral derivatives. Thus for

$$\tilde{M} := F_N^{-1}(\mathfrak{M}^2 \odot F_N)$$

where \mathfrak{M}^2 contains the discrete Fourier multipliers (compare (4.4)), A_j^n has to satisfy

$$\tilde{M} A_j^n = -\varepsilon h \text{Im}(\bar{\psi}^n D_j \psi^n) - \varepsilon^2 n^n A_j^n$$

where $D_1 = D_x$ and $D_2 = D_y$.

To construct an iteration, one starts with inverting \tilde{M} , avoiding singularities by adding a small parameter $\alpha < 0$ to the multiplier matrix \mathfrak{M}^2 (which contains only non-positive entries):

$$\tilde{M}_\alpha := F_N^{-1}((\mathfrak{M}^2 + \alpha \mathbf{1}) \odot F_N)$$

$\mathbf{1}$ denotes the matrix consisting of ones. \tilde{M}_α is invertible, since the DFT-matrix F is and

$$\tilde{M}_\alpha^{-1} = F_N^{-1}(\underbrace{(\mathfrak{M}^2 + \alpha \mathbf{1})^{\ominus 1}}_{\text{componentwise inverse}} \odot F_N)$$

Hence

$$\begin{aligned} A_j^n &= \tilde{M}_\alpha^{-1} \left(-\varepsilon h \operatorname{Im}(\bar{\psi}^n D_j^2 \psi^n) - \varepsilon^2 n^n A_j^n \right) \\ &= \underbrace{\tilde{M}_\alpha^{-1} \left(-\varepsilon h \operatorname{Im}(\bar{\psi}^n D_j^2 \psi^n) \right)}_{=: \mathbf{b}} - \tilde{M}_\alpha^{-1} (\varepsilon^2 n^n A_j^n) \end{aligned}$$

This suggests the iteration

$$\begin{aligned} A_0 &:= A_j^{n-1} \\ A_{k+1} &= \mathbf{b} - \underbrace{\tilde{M}_\alpha^{-1} (\varepsilon^2 n^n + \alpha I)}_{=: M_\alpha} A_k, \quad k \geq 0 \end{aligned}$$

Note the additional α at the right hand side of this equation - it guarantees $\rho(M_\alpha) < 1$.

4.3 Finite difference methods

In order to numerically solve the Pauli equation (3.26), a finite difference scheme called 'Leap Frog' is introduced.

This chapter contains an overview of the theory of finite difference methods and concepts for analysing their behaviour are introduced. Details and proofs of the results can be found in [LR] and [ST].

The basic idea of these methods is to replace the differential quotients in differential equations (partly) by difference quotients. This yields difference equations for the function values of an approximation in the grid points.

As before, considerations are restricted to the domain $Q \subseteq \mathbb{R}^2$, covered by a grid (x_j, y_k) , $j, k \in \{0, 1, \dots, N-1\}$ (compare page 37). Similar results hold in the multidimensional case.

Example 24. Consider the 1D transport equation

$$\begin{aligned} \frac{\partial}{\partial t} u + a \frac{\partial}{\partial x} u &= 0 \\ u(x, 0) &= u_0(x) \end{aligned}$$

Replacing with forward difference quotients leads to the 'forward time, forward space scheme':

$$\frac{u_j^{n+1} - u_j^n}{\Delta t} + a \frac{u_{j+1}^n - u_j^n}{\Delta x} = 0$$

Another example is the 'forward time, central space scheme':

$$\frac{u_j^{n+1} - u_j^n}{\Delta t} + a \frac{u_{j+1}^{n+1} - u_{j-1}^{n+1}}{2\Delta x} = 0$$

both using the initial condition

$$\{u_j^0\}_j = \{u_0(x_j)\}$$

Methods involving the timesteps t^{n+1} and t^n only are called *one-step schemes*, otherwise *multistep schemes*. If u_j^{n+1} can be calculated explicitly, the scheme is called *explicit*, if one has to solve a linear or even nonlinear system of difference equations in each step, it is called *implicit*.

Implicit schemes are generally more tolerant concerning step sizes, but the implementation of explicit schemes is easier.

A multistep scheme needs more than one time-level to initialize, the lacking initial data can be computed for example by a one-step scheme.

4.3.1 Convergence, consistency and stability

The main property a finite difference scheme must have is convergence to an actual solution of the corresponding PDE. In this case, convergence is measured in the Banach space of complex valued, square Lebesgue-integrable functions $(L_{per}^2(Q), \|\cdot\|_{L^2})$, which contains all quantum mechanical states as unit vectors.

Approximate solutions, which are only calculated in the grid points, can be considered as L_{per}^2 -functions too (by interpolation).

The difference schemes constructed in this section are intended for a numerical treatment of PDEs of the form

$$P\mathbf{u}(\mathbf{x}, t) := \frac{\partial}{\partial t}\mathbf{u}(\mathbf{x}, t) - L\mathbf{u}(\mathbf{x}, t) = 0, \text{ for } x \text{ in } Q, t \geq 0 \quad (4.8)$$

$$\mathbf{u}(\mathbf{x}, 0) = \mathbf{u}_0(\mathbf{x}) \quad (4.9)$$

Where L is a linear differential operator with constant coefficients and periodic boundary conditions are assumed. The Pauli equation does not satisfy this condition, but one can assume constant coefficients during calculations and impose bounds later.

Note that the function \mathbf{u} is vector valued. This is necessary to include systems of PDEs -

like the Pauli equation. All norms are considered component wise.

Definition 25. An initial value problem of the form (4.8)-(4.9) is called *well-posed* if for every $T \geq 0$ there is a constant $C_T > 0$, such that any solution \mathbf{u}^* satisfies

$$\|\mathbf{u}^*(\cdot, t)\|_{L^2} \leq C_T \|\mathbf{u}_0\|_{L^2}$$

for $0 \leq t \leq T$ and every initial data $\mathbf{u}_0 \in L^2$.

Remark 26. • One can show that only well-posed equations are suitable to model physical processes.

- From now on, \mathbf{u}^* denotes an exact solution of (4.8)-(4.9).

Let $\mathbf{u}^n(x)$ denote the trigonometric polynomial interpolating the calculated approximations at time t^n (actually, \mathbf{u}^n is a vector of interpolating polynomials, one for each component of \mathbf{u}). The difference schemes resulting from replacing differential quotients by difference quotients are generally of the form

$$\sum_{l_1, l_2 \in H} I_1(l_1, l_2) \mathbf{u}^{n+1}(x_j + l_1 \Delta x, y_k + l_2 \Delta y) + I_2(l_1, l_2) \mathbf{u}^n(x_j + l_1 \Delta x, y_k + l_2 \Delta y) = 0 \quad (4.10)$$

or in operator form

$$P_d(\Delta x, \Delta y, \Delta t) \mathbf{u}^n(\mathbf{x}, t) = 0 \quad (4.11)$$

where $H \subseteq \mathbb{N}$ is a finite index set, $j, k \in \{0, \dots, N-1\}$ and I_1, I_2 are matrices depending on $l_1, l_2, \Delta x, \Delta y, \Delta t$.

The value of \mathbf{u}^{n+1} at a grid point (x_j, y_k) is given by a linear combination of the values of \mathbf{u}^n (and \mathbf{u}^{n+1} in the implicit case) at a finite number of neighbouring points. Sometimes, interpolated values between the grid points are included in this calculation.

It is assumed, that this scheme has a unique solution for \mathbf{u}^{n+1} , therefore all matrices $I_1(l_1, l_2)$ are non-singular. More than two time levels are handled by introducing auxiliary variables.

Equation (4.10) can be written equivalently in the form

$$\mathbf{u}^{n+1} = B(\Delta t, \Delta x, \Delta y) \mathbf{u}^n, \quad n \geq 0 \quad (4.12)$$

where B is a linear finite difference operator - it may contain the inverses of the matrices I_1 if the scheme is implicit.

In the analysis of finite difference schemes, it is customary to assume that the space steps

Δx and Δy are related to the time step Δt , i.e.:

$$\Delta x = f_1(\Delta t)$$

$$\Delta y = f_2(\Delta t)$$

in a way such that $\Delta x \rightarrow 0$, $\Delta y \rightarrow 0$ as Δt converges to 0.

In this case, (4.12) transforms to

$$\mathbf{u}^{n+1} = C(\Delta t)\mathbf{u}^n = C(\Delta t)^n\mathbf{u}^0, \quad n \geq 0 \quad (4.13)$$

Definition 27 (Convergence). A scheme of the form (4.13) is called *convergent*, if for every initial data $u_0 \in L^2_{per}(Q)$ and every pair of sequences $\{\Delta t_j\}_j, \{n_j\}_j$ with

$$\begin{aligned} \Delta t_j &\xrightarrow{j \rightarrow \infty} 0 \\ n_j \Delta t_j &\xrightarrow{j \rightarrow \infty} t \quad (t \geq 0) \end{aligned}$$

the following holds:

$$\|C(\Delta t_j)^{n_j}\mathbf{u}_0 - \mathbf{u}^*(\cdot, t)\|_{L^2_{per}} \xrightarrow{j \rightarrow \infty} 0$$

In most cases, convergence of a scheme is not easy to prove, therefore alternative characterizations are needed.

At first, a property called *consistency* assures that if the scheme in question is convergent, then it converges to a solution of the corresponding PDE.

Definition 28 (Consistency). A scheme of the form (4.11) is called *consistent* with the initial value problem (4.8)-(4.9), if

$$P\phi - P_d(\Delta x, \Delta y, \Delta t)\phi \rightarrow 0 \text{ pointwise for } \Delta x, \Delta y, \Delta t \rightarrow 0$$

for $\phi \in \mathcal{C}^\infty(\mathbb{R}^2 \times \mathbb{R}^+)$ arbitrary.

Consistency can usually be checked with the help of Taylor expansions.

The next property is an analogon to well-posedness for the difference approximation:

Definition 29 (Stability). A scheme of the form (4.13) is called *stable*, if for every $T \geq 0$ and $\tau > 0$ the set of operators

$$\{C(\Delta t)^n \mid 0 < \Delta t \leq \tau, 0 \leq n\Delta t \leq T\}$$

is uniformly bounded in the operator norm $\|\cdot\|$ (defined as the matrix norm in Definition 19).

Equivalently, for arbitrary $T \geq 0, \Delta t > 0$ there is a constant $C_T > 0$, such that

$$\|\mathbf{u}^n\|_{L_{per}^2} = \|C(\Delta t)^n \mathbf{u}_0\|_{L_{per}^2} \leq \|C(\Delta t)^n\| \|\mathbf{u}^0\|_{L_{per}^2} \leq C_T \|\mathbf{u}^0\|_{L_{per}^2}$$

for every initial data $\mathbf{u}^0 \in L_{per}^2(Q)$ and $0 \leq n\Delta t \leq T$.

Finally, the well-known

Theorem 30 (Lax-Richtmyer Equivalence Theorem). A consistent scheme of the form (4.13) for a well-posed initial value problem (4.8)-(4.9) is convergent if and only if it is stable.

4.3.2 Von Neumann stability analysis

In this section, an important result on the stability of finite difference schemes is presented, the von Neumann condition, which is based on Fourier analytical calculations.

If $\mathbf{f} : \mathbb{R}^2 \rightarrow \mathbb{C}^n$ is periodic and square integrable with period $p = b - a$ (remember the domain of interest is $Q := [a, b) \times [a, b)$) in both coordinate directions, it can be expanded into an infinite Fourier series in each component, i.e.:

$$\mathbf{f}(\mathbf{x}) = \sum_{\mathbf{k} \in K} \mathbf{c}(\mathbf{k}) e^{i\mathbf{k} \cdot \mathbf{x}}$$

where

$$K = \left\{ \mathbf{k} = \begin{pmatrix} k_1 \\ k_2 \end{pmatrix} = \begin{pmatrix} \frac{2\pi l_1}{p} \\ \frac{2\pi l_2}{p} \end{pmatrix} \mid l_1, l_2 \in \mathbb{Z} \right\}$$

and $\mathbf{x} = \begin{pmatrix} x \\ y \end{pmatrix}$, $\mathbf{c}(\mathbf{k}) \in \mathbb{C}^n$.

As in the case of discrete Fourier series, uniqueness of the expansion in every component of \mathbf{f} is given:

Proposition 31. i. The map

$$\mathcal{F} : L_{per}^2(Q) \rightarrow l^2(\mathbb{C})$$

$$f \mapsto c(\mathbf{k})_{\mathbf{k} \in K}$$

which maps every L_{per}^2 function on Q to a square summable complex sequence, is an

isometric isomorphism, i.e. *Parseval's equation* holds:

$$\|f\|_{L^2}^2 = \int_{\mathbb{R}^2} |f(\mathbf{x})|^2 d\mathbf{x} = \sum_{\mathbf{k} \in K} |c(\mathbf{k})|^2 = \|c\|_{l^2}^2 \quad (4.14)$$

ii. If $p_N = \sum_{\mathbf{k} \in K} c(\mathbf{k})e^{i\mathbf{k} \cdot \mathbf{x}}$, $K = \{\mathbf{k}_1, \dots, \mathbf{k}_m\}$, is a trigonometric polynomial of order N in Q , then

$$\mathcal{F}p_N = (c(\mathbf{k}_1), \dots, c(\mathbf{k}_m), 0, 0, \dots)$$

For a proof of this proposition, see your favourite course in functional analysis or [HA]. Since every trigonometric polynomial in Q can be interpreted as infinite Fourier series (by adding terms with coefficients $c(\mathbf{k}) = 0$), uniqueness of part (i.) proves part (ii.) of this proposition. As consequence of the norm preserving property of the map \mathcal{F} , one can analyse stability properties of finite difference scheme in the Fourier space $l^2(\mathbb{C})$:

Consider the scheme (4.10); since \mathbf{u}^n is a trigonometric interpolation polynomial:

$$\mathbf{u}^n = \sum_{\mathbf{k} \in K} \mathbf{v}^n(\mathbf{k})e^{i\mathbf{k} \cdot \mathbf{x}}$$

Hence

$$\begin{aligned} & \sum_{l_1, l_2 \in H} I_1(l_1, l_2) \sum_{\mathbf{k} \in K} \left(\mathbf{v}^{n+1}(\mathbf{k})e^{i(k_1(x_j+l_1\Delta x)+k_2(y_k+l_2\Delta y))} \right) \\ & + I_2(l_1, l_2) \sum_{\mathbf{k} \in K} \left(\mathbf{v}^n(\mathbf{k})e^{i(k_1(x_j+l_1\Delta x)+k_2(y_k+l_2\Delta y))} \right) = 0 \end{aligned}$$

Comparing coefficients yields the equation

$$\sum_{l_1, l_2 \in H} I_1(l_1, l_2) \mathbf{v}^{n+1}(\mathbf{k})e^{i(k_1(x_j+l_1\Delta x)+k_2(y_k+l_2\Delta y))} + I_2(l_1, l_2) \mathbf{v}^n(\mathbf{k})e^{i(k_1(x_j+l_1\Delta x)+k_2(y_k+l_2\Delta y))} = 0$$

for arbitrary $\mathbf{k} \in K$. Now, after cancelling the common factor $e^{i\mathbf{k} \cdot \mathbf{x}}$ and setting

$$G_m = G_m(\Delta x, \Delta y, \Delta t, \mathbf{k}) := \sum_{l_1, l_2 \in H} I_m(l_1, l_2)e^{i(k_1 l_1 \Delta x + k_2 l_2 \Delta y)}, \quad m = 1, 2$$

one gets

$$\begin{aligned} G_1 \mathbf{v}^{n+1}(\mathbf{k}) + G_2 \mathbf{v}^n(\mathbf{k}) &= 0 \\ \Rightarrow \mathbf{v}^{n+1}(\mathbf{k}) &= \underbrace{-G_1^{-1} G_2}_{=: G} \mathbf{v}^n(\mathbf{k}) \end{aligned}$$

G_1 is invertible because of the uniqueness of Fourier expansions and the solvability as-

sumption made before. $G(\Delta x, \Delta y, \Delta t, \mathbf{k})$ is called *amplification matrix* (actually, G is a set of matrices), it reflects the amount the amplitude of each pure frequency changes in calculating the next time step.

If the space steps depend on the time step as before ($\Delta x = f_1(\Delta t), \Delta y = f_2(\Delta t)$) one can see that the scheme (4.10) is stable iff for all $T \geq 0, \tau > 0$ the set

$$\{G(\Delta t, \mathbf{k})^n \mid 0 < \Delta t \leq \tau, 0 \leq n\Delta t \leq T\}$$

is uniformly bounded with respect to all $\mathbf{k} \in K$, because in this case for every $T \geq 0, \Delta t > 0$, there is a constant $C_T > 0$, such that for all n satisfying $0 \leq n\Delta t \leq T$ and all $u_0 \in L^2_{per}(\mathbb{R}^2)$

$$\|\mathbf{u}^n\|_{L^2} = \|\mathbf{v}^n\|_{l^2} = \|G(\Delta t, \cdot)^n \mathbf{v}_0\|_{l^2} \leq C_T \|\mathbf{v}_0\|_{l^2} = C_T \|u_0\|_{L^2}$$

Here Parseval's equation (4.14) was used.

As in the preceding section, the spectral radius of the amplification matrix is used to generalize this statement:

Theorem 32 (Von Neumann stability condition). Let

$$\rho_1(G, \Delta t) := \max_{\mathbf{k} \in K} \rho(G(\Delta t, \mathbf{k}))$$

$$\rho_2(G, \Delta t) := \max_{\mathbf{k} \in K} \sqrt{\rho(G(\Delta t, \mathbf{k})^* G(\Delta t, \mathbf{k}))}$$

i. If (4.10) is stable, then

$$\rho_1(G, \Delta t) \leq 1 + O(\Delta t) \tag{4.15}$$

ii. If $\rho_2(G, \Delta t) \leq 1 + O(\Delta t)$, then (4.10) is stable.

iii. If G is normal, i.e. $G^*G = GG^*$, then condition (4.15) is also sufficient for the stability of scheme (4.10).

Corollary 33. Let G be the amplification factor of a stable scheme and \tilde{G} another amplification factor. If there are constants $\gamma_1 \geq 0, \gamma_2 \geq 1$ such that

$$\|G - \tilde{G}\| \leq \gamma_1 \Delta t$$

and

$$\|\tilde{G}\| \geq \gamma_2$$

then the scheme corresponding to \tilde{G} is stable.

4.3.3 Application to the Pauli equation

As mentioned above, a finite difference scheme is used to solve the Pauli equation (3.26), the Leap Frog method:

Let Q and (x_j, y_k) be defined as before (cf. page 37) and denote the calculated approximations for $\psi = \begin{pmatrix} \psi_\uparrow \\ \psi_\downarrow \end{pmatrix}$, $\mathbf{A} = \begin{pmatrix} A_1 \\ A_2 \end{pmatrix}$, V, n at time t^m , $m \geq 0$ by a superscript:

$$\psi^m = \left\{ \begin{pmatrix} \psi_{\uparrow,j,k}^m \\ \psi_{\downarrow,j,k}^m \end{pmatrix} \right\}_{j,k}, \mathbf{A}^m = \left\{ \begin{pmatrix} A_{1,j,k}^m \\ A_{2,j,k}^m \end{pmatrix} \right\}_{j,k}, V^m = \{V_{j,k}^m\}_{j,k}, n^m = \{n_{j,k}^m\}_{j,k}$$

Since the scheme is a two-step scheme, the lacking initial data is calculated by one step of a Runge-Kutta algorithm of second order:

ψ^0 is given by the initial data and let $c := -\frac{i\Delta t}{h}$, then

$$\psi_\uparrow^1 = \psi_\uparrow^0 + c \cdot (g_\uparrow(\psi^0, 0) + g_\uparrow(\psi^0 + cg_\uparrow(\psi^0, 0), 0))$$

$$\psi_\downarrow^1 = \psi_\downarrow^0 + c \cdot (g_\downarrow(\psi^0, 0) + g_\downarrow(\psi^0 + cg_\downarrow(\psi^0, 0), 0))$$

where $\mathbf{g}(f, m) = \begin{pmatrix} g_\uparrow(f, m) \\ g_\downarrow(f, m) \end{pmatrix}$, $m \in \mathbb{N}$, denotes the evaluation of the right hand side of (3.26) by Fourier-pseudospectral derivatives at time t^m for the approximation of a 2-spinor $f = \left\{ \begin{pmatrix} f_{\uparrow,j,k} \\ f_{\downarrow,j,k} \end{pmatrix} \right\}_{j,k}$, i.e.:

$$g_\uparrow(f, m) = \frac{1}{2} (h^2 \Delta_{\mathcal{F}} f_\uparrow - ih\varepsilon(A_1^m \odot D_x f_\uparrow + A_2^m \odot D_y f_\uparrow) - \varepsilon h(i(D_x A_1^m) \odot f_\uparrow - (D_y A_1^m) \odot f_\downarrow) - (i(D_y A_2^m) \odot f_\uparrow + (D_x A_2^m) \odot f_\downarrow) + (\varepsilon^2 |\mathbf{A}^m|^2 + 2V^m) \odot f_\uparrow)$$

$$g_\downarrow(f, m) = \frac{1}{2} (h^2 \Delta_{\mathcal{F}} f_\downarrow - ih\varepsilon(A_1^m \odot D_x f_\downarrow + A_2^m \odot D_y f_\downarrow) - \varepsilon h(i(D_x A_1^m) \odot f_\downarrow - (D_y A_1^m) \odot f_\uparrow) - (i(D_y A_2^m) \odot f_\downarrow + (D_x A_2^m) \odot f_\uparrow) + (\varepsilon^2 |\mathbf{A}^m|^2 + 2V^m) \odot f_\downarrow)$$

Here, $|\mathbf{A}^m|^2 = \left\{ |A_{1,j,k}^m|^2 + |A_{2,j,k}^m|^2 \right\}_{j,k}$.

Now assume that the approximation at time t^m is already calculated, then the Leap Frog method for this equation reads as follows:

For every $j, k \in \{0, \dots, N-1\}$

$$\psi_{\uparrow,j,k}^{m+1} = \psi_{\uparrow,j,k}^{m-1} - \frac{2i\Delta t}{h} g_\uparrow(\psi^m, m)_{j,k} \quad (4.16)$$

$$\psi_{\downarrow j,k}^{m+1} = \psi_{\downarrow j,k}^{m-1} - \frac{2i\Delta t}{h} g_{\downarrow}(\psi^m, m)_{j,k} \quad (4.17)$$

Stability of the Leap Frog scheme

Now the stability and consistency properties of the introduced scheme are checked.

Using trigonometric interpolation of the data yields the approximations

$$\begin{aligned} \psi_{\uparrow}^m(x, y) &\approx \sum_{k_1, k_2=0}^{N-1} a^m(k_1, k_2) e^{i(k_1 x + k_2 y)} \\ \psi_{\downarrow}^m(x, y) &\approx \sum_{k_1, k_2=0}^{N-1} b^m(k_1, k_2) e^{i(k_1 x + k_2 y)} \\ \psi_{\uparrow}^{m-1}(x, y) &\approx \sum_{k_1, k_2=0}^{N-1} c^m(k_1, k_2) e^{i(k_1 x + k_2 y)} \\ \psi_{\downarrow}^{m-1}(x, y) &\approx \sum_{k_1, k_2=0}^{N-1} d^m(k_1, k_2) e^{i(k_1 x + k_2 y)} \end{aligned}$$

(i.e.: $a^m(k_1, k_2) = c^{m+1}(k_1, k_2)$, $b^m(k_1, k_2) = d^{m+1}(k_1, k_2)$ for all $k_1, k_2 \in \{0, \dots, N-1\}$).

Putting this expansions into the Leap Frog scheme and comparing the coefficients as described on page 55 yields the following relations for the Fourier coefficients:

For fixed $k_1, k_2 \in \{0, \dots, N-1\}$:

$$a^{m+1} = c^m + \Delta t \underbrace{\left((k_1^2 + k_2^2)\alpha_0 + k_1\varepsilon\alpha_1 + k_2\varepsilon\alpha_2 + \varepsilon\alpha_3 + \varepsilon^2\alpha_4 + \alpha_5 \right)}_{:=\beta(\varepsilon, k_1, k_2)} a^m + \Delta t \varepsilon \alpha_6 b^m$$

$$b^{m+1} = d^m + \Delta t \varepsilon \alpha_6 a^m + \Delta t \left((k_1^2 + k_2^2)\alpha_0 + k_1\varepsilon\alpha_1 + k_2\varepsilon\alpha_2 + \varepsilon\alpha_3 + \varepsilon^2\alpha_4 + \alpha_5 \right) b^m$$

$$c^{m+1} = a^m$$

$$d^{m+1} = b^m$$

with coefficients

$$\begin{aligned}
 \alpha_0 &:= ih \\
 \alpha_1 &:= 2iA_1^m{}_{j,k} \\
 \alpha_2 &:= 2iA_2^m{}_{j,k} \\
 \alpha_3 &:= -(D_x A_1^m)_{j,k} - (D_y A_2^m)_{j,k} \\
 \alpha_1 &:= 2iA_1^m{}_{j,k} \\
 \alpha_2 &:= 2iA_2^m{}_{j,k} \\
 \alpha_3 &:= -(D_x A_1^m)_{j,k} - (D_y A_2^m)_{j,k} \\
 \alpha_4 &:= -\frac{i}{h}(|A_1^m{}_{j,k}|^2 + |A_2^m{}_{j,k}|^2) \\
 \alpha_5 &:= V_{j,k}^m \\
 \alpha_6 &:= i\varepsilon(-(D_y A_1^m)_{j,k} + (D_x A_2^m)_{j,k})
 \end{aligned}$$

This yields the amplification matrix

$$G(\Delta t, k_1, k_2, \varepsilon) = \begin{pmatrix} \Delta t\beta(\varepsilon, k_1, k_2) & \Delta t\varepsilon\alpha_6 & 1 & 0 \\ \Delta t\varepsilon\alpha_6 & \Delta t\beta(\varepsilon, k_1, k_2) & 0 & 1 \\ 1 & 0 & 0 & 0 \\ 0 & 1 & 0 & 0 \end{pmatrix}$$

Note that here and in the following a dependency of ε is included. This is done to check the influence of the parameter on the stability of the system.

This can be split into the two parts

$$G(\Delta t, k_1, k_2, \varepsilon) = \underbrace{\begin{pmatrix} 0 & \Delta t\varepsilon\alpha_6 & 1 & 0 \\ \Delta t\varepsilon\alpha_6 & 0 & 0 & 1 \\ 1 & 0 & 0 & 0 \\ 0 & 1 & 0 & 0 \end{pmatrix}}_{=:G'(\Delta t, k_1, k_2, \varepsilon)} + \underbrace{\begin{pmatrix} \Delta t\beta(\varepsilon, k_1, k_2) & 0 & 0 & 0 \\ 0 & \Delta t\beta(\varepsilon, k_1, k_2) & 0 & 0 \\ 0 & 0 & 0 & 0 \\ 0 & 0 & 0 & 0 \end{pmatrix}}_{=:G''(\Delta t, k_1, k_2, \varepsilon)}$$

satisfying

$$\|G' - G\| = \|G''\| = |\beta|\Delta t \leq \gamma_1 \Delta t$$

and $\|G\| < \infty$ if A_1, A_2 are bounded together with their partial derivatives of first order and V is bounded. The second requirement of Corollary 33 is not generally satisfied, it has to be checked for given potentials.

Thus one has to prove stability of the scheme corresponding to the amplification matrix G' to show the stability of the Leap Frog scheme.

G' is not normal, therefore condition 32(ii.) has to be checked:

The eigenvalues of $(G')^*G'$ are given by

$$\mu_{1,2} = \frac{1}{2}(2 + \Delta t^2 \varepsilon^2 |\alpha_6|^2 \pm \Delta t \varepsilon |\alpha_6| \sqrt{4 + \Delta t^2 \varepsilon^2 |\alpha_6|^2})$$

Using Taylor expansions of $\sqrt{|\mu_1|}$, $\sqrt{|\mu_2|}$ yields

$$\rho_2(G', \Delta t) = 1 + O(\Delta t)$$

Hence, the scheme corresponding to G' is stable according to Theorem 32 and the Leap Frog scheme is stable.

Consistency of the Leap Frog scheme

Choose an arbitrary $\phi \in (C^\infty(\mathbb{R}^2 \times \mathbb{R}^+))^2$, the applied scheme is of the form (compare Definition 28, which is generalized in an obvious way to incorporate 2-spinors):

$$P_d(\Delta x, \Delta y, \Delta t)\phi_{j,k}^m = \frac{i}{2\Delta t}(\phi_{j,k}^{m+1} - \phi_{j,k}^{m-1}) - \mathbf{g}(\phi^m, m)$$

Here the notation $\phi_{j,k}^m$ is used for the exact value of the test function ϕ at (x_j, y_k, t^m) .

Using Taylor expansions of first order yields

$$\begin{aligned} P_d(\Delta x, \Delta y, \Delta t)\phi_{j,k}^m &= \frac{i}{2\Delta t} \left(\phi_{j,k}^m + \Delta t \left(\frac{\partial \phi}{\partial t} \right)_{j,k}^m - \phi_{j,k}^m + \Delta t \left(\frac{\partial \phi}{\partial t} \right)_{j,k}^m \right) - \mathbf{g}(\phi^m, m) + O((\Delta t)^2) \\ &= i \left(\frac{\partial \phi}{\partial t} \right)_{j,k}^m - \mathbf{g}(\phi^m, m) + O((\Delta t)^2) \end{aligned}$$

Hence, if $\mathcal{A}\phi$ denotes the right hand side of the Pauli Equation (3.26):

$$\begin{aligned} P\phi(x_j, y_k, t^m) - P_d(\Delta x, \Delta y, \Delta t)\phi_{j,k}^m &= \\ &= i \frac{\partial \phi}{\partial t}(x_j, y_k, t^m) - i \left(\frac{\partial \phi}{\partial t} \right)_{j,k}^m - \mathcal{A}\phi(x_j, y_k, t^m) + \mathbf{g}(\phi^m, m) + O((\Delta t)^2) \\ &= \underbrace{-\mathcal{A}\phi(x_j, y_k, t^m) + \mathbf{g}(\phi^m, m)}_{\rightarrow 0 \text{ for } \Delta x, \Delta y \rightarrow 0} + O((\Delta t)^2) \rightarrow 0 \text{ for } \Delta x, \Delta y, \Delta t \rightarrow 0 \end{aligned}$$

$-\mathcal{A} + g$ converges to 0 because of the spectral accuracy of the pseudospectral derivative.

4.4 Numerical approximation of the Pauli-Poiswell system

Now the numerical methods that were developed in the preceding sections of this chapter are applied to calculate an approximate solution of the Pauli-Poiswell system (3.26)-(3.33).

Note that the convergence analysis of these methods was not performed rigorously: Only the linear case was considered and the well-posedness of the Pauli-Poiswell system was not shown. But as these topics are very involved, they are not part of this thesis.

The following algorithm is used (with the same notation as presented on page 57):

Assume that, starting with the initial condition $\psi_{j,k}^0 = \psi_0(x_j, y_k)$, $j, k = 0, \dots, N - 1$ as given in (3.27), ψ^m , $m \in \mathbb{N}$ has already been computed, then:

1. Calculate $n^m = (\psi^m)^* \odot \psi^m$.
2. Use the Fourier-pseudospectral method (4.4) to solve (3.32) for V_{int}^m numerically and set $V^m = V_{int}^m + V_{ext}^m$ (where V_{ext}^m is given).
3. Approximate (3.33) for \mathbf{A}_{int}^m in each component using the relaxation iteration (4.7) and get \mathbf{A}^m via $\mathbf{A}^m = \mathbf{A}_{int}^m + \mathbf{A}_{ext}^m$ (with given \mathbf{A}_{ext}^m).
4. Use the Leap Frog method (4.16)-(4.17) to calculate ψ^{m+1} .

It may be necessary to adjust boundary values during calculations to satisfy the periodic boundary conditions.

Chapter 5

Numerical results

This chapter is devoted to the presentation and interpretation of simulation results concerning the Pauli-Poiswell system in two space dimensions. The system was solved numerically as described in the previous chapter. The algorithm was implemented in FORTRAN 77 by Yanzhi Zhang and compiled using the Intel FORTRAN compiler ifort (IFORT), version '9.0 20050809'.

All calculations are based on a grid size of 256×256 on the spacial domain $\Omega = [-16, 16] \times [-16, 16]$ and a time step of 0.0001 in the time interval $[0, 10]$.

5.1 Setup of the numerical experiments

The experiments deal with the planar movement of an electron in three spacial dimensions - i.e. the movement of an electron in a thin metallic plate. As mentioned in remark 5, the magnetic field \mathbf{B} caused by the (in this case: 2-dimensional) magnetic vector potential \mathbf{A} via $\mathbf{B} = \text{curl}\mathbf{A}$ acts perpendicularly on the plate.

To be consistent with the notation used before, the coordinates of a point \mathbf{x} in \mathbb{R}^3 are

$$\mathbf{x} = \begin{pmatrix} x_1 \\ x_2 \\ x_3 \end{pmatrix}$$

and, assuming the metal plate is a part of the x_2x_3 -plane, points in the plate have the coordinates $\begin{pmatrix} 0 \\ x_2 \\ x_3 \end{pmatrix}$, which corresponds to the point $\begin{pmatrix} x_2 \\ x_3 \end{pmatrix} =: \begin{pmatrix} x \\ y \end{pmatrix}$ when projected on the x_2x_3 -plane.

The (external) electric potential V_{ext} is a parabolic 'confining potential', i.e.: a harmonic

oscillator potential of the form

$$V_{ext}(x, y) = -\frac{1}{2}(x^2 + y^2)$$

Potentials of this form are of particular importance as they can be used to approximate arbitrary potentials in a neighbourhood of a local minimum - cf. [G]. Comparing equation (3.16), one can see that with this choice of the potential V_{ext} , which is centered at 0, the electric field $\mathbf{E} = -\nabla V - \frac{1}{c}\partial_t \mathbf{A}$ pulls the electron towards the origin (when the internal potential V_{int} is small).

The (external) magnetic vector potential \mathbf{A}_{ext} is defined as

$$\mathbf{A}_{ext}(x_1, x_2, x_3) = \begin{pmatrix} 0 \\ 0 \\ 5x_2 \end{pmatrix}$$

In this case, the Pauli equation reads

$$ih\partial_t\psi = \frac{1}{2}(ih\nabla + \varepsilon\mathbf{A})^2\psi - V\psi - \frac{\varepsilon h}{2} \underbrace{\begin{pmatrix} 0 & 1 \\ 1 & 0 \end{pmatrix}}_{\hat{\sigma}^1} \underbrace{5}_{\text{curl}_1(\mathbf{A})} \psi$$

since only the first component of $\text{curl}\mathbf{A}$ is nonzero.

The following 4 systems are compared using two different initial conditions (always considering ψ as a 2-spinor).

- The **Pauli-Poiswell system**:

$$\begin{aligned} ih\partial_t\psi &= \frac{1}{2}(ih\nabla + \varepsilon\mathbf{A})^2\psi - V\psi - \frac{\varepsilon h}{2} \begin{pmatrix} 0 & 1 \\ 1 & 0 \end{pmatrix} \text{curl}_1(\mathbf{A})\psi \\ \psi(\mathbf{x}, 0) &= \psi_I(\mathbf{x}) \\ n(\mathbf{x}, t) &= |\psi_1(\mathbf{x}, t)|^2 + |\psi_2(\mathbf{x}, t)|^2 \\ J_k(\mathbf{x}, t) &= \text{Im}(\bar{\psi}(h\partial_k + i\varepsilon A_k)\psi) + \text{curl}_k(\bar{\psi} \cdot \vec{\sigma}\psi), \quad k = 1, 2 \\ V &= \theta V_{int} + V_{ext} \\ \mathbf{A} &= \theta \mathbf{A}_{int} + \mathbf{A}_{ext} \\ \Delta V_{int} &= -n \\ \Delta \mathbf{A}_{int} &= -\varepsilon \mathbf{J} \end{aligned}$$

- The linear Pauli equation

$$ih\partial_t\psi = \frac{1}{2}(ih\nabla + \varepsilon\mathbf{A})^2\psi - V\psi - \frac{\varepsilon h}{2} \begin{pmatrix} 0 & 1 \\ 1 & 0 \end{pmatrix} \text{curl}_1(\mathbf{A})\psi$$

$$\psi(\mathbf{x}, 0) = \psi_I(\mathbf{x})$$

- The magnetic Schrödinger-Poiswell system

$$ih\partial_t\psi = \frac{1}{2}(ih\nabla + \varepsilon\mathbf{A})^2\psi - V\psi$$

$$\psi(\mathbf{x}, 0) = \psi_I(\mathbf{x})$$

$$n(\mathbf{x}, t) = |\psi_1(\mathbf{x}, t)|^2 + |\psi_2(\mathbf{x}, t)|^2$$

$$J_k(\mathbf{x}, t) = \text{Im}(\bar{\psi}(h\partial_k + i\varepsilon A_k)\psi) + \text{curl}_k(\bar{\psi} \cdot \vec{\sigma}\psi), \quad k = 1, 2$$

$$V = \theta V_{int} + V_{ext}$$

$$\mathbf{A} = \theta \mathbf{A}_{int} + \mathbf{A}_{ext}$$

$$\Delta V_{int} = -n$$

$$\Delta \mathbf{A}_{int} = -\varepsilon \mathbf{J}$$

- The linear magnetic Schrödinger equation

$$ih\partial_t\psi = \frac{1}{2}(ih\nabla + \varepsilon\mathbf{A})^2\psi - V\psi$$

$$\psi(\mathbf{x}, 0) = \psi_I(\mathbf{x})$$

Here θ is a factor amplifying the influence of the internal parts of the potentials.

The initial data used are eigenstates of the stationary Schrödinger equation with harmonic oscillator potential (cf. [G] for a derivation in a similar scaling):

The first one reads

$$\psi_{I\uparrow}(x, y) = \frac{\overbrace{1}^{(i.)}}{\sqrt{\pi}} \overbrace{e^{-\frac{1}{2}(\frac{x}{y}) - (\frac{1}{1})^2}}^{(ii.)}} \overbrace{e^{i(\frac{x}{y}) \cdot (\frac{-5}{5})}}^{(iii.)}}$$

$$\psi_{I\downarrow}(x, y) = 0$$

Where

- (i.) is a normalization factor,
- (ii.) the main part of the wavefunction with maximum at $\begin{pmatrix} 1 \\ 1 \end{pmatrix}$,
- (iii.) a phase factor with wave vector $\begin{pmatrix} -5 \\ 5 \end{pmatrix}$

In the Pauli equation, the potential \mathbf{A} influences the impulse of the resulting wave function - in the considered example, this influence is exerted parallel to the y-axis (w.r.t. the coordinates in the metallic plate).

Together with the influence of V and the translation of the position expectation in part (ii.) of the wavefunction, this causes a *rotation* of the position expectation over time.

Part (iii.) governs the direction of propagation of the wavefunction.

Here a scaling of $\theta = 99$ is used (which corresponds to a strongly dominating self-consistent field).

The second initial condition is

$$\psi_{I\uparrow}(x, y) = \frac{1 - (x^2 + y^2)}{\sqrt{\pi}} e^{-\frac{x^2 + y^2}{2}}$$

$$\psi_{I\downarrow}(x, y) = 0$$

In this case, a scaling of $\theta = 33$ is used (i.e. a moderately strong self-consistent field).

The following effects can be observed in the results of the simulations:

- The spin-magnetic field coupling (in the Pauli-Poiswell system and the Pauli equation) leads to an oscillation between up-state and down-state.
- The frequency and period of this oscillation does not depend on initial condition and scaling of the self-consistent part (cf. page 86).
- Scaling of the self-consistent part leads to a blur of the position densities.

Scaling of the self-consistent part yields an inconsistent model: a particle moving at 'slow' speed is assumed to generate a self-consistent field corresponding to a 'fast' particle. This leads to a violation of the conservation of mass - as can be observed in the following images.

5.2 Numerical data

First initial condition at time $t=0.1$

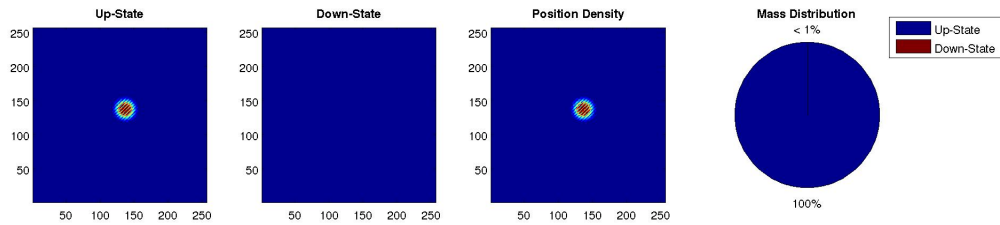


Figure 5.1: Pauli-Poiswell at time $t=0.1$

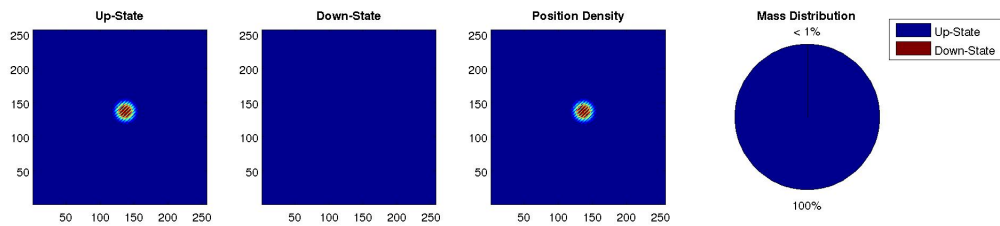


Figure 5.2: linear Pauli at time $t=0.1$

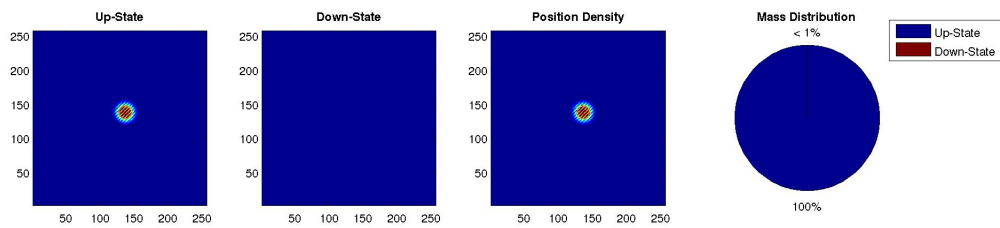


Figure 5.3: Magnetic Schrödinger-Poiswell at time $t=0.1$

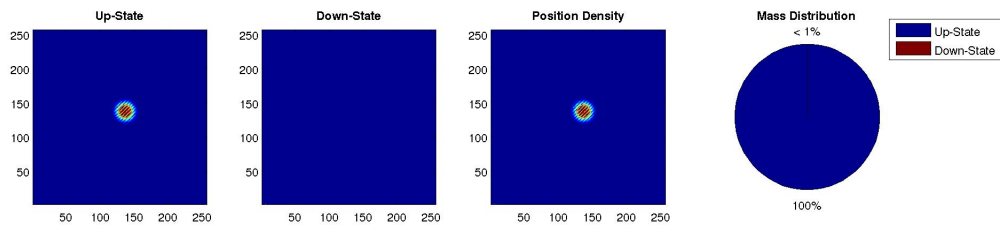
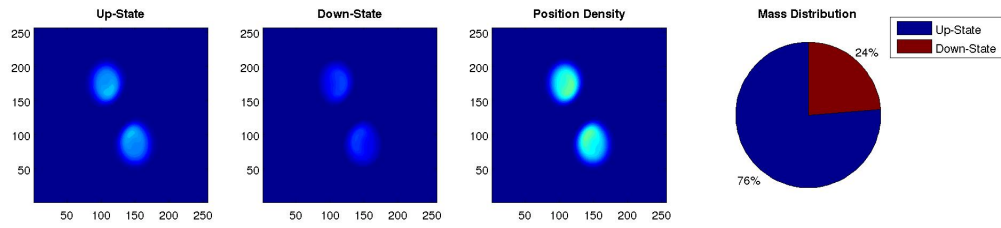
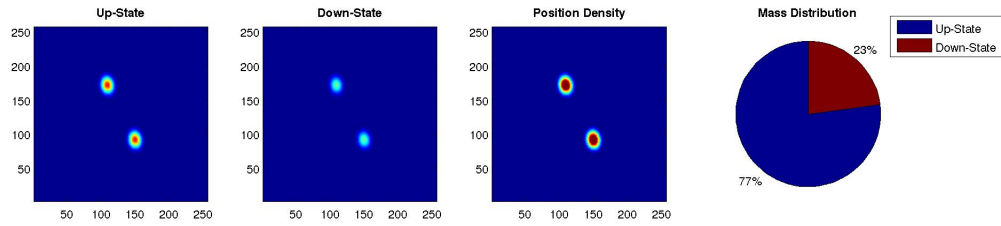
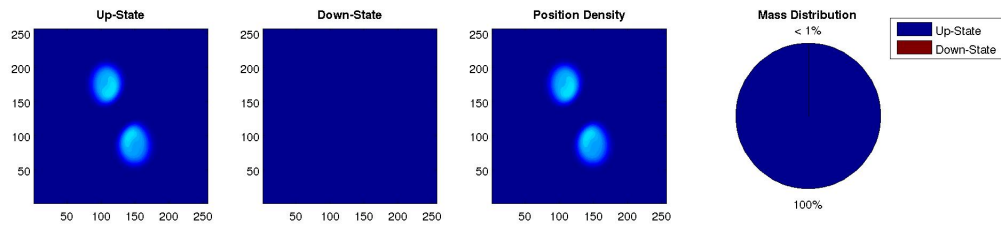
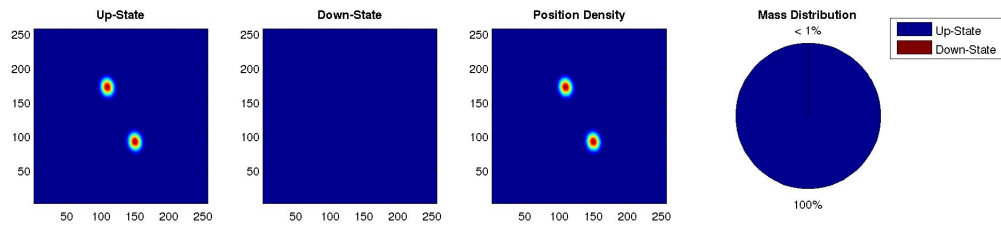


Figure 5.4: linear Magnetic Schrödinger at time $t=0.1$

Time $t=1.1$ Figure 5.5: Pauli-Poiswell at time $t=1.1$ Figure 5.6: linear Pauli at time $t=1.1$ Figure 5.7: Magnetic Schrödinger-Poiswell at time $t=1.1$ Figure 5.8: linear Magnetic Schrödinger at time $t=1.1$

Time $t=2.1$

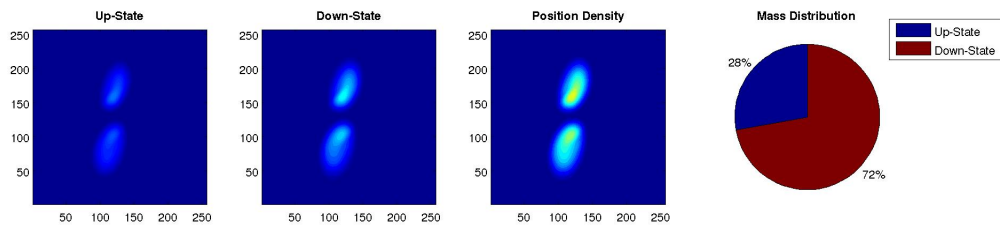


Figure 5.9: Pauli-Poiswell at time $t=2.1$

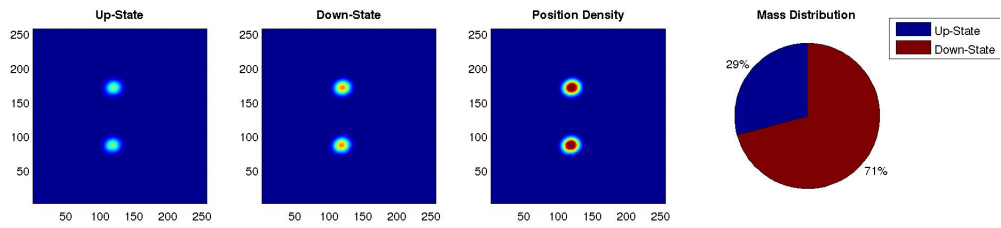


Figure 5.10: linear Pauli at time $t=2.1$

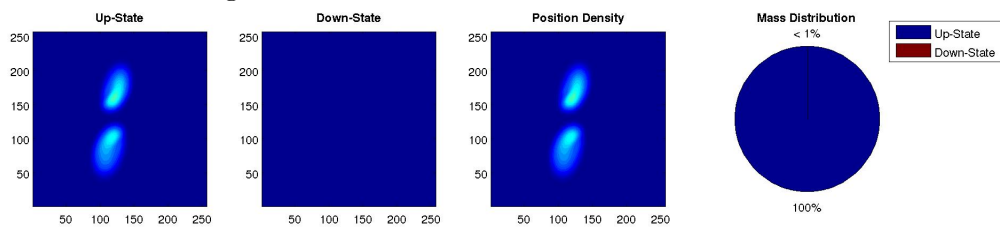


Figure 5.11: Magnetic Schrödinger-Poiswell at time $t=2.1$

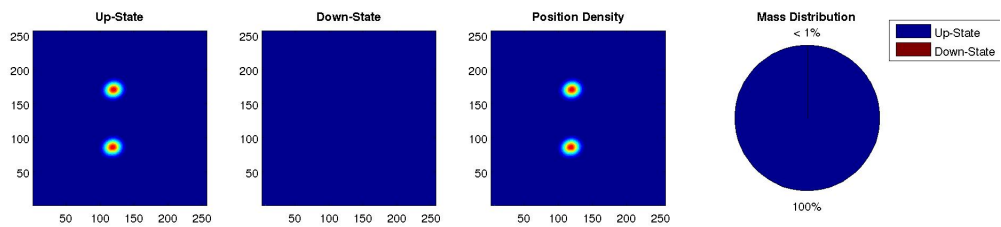
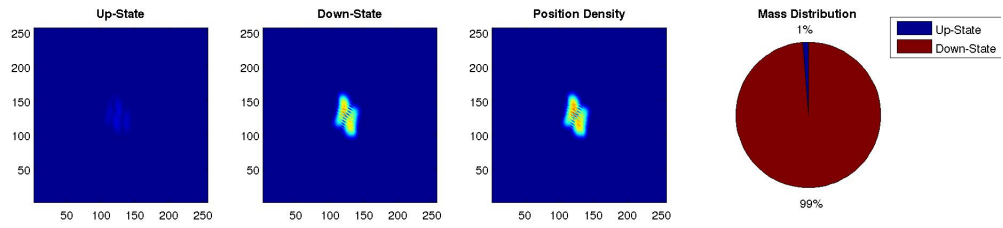
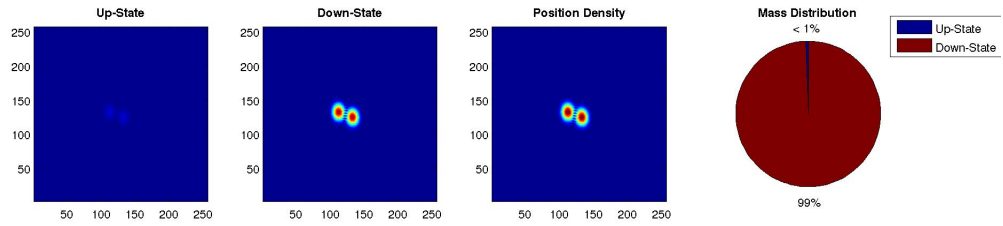
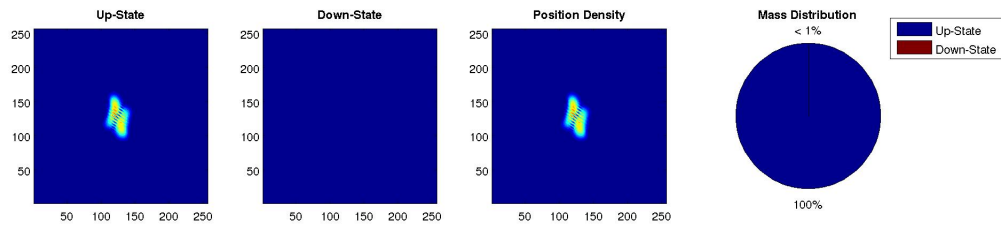
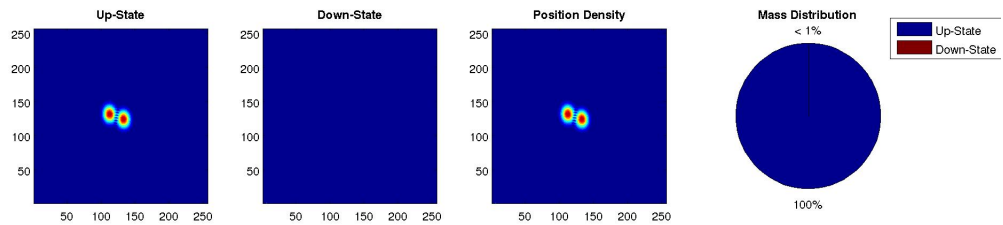


Figure 5.12: linear Magnetic Schrödinger at time $t=2.1$

Time $t=3.1$ Figure 5.13: Pauli-Poiswell at time $t=3.1$ Figure 5.14: linear Pauli at time $t=3.1$ Figure 5.15: Magnetic Schrödinger-Poiswell at time $t=3.1$ Figure 5.16: linear Magnetic Schrödinger at time $t=3.1$

Time $t=4.1$

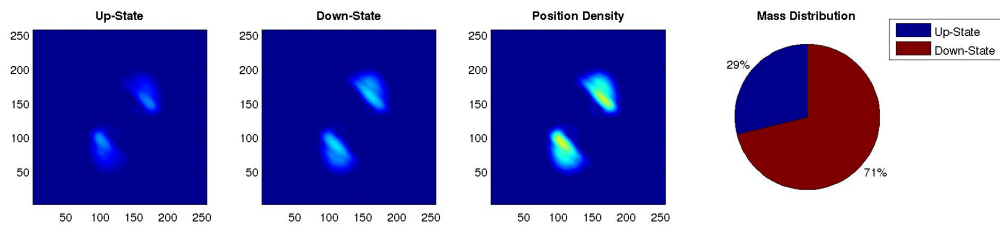


Figure 5.17: Pauli-Poiswell at time $t=4.1$

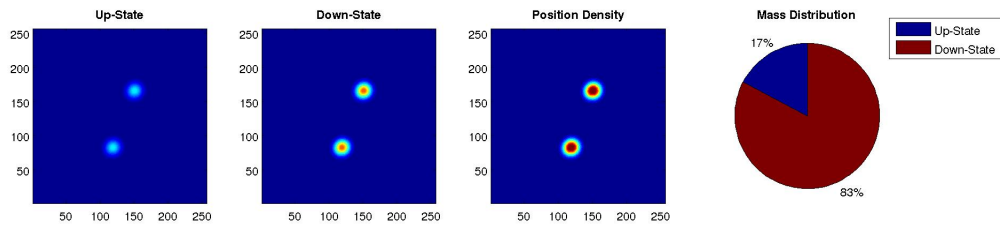


Figure 5.18: linear Pauli at time $t=4.1$

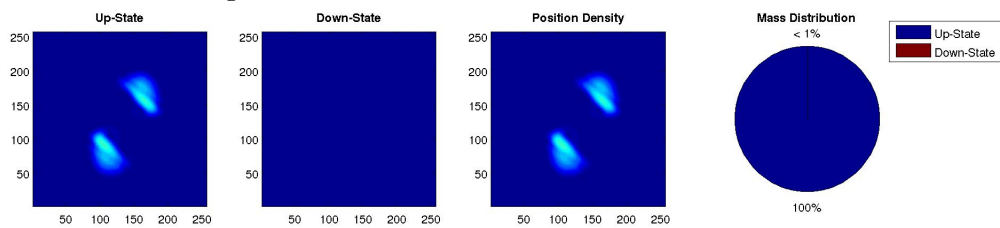


Figure 5.19: Magnetic Schrödinger-Poiswell at time $t=4.1$

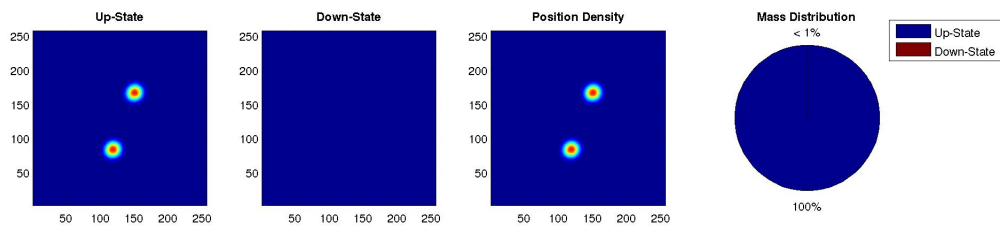
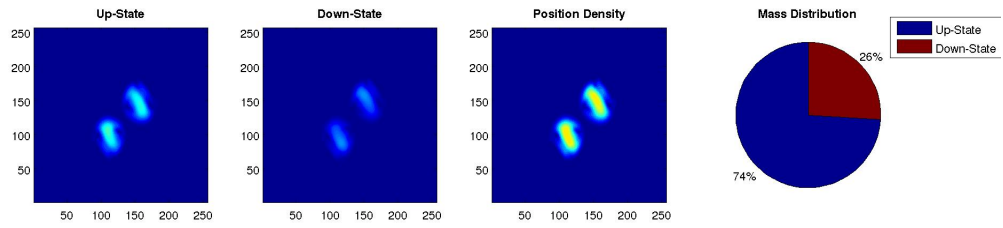
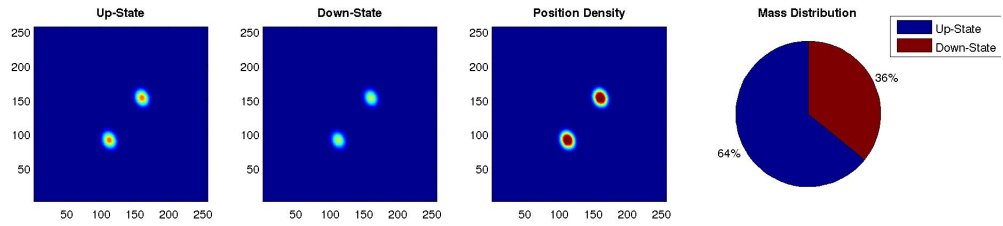
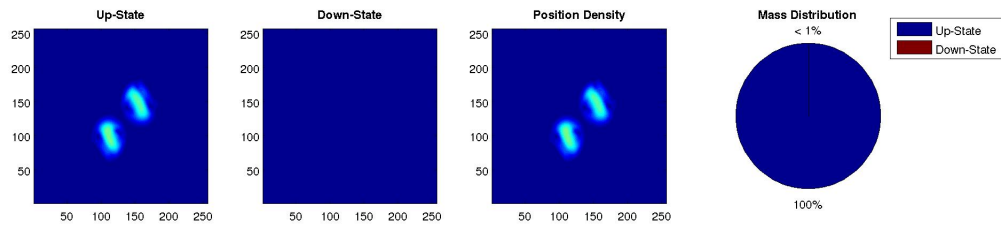
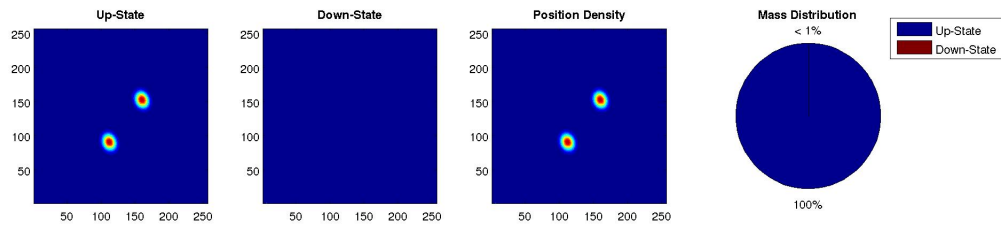


Figure 5.20: linear Magnetic Schrödinger at time $t=4.1$

Time $t=5.1$ Figure 5.21: Pauli-Poiswell at time $t=5.1$ Figure 5.22: linear Pauli at time $t=5.1$ Figure 5.23: Magnetic Schrödinger-Poiswell at time $t=5.1$ Figure 5.24: linear Magnetic Schrödinger at time $t=5.1$

Time $t=6.1$

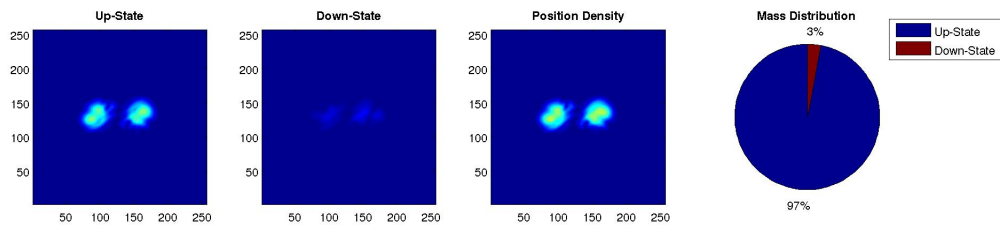


Figure 5.25: Pauli-Poiswell at time $t=6.1$

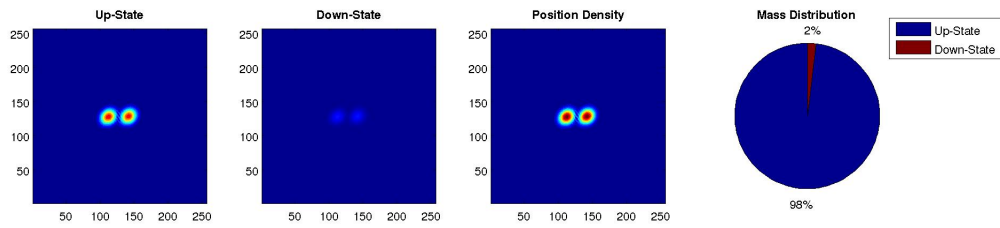


Figure 5.26: linear Pauli at time $t=6.1$

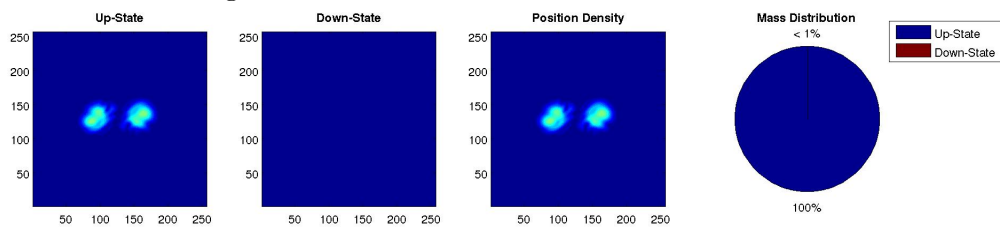


Figure 5.27: Magnetic Schrödinger-Poiswell at time $t=6.1$

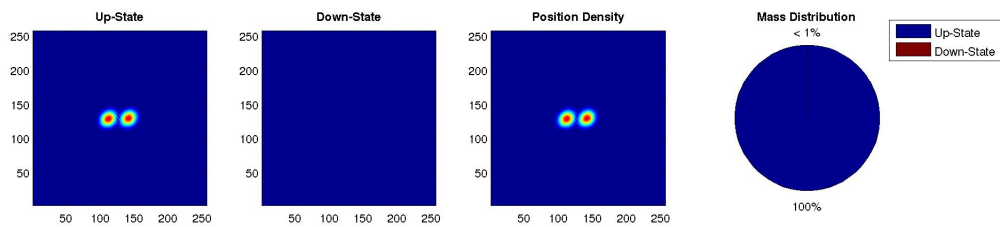
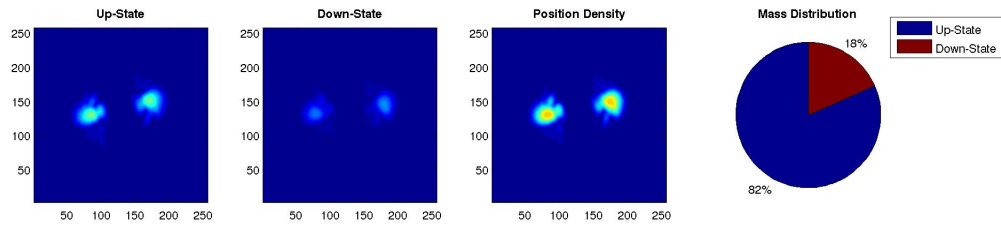
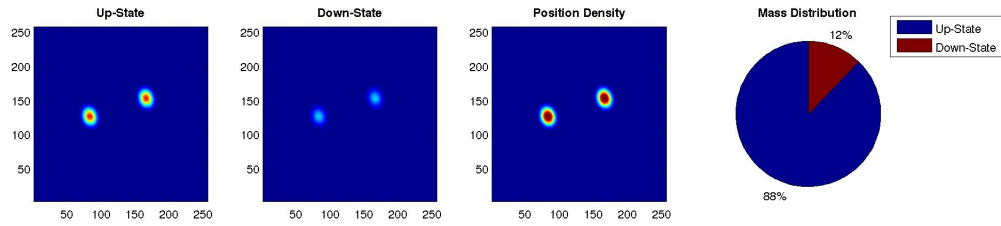
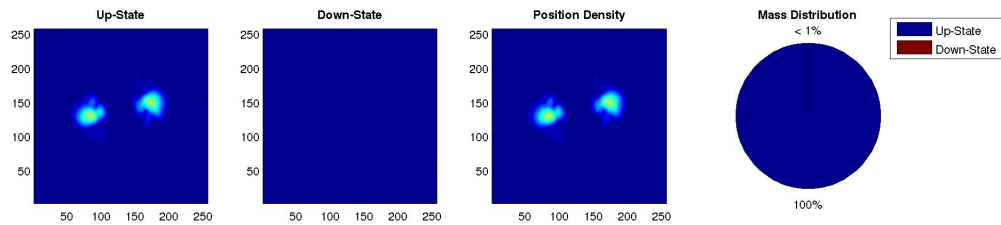
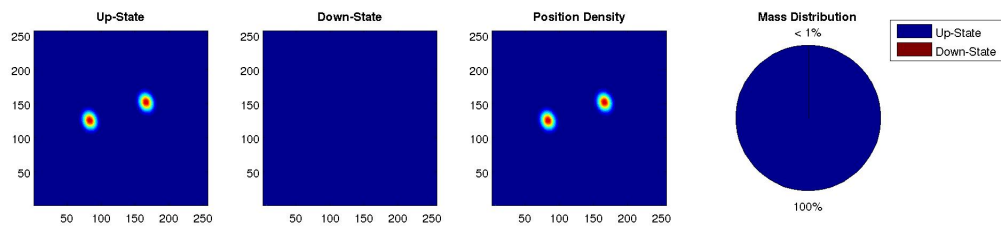


Figure 5.28: linear Magnetic Schrödinger at time $t=6.1$

Time $t=7.1$ Figure 5.29: Pauli-Poiswell at time $t=7.1$ Figure 5.30: linear Pauli at time $t=7.1$ Figure 5.31: Magnetic Schrödinger-Poiswell at time $t=7.1$ Figure 5.32: linear Magnetic Schrödinger at time $t=7.1$

Time $t=8.1$

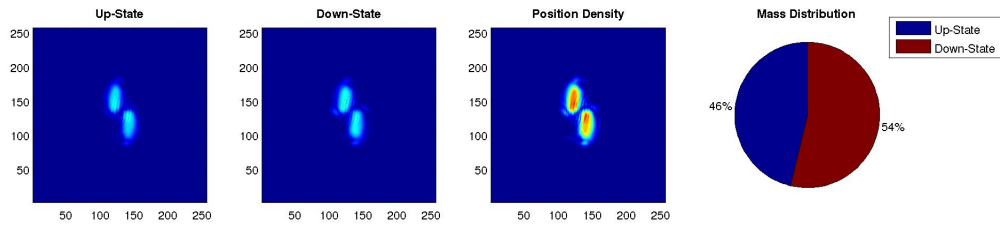


Figure 5.33: Pauli-Poiswell at time $t=8.1$

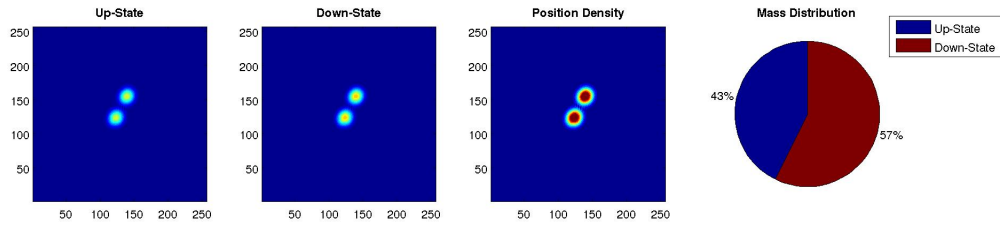


Figure 5.34: linear Pauli at time $t=8.1$

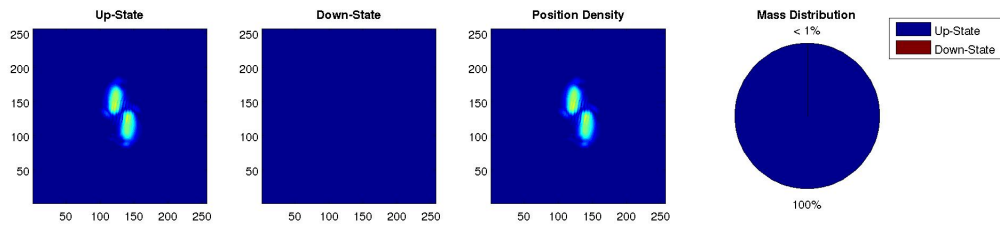


Figure 5.35: Magnetic Schrödinger-Poiswell at time $t=8.1$

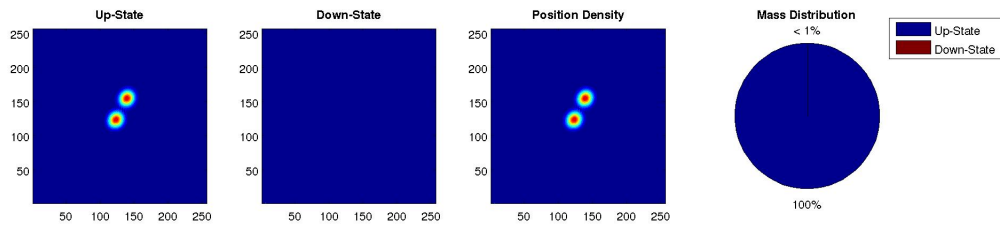
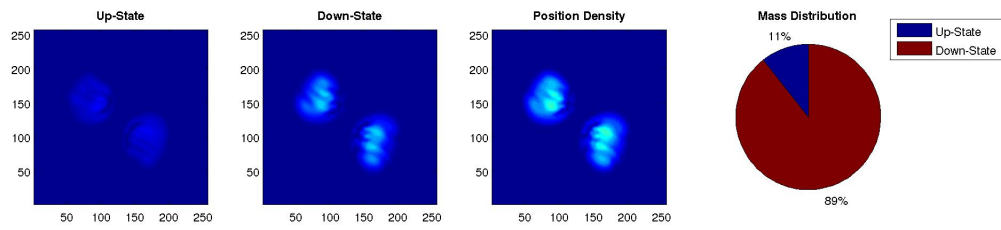
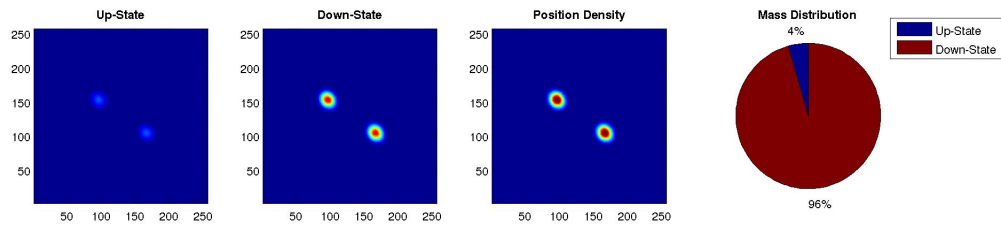
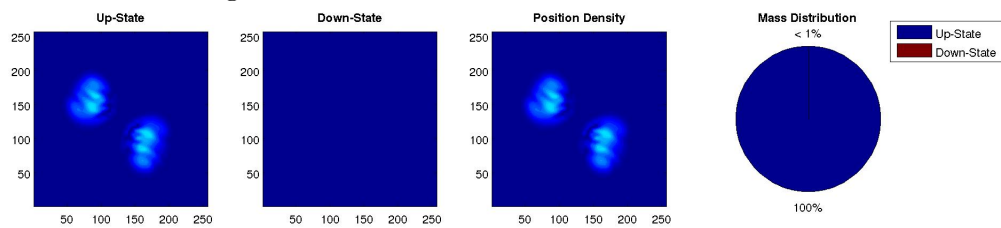
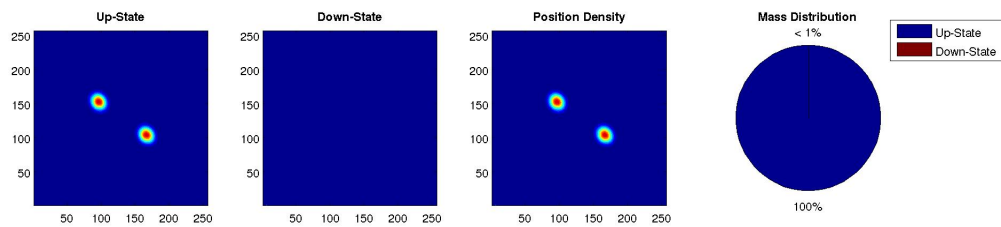


Figure 5.36: linear Magnetic Schrödinger at time $t=8.1$

Time $t=9.1$ Figure 5.37: Pauli-Poiswell at time $t=9.1$ Figure 5.38: linear Pauli at time $t=9.1$ Figure 5.39: Magnetic Schrödinger-Poiswell at time $t=9.1$ Figure 5.40: linear Magnetic Schrödinger at time $t=9.1$

Second initial condition at time $t=0.1$

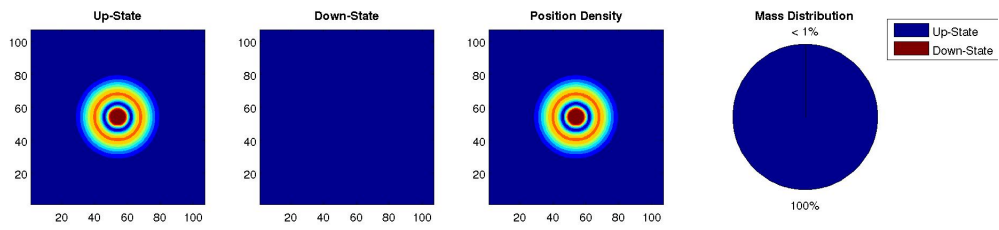


Figure 5.41: Pauli-Poiswell at time $t=0.1$

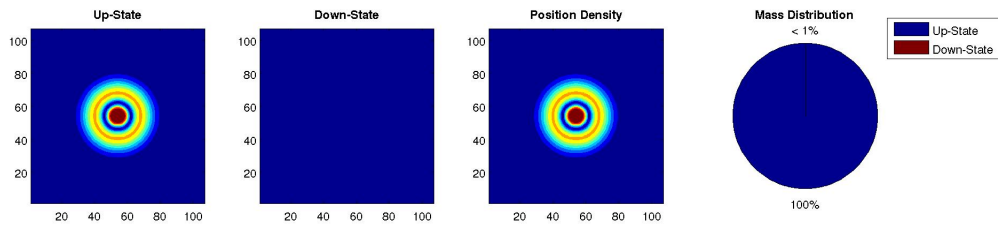


Figure 5.42: linear Pauli at time $t=0.1$

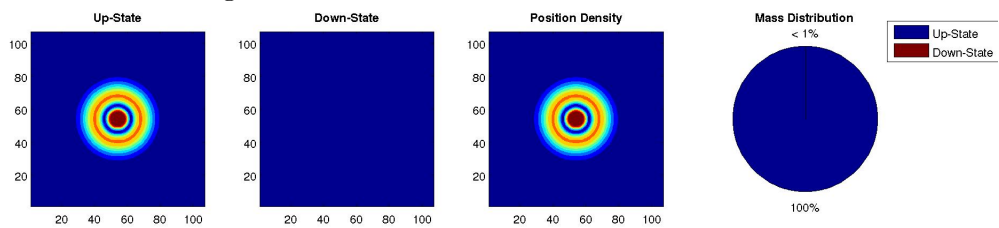


Figure 5.43: Magnetic Schrödinger-Poiswell at time $t=0.1$

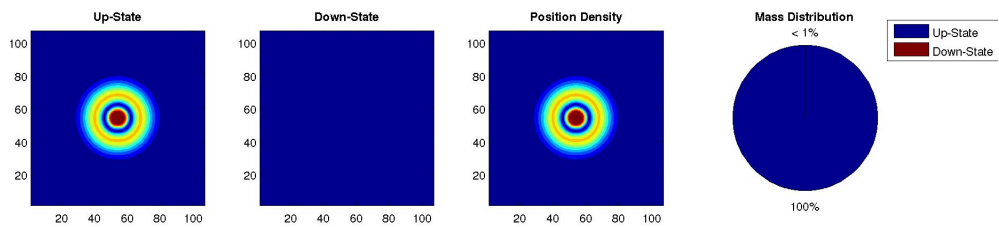
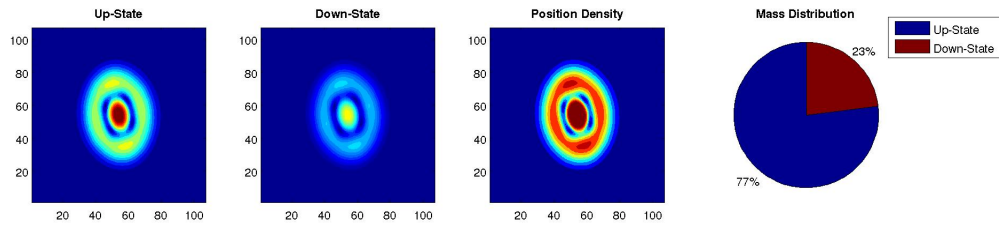
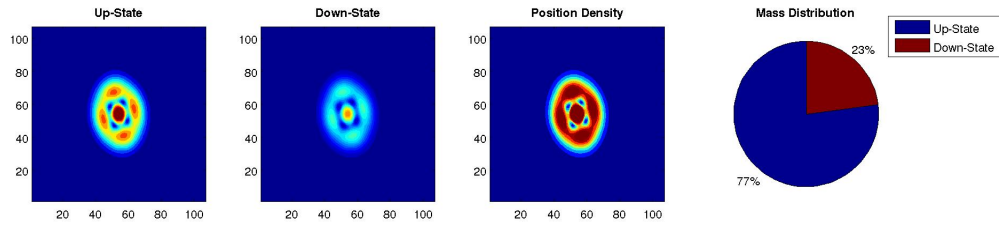
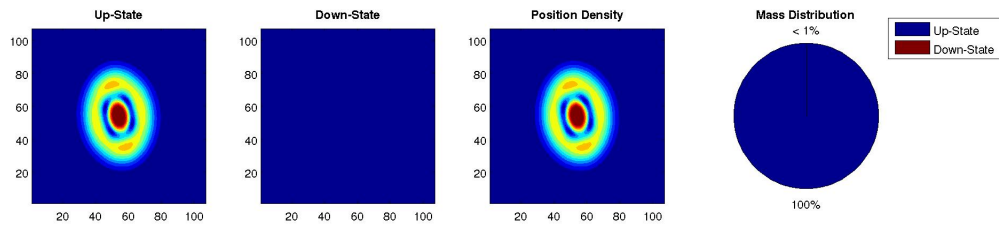
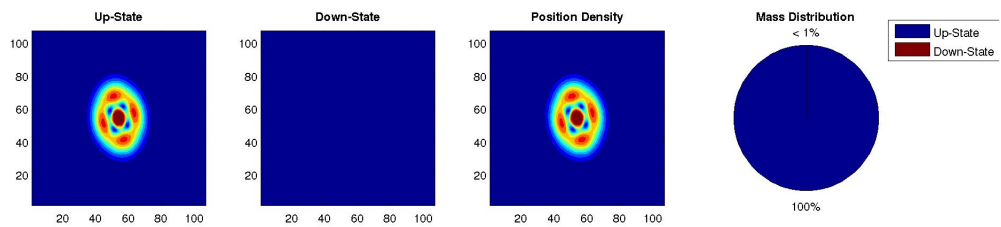


Figure 5.44: linear Magnetic Schrödinger at time $t=0.1$

Time $t=1.1$ Figure 5.45: Pauli-Poiswell at time $t=1.1$ Figure 5.46: linear Pauli at time $t=1.1$ Figure 5.47: Magnetic Schrödinger-Poiswell at time $t=1.1$ Figure 5.48: linear Magnetic Schrödinger at time $t=1.1$

Time $t=2.1$

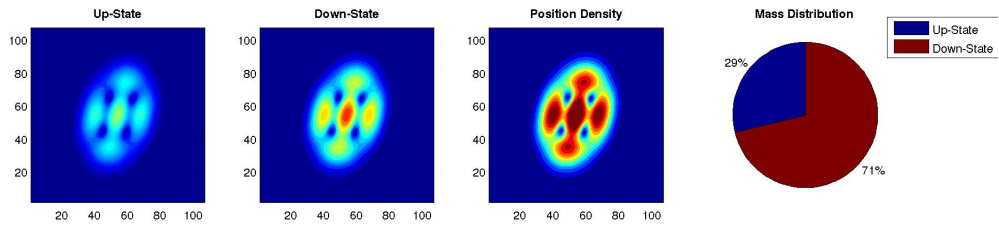


Figure 5.49: Pauli-Poiswell at time $t=2.1$

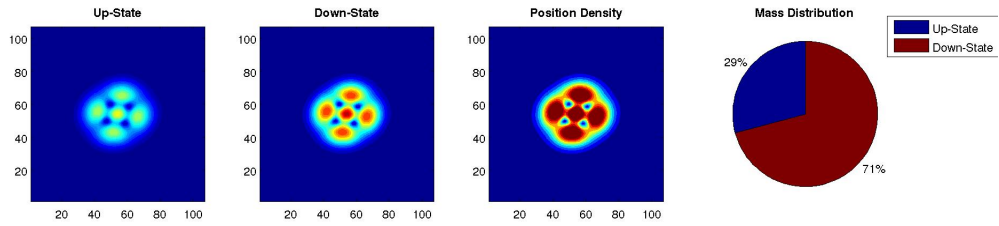


Figure 5.50: linear Pauli at time $t=2.1$

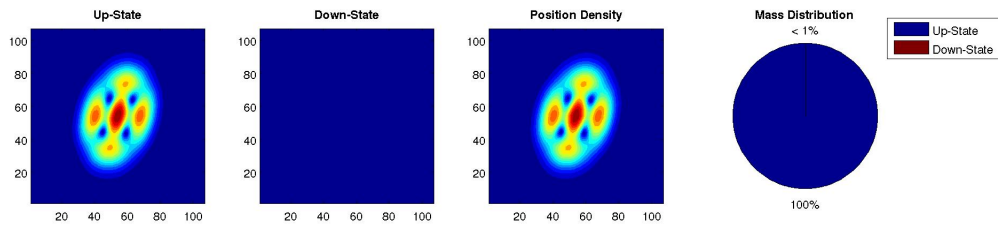


Figure 5.51: Magnetic Schrödinger-Poiswell at time $t=2.1$

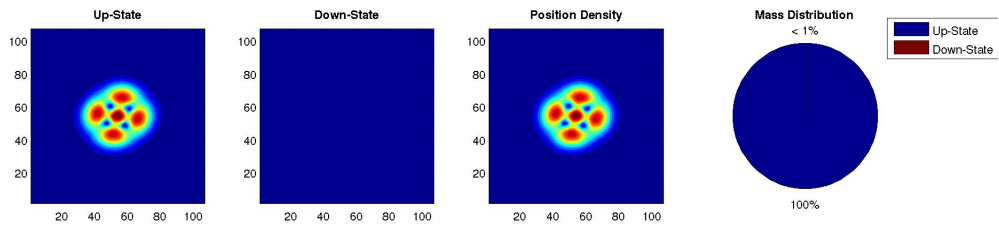
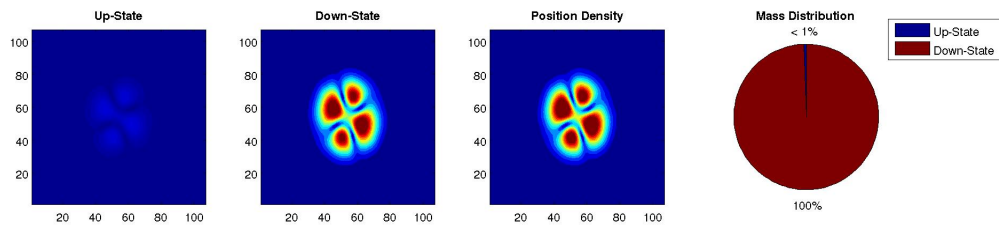
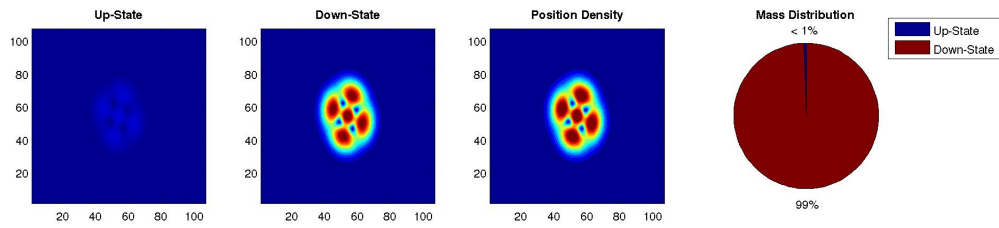
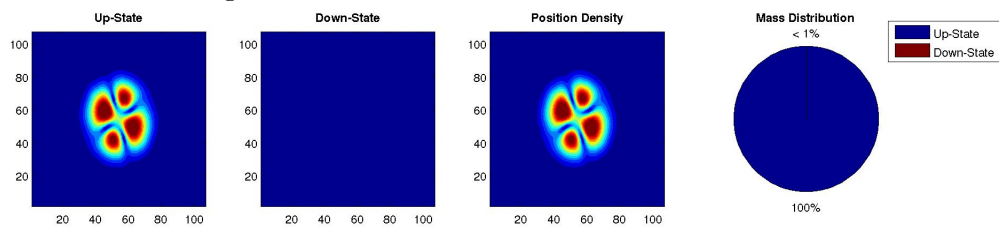
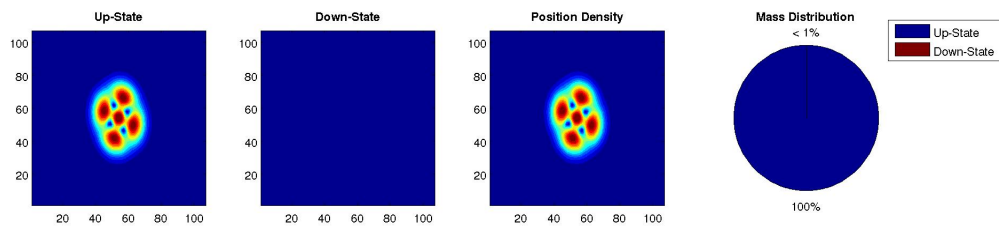


Figure 5.52: linear Magnetic Schrödinger at time $t=2.1$

Time $t=3.1$ Figure 5.53: Pauli-Poiswell at time $t=3.1$ Figure 5.54: linear Pauli at time $t=3.1$ Figure 5.55: Magnetic Schrödinger-Poiswell at time $t=3.1$ Figure 5.56: linear Magnetic Schrödinger at time $t=3.1$

Time $t=4.1$

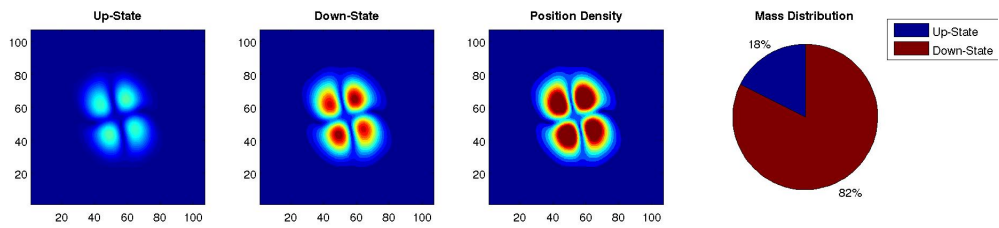


Figure 5.57: Pauli-Poiswell at time $t=4.1$

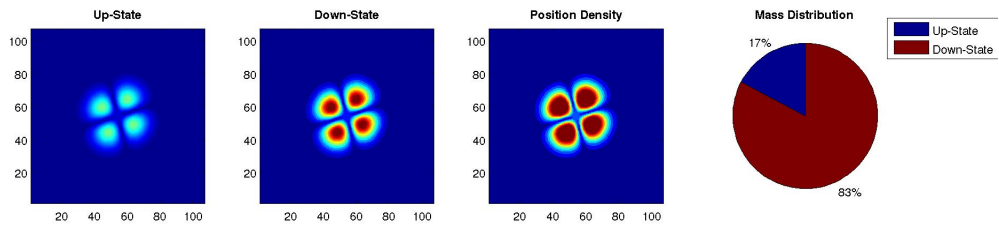


Figure 5.58: linear Pauli at time $t=4.1$

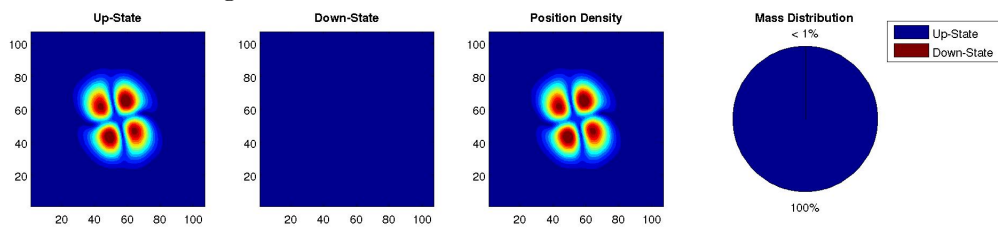


Figure 5.59: Magnetic Schrödinger-Poiswell at time $t=4.1$

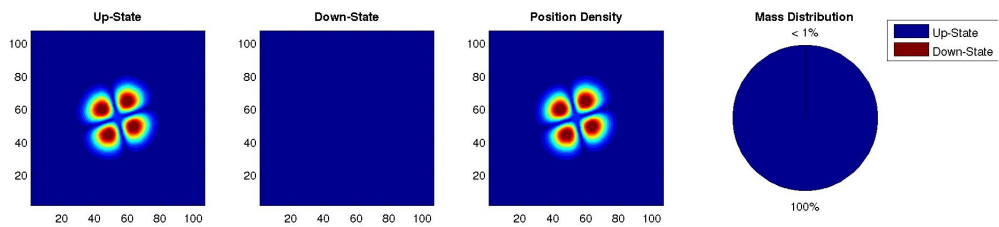
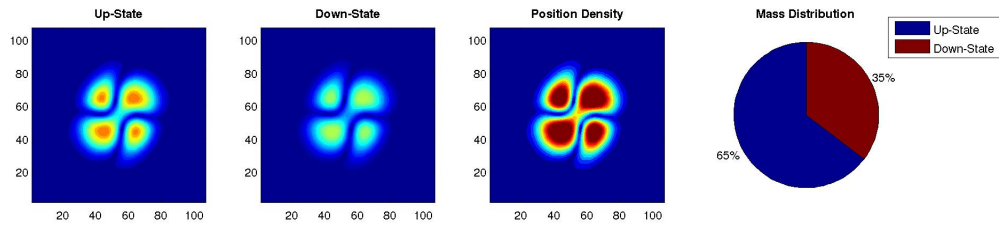
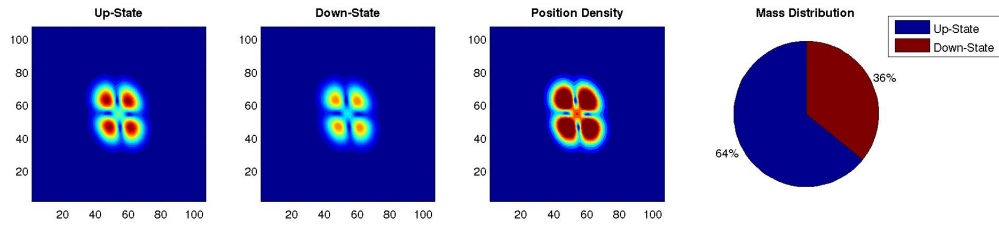
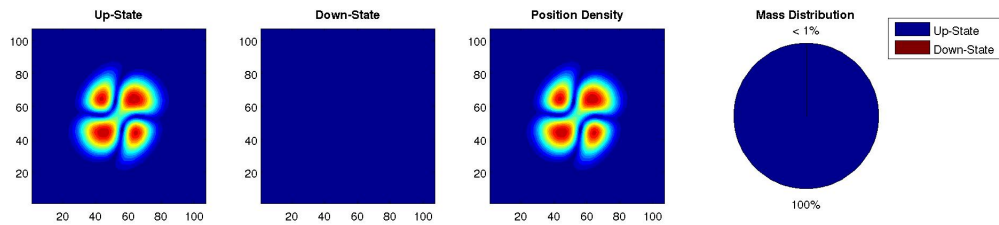
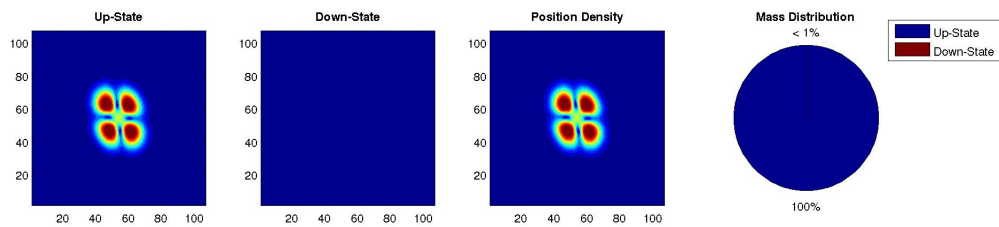


Figure 5.60: linear Magnetic Schrödinger at time $t=4.1$

Time $t=5.1$ Figure 5.61: Pauli-Poiswell at time $t=5.1$ Figure 5.62: linear Pauli at time $t=5.1$ Figure 5.63: Magnetic Schrödinger-Poiswell at time $t=5.1$ Figure 5.64: linear Magnetic Schrödinger at time $t=5.1$

Time $t=6.1$

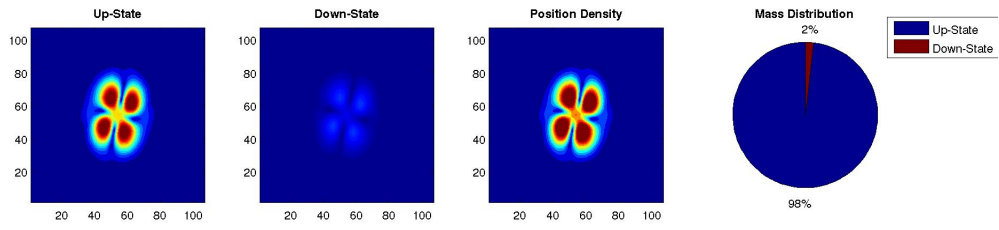


Figure 5.65: Pauli-Poiswell at time $t=6.1$

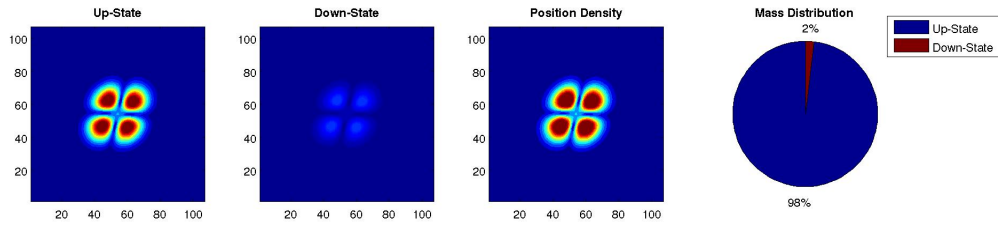


Figure 5.66: linear Pauli at time $t=6.1$

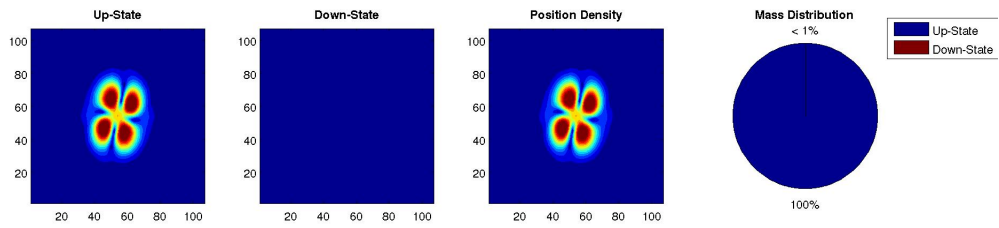


Figure 5.67: Magnetic Schrödinger-Poiswell at time $t=6.1$

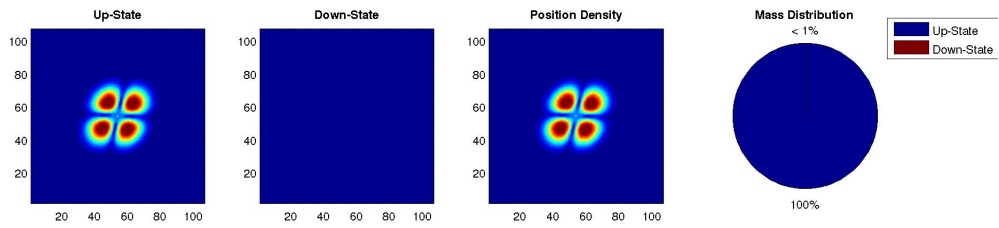
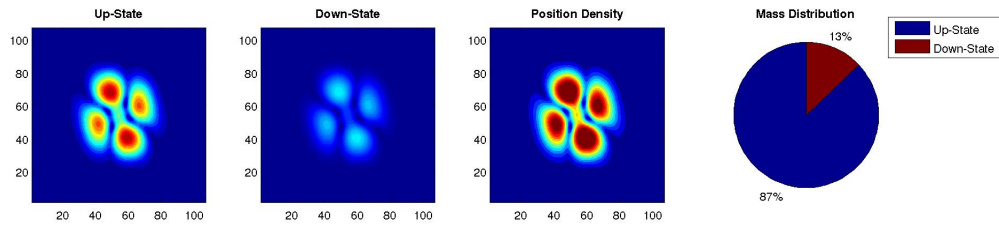
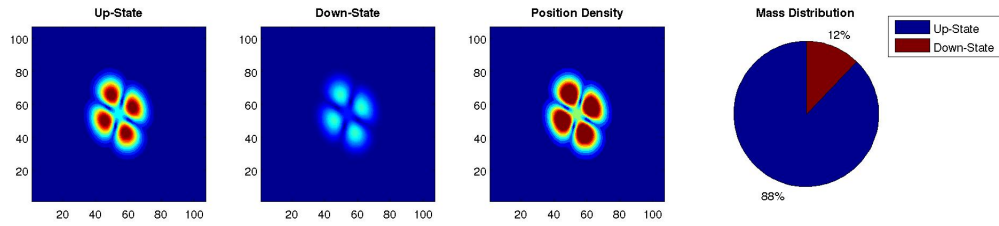
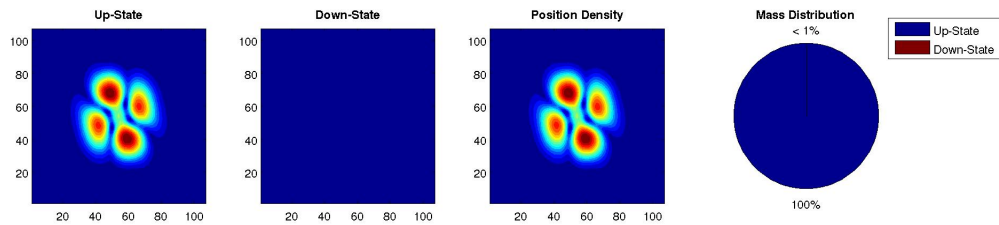
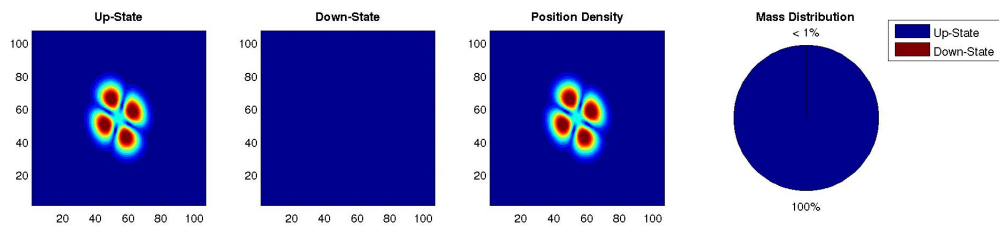


Figure 5.68: linear Magnetic Schrödinger at time $t=6.1$

Time $t=7.1$ Figure 5.69: Pauli-Poiswell at time $t=7.1$ Figure 5.70: linear Pauli at time $t=7.1$ Figure 5.71: Magnetic Schrödinger-Poiswell at time $t=7.1$ Figure 5.72: linear Magnetic Schrödinger at time $t=7.1$

Time $t=8.1$

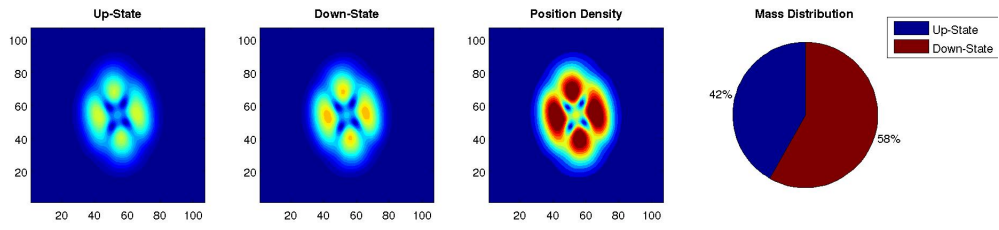


Figure 5.73: Pauli-Poiswell at time $t=8.1$

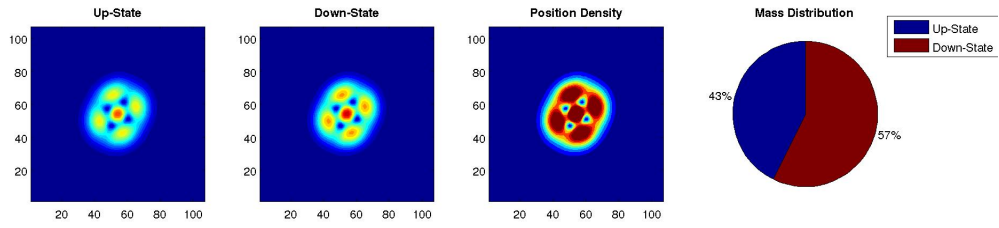


Figure 5.74: linear Pauli at time $t=8.1$

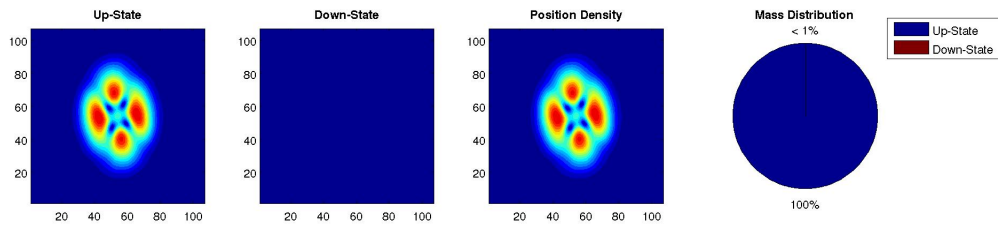


Figure 5.75: Magnetic Schrödinger-Poiswell at time $t=8.1$

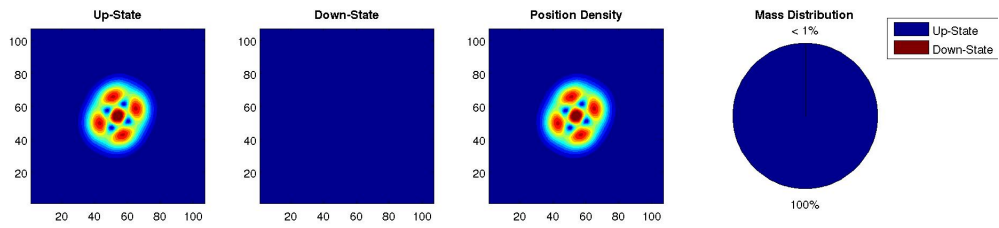
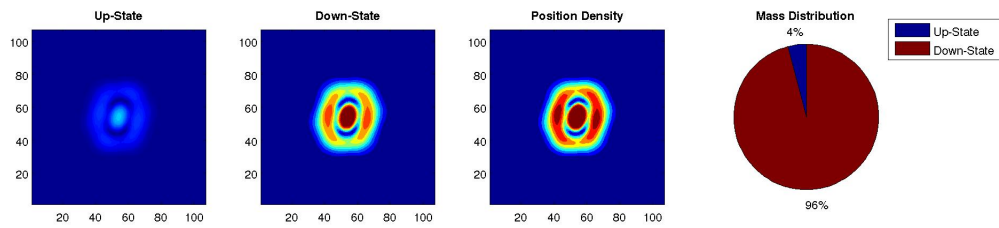
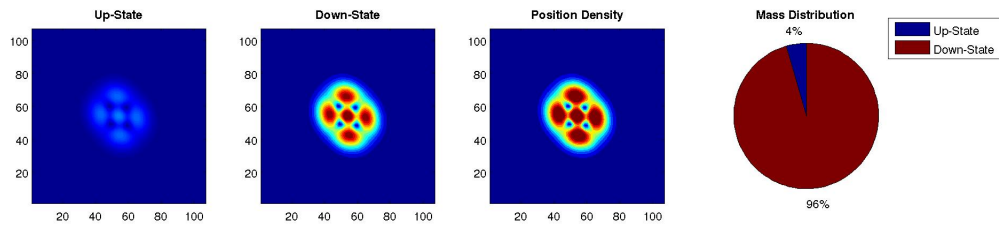
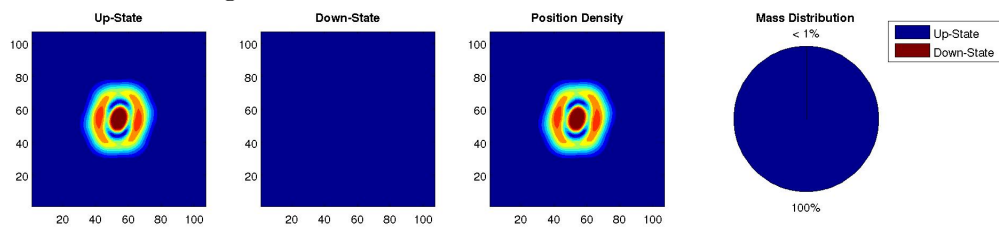
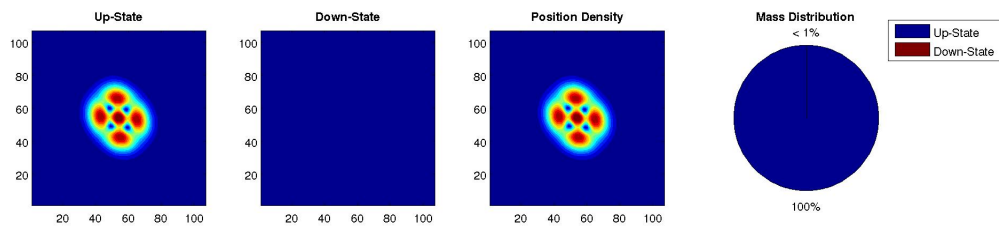


Figure 5.76: linear Magnetic Schrödinger at time $t=8.1$

Time $t=9.1$ Figure 5.77: Pauli-Poiswell at time $t=9.1$ Figure 5.78: linear Pauli at time $t=9.1$ Figure 5.79: Magnetic Schrödinger-Poiswell at time $t=9.1$ Figure 5.80: linear Magnetic Schrödinger at time $t=9.1$

Oscillation between up-state and down-state

As mentioned above, the spin-magnetic field coupling leads to an oscillation between up-state and down-state. The frequency and period of this oscillation depend only on the strength of the magnetic field and are independent of initial condition and scaling of the self-consistent part.

These plots are made from the data of the simulations described above:

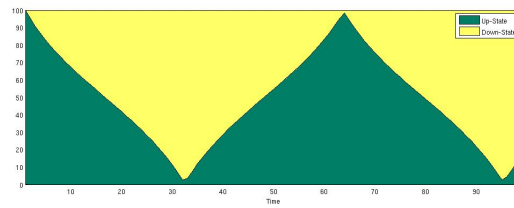


Figure 5.81: Pauli-Poiswell, first initial condition

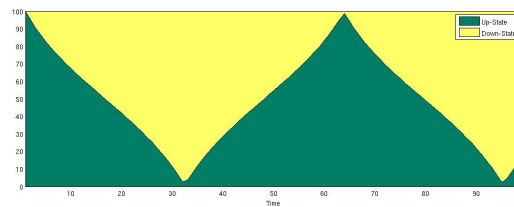


Figure 5.82: linear Pauli, first initial condition

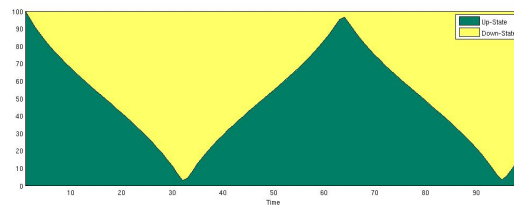


Figure 5.83: Pauli-Poiswell, second initial condition

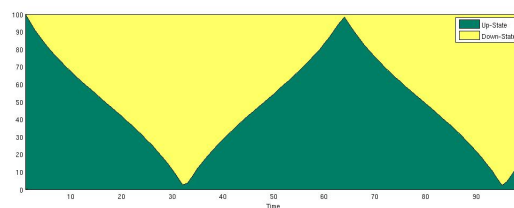


Figure 5.84: linear Pauli, second initial condition

Interference phenomena

Here are some close-ups of the interference phenomena occurring in the Pauli-Poiswell- and the linear Pauli approximation with the first initial condition.

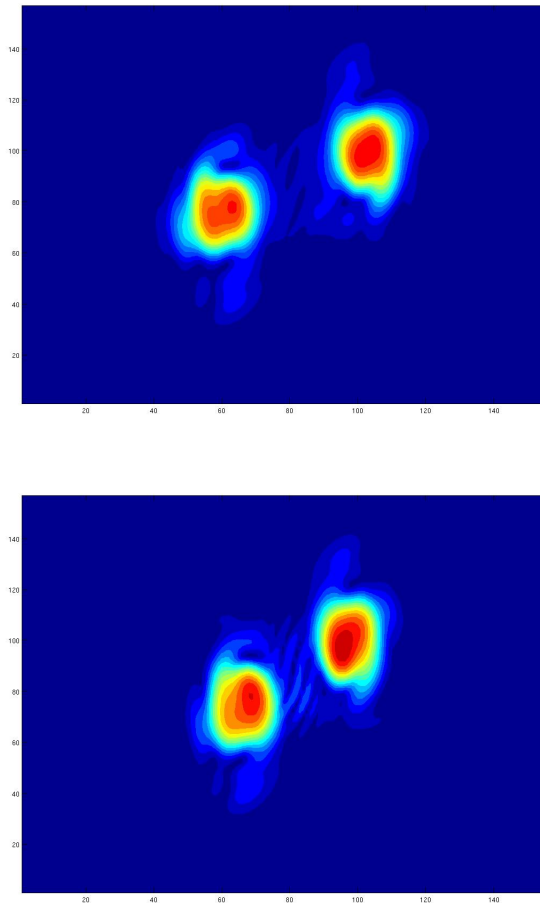


Figure 5.85: Pauli-Poiswell system

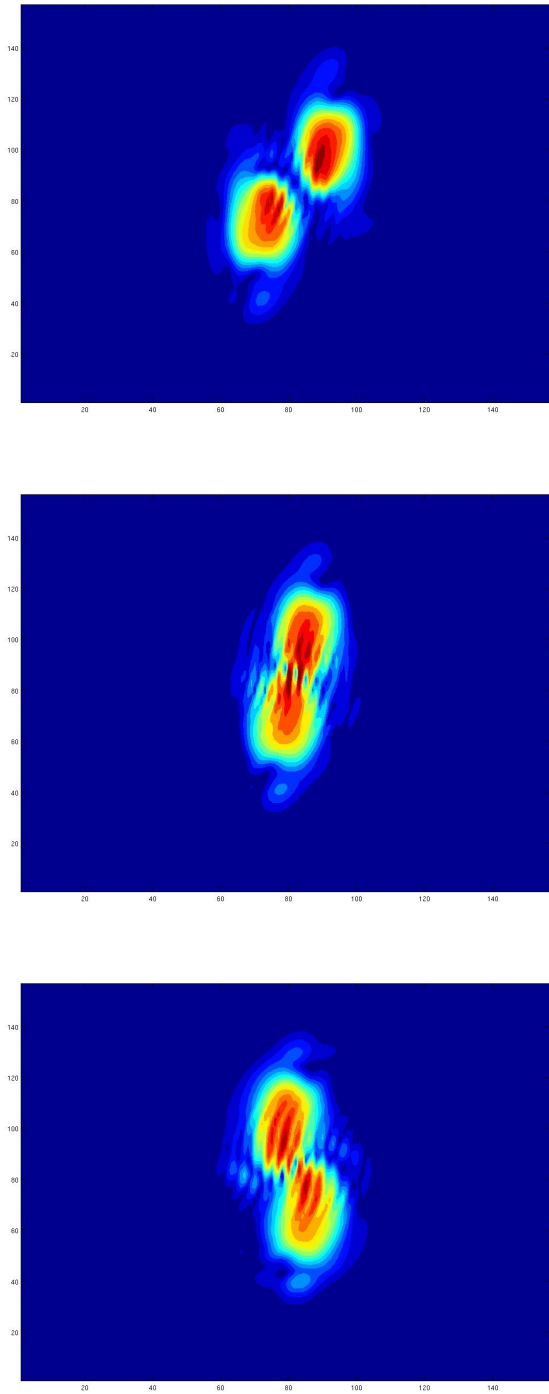


Figure 5.86: Pauli-Poiswell system

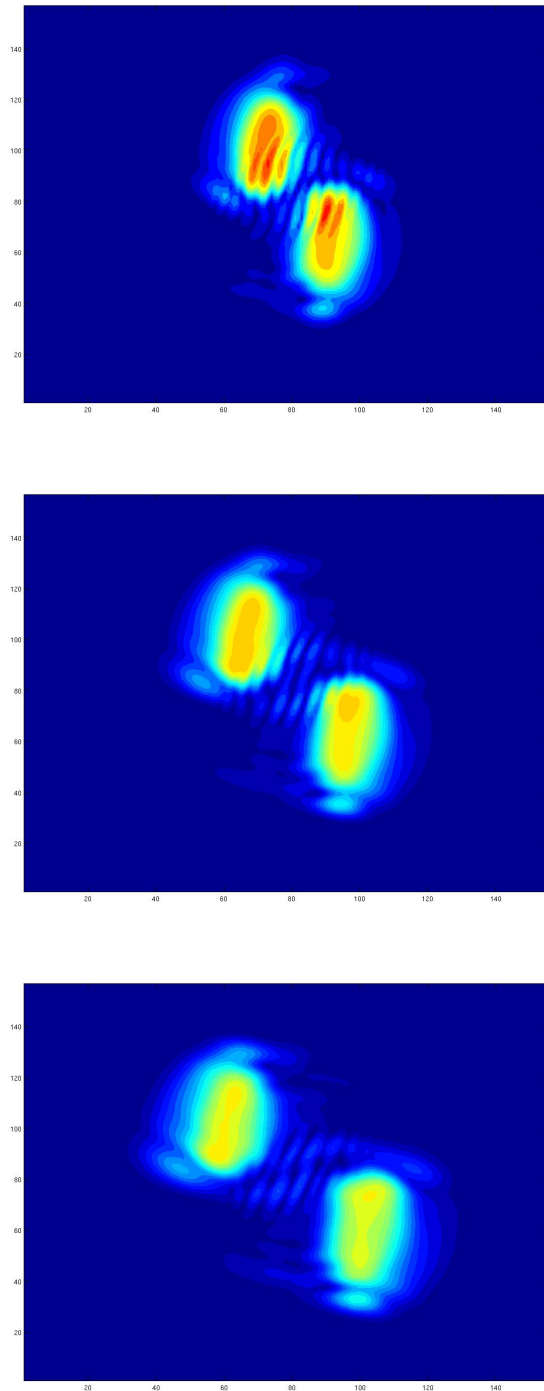


Figure 5.87: Pauli-Poiswell system

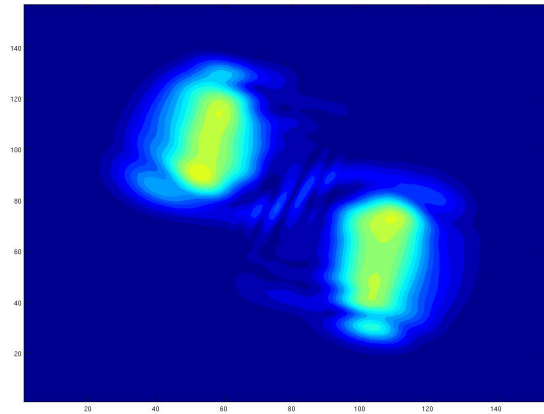


Figure 5.88: Pauli-Poiswell system

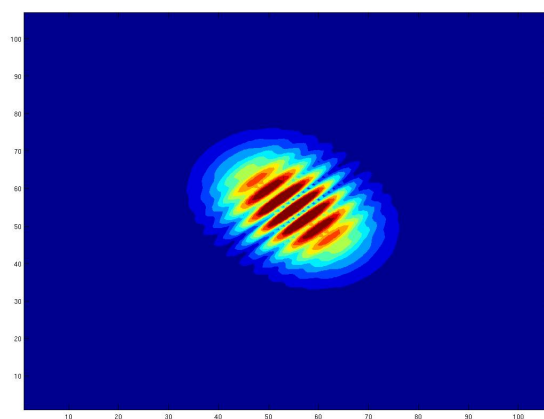
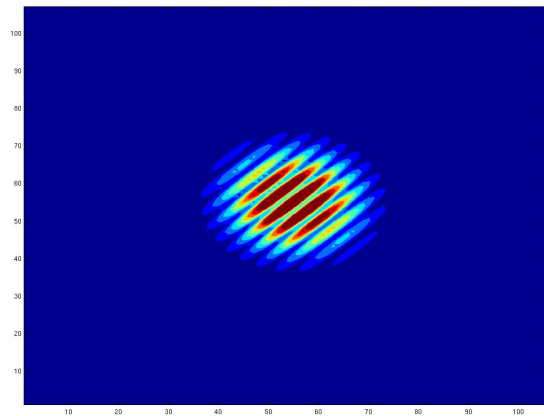


Figure 5.89: linear Pauli

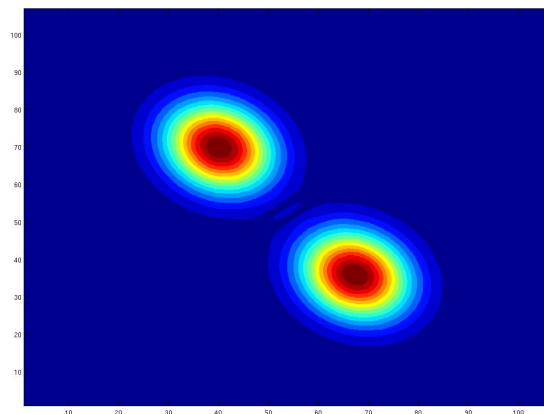
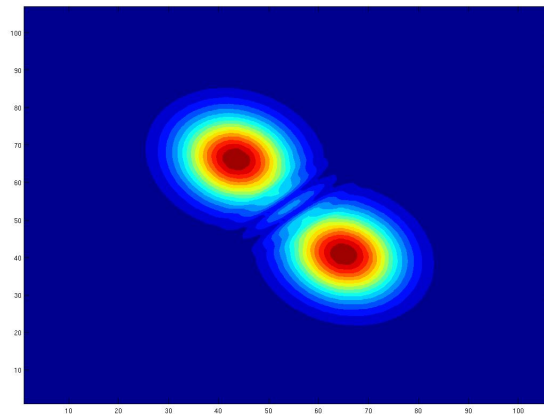
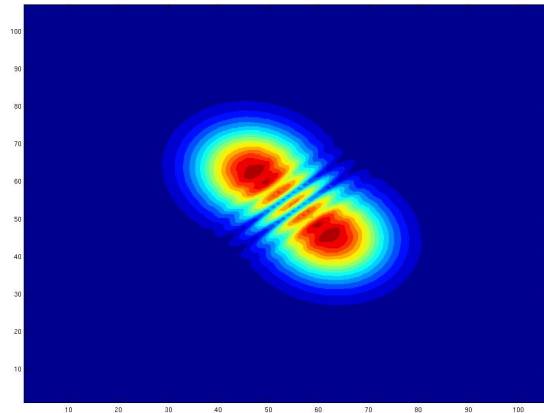


Figure 5.90: linear Pauli

Appendix A

Curriculum Vitae

Personal Data

- Name: David Wimmesberger
- Born on March 6th, 1985 in Salzburg, Austria
- Nationality: Austria

Education

- 1991-1995: Volksschule Oberndorf bei Salzburg
- 1995-2003: Musisches Gymnasium Salzburg, Matura on June 30th, 2003
- 2004- : Diploma Studies of Mathematics at the University of Vienna, Austria
- Summer term 2008: Exchange semester in Cork, Ireland

Work experience related to mathematics

- Tutor at the Faculty of Mathematics of the University of Vienna (2009 and 2010)
- Implementation of several algorithms for the Computer Mathematics Group of the Faculty of Mathematics of the University of Vienna

Bibliography

- [AA] A. Azzollini, P. d'Avenia, A. Pomponio, On the Schrödinger-Maxwell equations under the effect of a general nonlinear term, *Ann. I. H. Poincaré - AN* 27 (2010) 779-791
- [AJ] G. F. De Angelis, G. Jona-Lasinio, A stochastic description of a spin-1/2 particle in a magnetic field, *J. Phys. A: Math. Gen.* 15 2053 (1982)
- [AP] A. Azzollini, A. Pomponio, Ground state solutions for the nonlinear Schrödinger-Maxwell equations, *J. Math. Anal. Appl.* 345 (2008) 90-108
- [BB] Y. Bouguerra, A. Bounames, M. Maamache, Y. Saadi, Time-dependent Pauli equation in the presence of the Aharonov-Bohm effect, *Journal of Mathematical Physics* 49, 042107 (2008)
- [BD] A. Borzi, E. Decker, Analysis of a leap-frog pseudospectral scheme for the Schrödinger equation, *Journal of Computational and Applied Mathematics* 193 (2006) 65 - 88
- [BM] P. Bechouche, N.J. Mauser, F. Poupaud, (Semi-) Nonrelativistic Limits of the Dirac Equation with External Time-Dependent Electromagnetic Field, *Commun. Math. Phys.* 197, 405 - 425 (1998)
- [BM1] P. Bechouche, N.J. Mauser, S. Selberg, Nonrelativistic limit of Klein-Gordon Maxwell to Schrödinger-Poisson, *Amer. J. Math.* 126 (1) (2004) 31-64
- [BM2] P. Bechouche, N.J. Mauser, S. Selberg, On the asymptotic analysis of the Dirac-Maxwell system in the nonrelativistic limit, *J. Hyp.Diff. Equ.* 2 (1) (2005) 129 182
- [CF] H.L. Cycon, R.G. Froese, W. Kirsch, B. Simon - Schrödinger Operators (2nd corrected printing, Springer 2008)
- [CG] J.M. Chadam, R.T. Glassey, On the Maxwell-Dirac Equations with Zero Magnetic field and their Solution in Two Space Dimensions, *Journal of Mathematical Analysis and Applications* 53, 495-507 (1976)
- [CH] C. Canuto, M.Y. Hussaini, A. Quarteroni, T.A. Zang - Spectral Methods in Fluid Dynamics (Springer, New York 1988)
- [CP] C. Chang, M. Pelissier, P. Durand, Regular Two-Component Pauli-Like Effective Hamiltonians in Dirac Theory, *Physica Scripta*. Vol. 34, 394-404 (1986)

- [CS] A.M. Candela, A. Salvatore, Multiple Solitary Waves for Non-Homogeneous SchrödingerMaxwell Equations, *Mediterr. j. math.* 3 (2006), 483-493
- [E] L. Erdős, Ground-State Density of the Pauli Operator in the Large Field Limit, *Letters in Mathematical Physics* 29: 219-240 (1993)
- [ES] L. Erdős, J.P. Solovej, Uniform Lieb-Thirring Inequality for the Three-Dimensional Pauli Operator with a Strong Non-Homogeneous Magnetic Field, *Ann. Henri Poincaré* 5 (2004) 671 - 741
- [ES1] L. Erdős, J.P. Solovej, Semiclassical Eigenvalue Estimates for the Pauli Operator with Strong Non-Homogeneous Magnetic Fields, *Commun. Math. Phys.* 188, 599 - 656 (1997)
- [K] C.T. Kelley, *Iterative Methods for Linear and Nonlinear Equations* (SIAM, Philadelphia 1995)
- [G] W. Greiner, *Quantum Mechanics - An Introduction*, Fourth edition (Springer, Berlin, Heidelberg 2001)
- [G1] W. Greiner, *Classical Electrodynamics* (Springer-Verlag, New York, 1998)
- [GN] D.R. Grigore, G. Nenciu, R. Purice, On the nonrelativistic limit of the Dirac hamiltonian, *Ann. Inst. Henri Poincaré*, Vol. 51, no. 3, (1989) p. 231-263
- [H] C. Heitzinger, *Applied Analysis - Lecture Notes Summer Semester 2010* (University of Vienna)
- [HA] F. Haslinger, *Funktionalanalysis I,II - Skriptum zur Vorlesung*, Studienjahr 2006/2007 (University of Vienna)
- [HU] W. Hunziker, On the Nonrelativistic Limit of the Dirac Theory, *Commun. math. Phys.*, 215-222 (1975)
- [L] C. Lubich, On splitting methods for Schrödinger-Poisson and cubic nonlinear Schrödinger equations, *Math. Comp.* 77(2008), 2141-2153
- [LR] P.D. Lax, R.D. Richtmyer, Survey of the Stability of Linear Finite Difference Equations, *Communications on Pure and Applied Mathematics*, Vol. IX, 267-293 (1956)
- [M] N.J. Mauser, Semi-relativistic approximations of the Dirac equation: first and second order corrections, *Transp.Theor.Stat.Phys.* 29 (2000) 122-137
- [M1] N.J. Mauser, Rigorous derivation of the Pauli equation with time-dependent electromagnetic field, *VLSI Design* 9 (4), (1999) 415-426
- [MA] V.P. Maslov, *Semi-classical approximation in quantum mechanics* (D. Reidel Publishing Company, 1981)
- [MM] N. Masmoudi, N.J. Mauser, The Selfconsistent Pauli Equation, *Monatshefte der Mathematik* 132, 19-24(2001)

-
- [MS] N.J. Mauser, S. Selberg, Convergence of the Dirac-Maxwell system to the Vlasov-Poisson system, *Comm. PDE* 32 (3) (2007) 503-524
- [N] B. Najman, The nonrelativistic limit of the nonlinear Dirac equation, *Ann. Inst. Henri Poincaré*, Vol. 9, no 1 (1992) p. 3-12
- [S] H. Schichl, *Numerik 1 - Skriptum zur Vorlesung WS2000/01* (University of Vienna)
- [SC] A.Y. Schoene, On the Nonrelativistic Limits of the Klein-Gordon and Dirac Equations, *Journal of Mathematical Analysis and Applications* 71, 36-47 (1979)
- [ST] J.C. Strikwerda, *Finite Difference Schemes and Partial Differential Equations* (Second Edition, SIAM 2004)
- [T] G. Teschl, *Mathematical Methods in Quantum Mechanics* (AMS 2009)
- [T1] A. Tip - Atoms in circularly polarised fields: the dilatation-analytic approach, *J. Phys. A : Math. Gen.* 16 (1983) 3237-3259
- [QS] A. Quarteroni, R. Sacco, F. Saleri, *Numerische Mathematik 2* (Springer, Berlin, Heidelberg 2002)
- [QV] A. Quarteroni, A. Valli, *Numerical Approximation of Partial Differential Equations* (Springer, Berlin, Heidelberg, New York 1994)
- [W] G.B. White, Splitting of the Dirac operator in the nonrelativistic limit, *Ann. Inst. Henri Poincaré*, Vol. 53, no. 1, (1990) p. 109-121
- [Y] K. Yosida, *Functional Analysis* (Springer, Berlin, Heidelberg 1995)
- [YA] H. Yamasaki, A New Derivation of Classical Models of the Spinning Electron from the WKB-Solutions to the Pauli and Dirac Equations, *Progress of Theoretical Physics* Vol. 36, No. 1 (July 1966)

Images: Image of the Photoelectric Effect (page 10): Wikimedia Commons, created by User Wolfmankurd, released under GNU free Documentation Licence 1.2 and the Creative Commons Attribution ShareAlike 3.0 License.

Image of the Stern-Gerlach Experiment (page 19): Wikimedia Commons, created by User Theresa Knott, released under GNU free Documentation Licence 1.2 and the Creative Commons Attribution ShareAlike 3.0 License.

Index

- amplification matrix, 56
- asymptotic expansion, 30

- conservation of mass, 23
- Copenhagen interpretation, 12
- correction, 31
- correspondence principle, 10
- current density
 - Pauli equation, 23
 - Schrödinger equation, 17

- Darwin term, 33
- dimension, 27
- Dirac equation, 24
- Dirac matrix, 24
- Dirac-Maxwell system, 26
- discrete Fourier transform
 - 1D, 40
 - 2D, 43

- explicit scheme, 51
- exponential accuracy, 46

- fast Fourier transform, 40
- Finite Difference scheme
 - consistency, 53
 - convergence, 53
 - stability, 53
- Fourier series, 54
- Fourier-pseudospectral derivative, 44
- Fourier-pseudospectral Laplacian, 44
- Fouriersynthesis
 - 1D, 40
 - 2D, 43

- Heisenberg uncertainty principle, 14

- implicit scheme, 51

- Leap Frog, 57
 - consistency, 60
 - stability, 58

- matrix norm, 47
- Maxwell equations
 - for fields, 25
 - for fields, 25
- multistep schemes, 51

- nondimensionalization, 27

- one-step schemes, 51

- Parseval's equation, 55
- particle current density, 16
- Pauli equation, 21
- Pauli matrix, 21
- Pauli-Poiswell system, 32
- photoelectric effect, 10
- photon, 10
- pseudospectral derivative, 38

- reduced problem, 31
- relative bound, 34
- relative boundedness, 34

- Schrödinger equation
 - magnetic, 19

general formulation, 16
 stationary, 16
self-consistency, 26
spectral accuracy, 46
spectral radius, 47
spin, 19, 20
spinor, 21
state, 12
Stern-Gerlach experiment, 19

trigonometric interpolation, 38

Von Neumann stability condition, 56

wave function, 12
well-posed, 52

zitterbewegung, 33